Nanoscale

REVIEW

Cite this: *Nanoscale*, 2023, **15**, 8044

Evolution of nanostructured skin patches towards multifunctional wearable platforms for biomedical applications

Daniel Rybak,[a] Yu-Chia Su,[b] Yang Li,[c] Bin Ding, *[d] Xiaoshuang Lv,[e] Zhaoling Li, [e] Yi-Cheun Yeh, [b] Pawel Nakielski,[a] Chiara Rinoldi,[a] Filippo Pierini *[a] and Jagan Mohan Dodda *[f]

Recent advances in the field of skin patches have promoted the development of wearable and implantable bioelectronics for long-term, continuous healthcare management and targeted therapy. However, the design of electronic skin (e-skin) patches with stretchable components is still challenging and requires an in-depth understanding of the skin-attachable substrate layer, functional biomaterials and advanced self-powered electronics. In this comprehensive review, we present the evolution of skin patches from functional nanostructured materials to multi-functional and stimuli-responsive patches towards flexible substrates and emerging biomaterials for e-skin patches, including the material selection, structure design and promising applications. Stretchable sensors and self-powered e-skin patches are also discussed, ranging from electrical stimulation for clinical procedures to continuous health monitoring and integrated systems for comprehensive healthcare management. Moreover, an integrated energy harvester with bioelectronics enables the fabrication of self-powered electronic skin patches, which can effectively solve the energy supply and overcome the drawbacks induced by bulky battery-driven devices. However, to realize the full potential offered by these advancements, several challenges must be addressed for next-generation e-skin patches. Finally, future opportunities and positive outlooks are presented on the future directions of bioelectronics. It is believed that innovative material design, structure engineering, and in-depth study of fundamental principles can foster the rapid evolution of electronic skin patches, and eventually enable self-powered close-looped bioelectronic systems to benefit mankind.

Received 20th February 2023,
Accepted 1st April 2023

DOI: 10.1039/d3nr00807j

rsc.li/nanoscale

1. Introduction

In recent years, biomedical sciences have made remarkable progress, owing to the advances in biomaterials, technology, the digital world, and medicine, which have directly impacted the human health sector. More importantly, biomedical systems such as skin patches, are in an evolutionary stage and can be easily handled for monitoring daily health care. Basically, a 'skin patch' was considered to be an adhesive patch that can be placed on the skin to deliver a timed release dose of medication through the skin into the bloodstream; however, technological innovation enabled the transformation of adhesive patches into a wearable device by the incorporation of electronic components, including sensors and actuators with appropriate processing, energy storage and communication, for tracking, detection, diagnosis, and treatment of diseases. The assembly of multicomponent electronics into skin patches resulted in the development of multifunctional skin patches with a broad range of biomedical applications. Wearable patches, which were developed through the evolution of skin patches, have extended to biomaterials with optimized mechanical, biocompatible, and physical properties that are responsive to external and internal stimuli.[1] In this case, adhesion strength and shear deformation sustainability are essential for bio-adhesives.[2] Repetitive on-demand topical administration with drug and immunomodulatory factors regulates the secretion of various signaling molecules,

[a]*Institute of Fundamental Technological Research, Polish Academy of Science, 02-106 Warsaw, Poland. E-mail: fpierini@ippt.pan.pl*
[b]*Institute of Polymer Science and Engineering, National Taiwan University, Taipei, Taiwan*
[c]*College of Electronic and Optical Engineering & College of Microelectronics, Institute of Flexible Electronics (Future Technology), Nanjing University of Posts & Telecommunications (NJUPT), Nanjing210023, China*
[d]*Innovation Center for Textile Science and Technology, Donghua University, Shanghai 200051, China. E-mail: binding@dhu.edu.cn*
[e]*Shanghai Frontier Science Research Center for Modern Textiles, College of Textiles, Donghua University, Shanghai 201620, China*
[f]*New Technologies – Research Centre (NTC), University of West Bohemia, Univerzitní 8, 301 00 Pilsen, Czech Republic. E-mail: jagan@ntc.zcu.cz*

enabling the stage-specific healing mechanism of wounds. Physical and chemical stimulations, such as mechanical, electrical, and thermal stimuli, play a crucial role in accelerating wound healing.[3] The real-time monitoring of physiological conditions and biomarkers is vital to controlling the wound-healing process. Furthermore, integrating biosensors with healing methods can trigger treatment on demand, depending on the wound state.[4]

Health monitoring gadgets, such as skin patches (SP), flexible electronics, biosensors, wireless optoelectronic patches, and printed electronics, have gained popularity on the global market.[5] The increasing demand for wearable skin patches, also known as smart patches, electronic skin, or e-skin patches, is due to advanced research that has made monitoring health much more accessible for everyone. Skin patches can be placed on any body part to monitor temperature, heartbeat, glucose level, *etc*., and can be conveniently used in hospitals, medical centers, or homes.[6] The patch adheres to the skin, creating close contact between the body and the embedded electronics, which helps monitor essential parts, including the heart, head, and stomach. They are frequently used not only to control the wound-healing process but also to detect cardiovascular problems, control diabetes, and maintaining proper health conditions.[7–9] During the COVID pandemic, skin patches were helpful for the early detection of individuals with serious illnesses (*e.g.*, blood pressure drop).[10]

Smart patches are designed by integrating multiple layers, predominantly consisting of a biocompatible flexible substrate, which attaches to the skin, and flexible electronic components such as sensors, self-power generators, processors, actuators, and communication systems.[11] Hence, all the components assembled in skin patches must possess extremely high mechanical strength and comply with desirable properties such as biocompatibility, good adhesion with the skin, ability to withstand different temperatures and humidity, breathability, and waterproofing, while maintaining economic feasibility.[12–14] Ongoing research aims to produce economic smart patches that can house multiple sensors and perform multiple detections simultaneously, which can be commercialized on a large scale to be utilized regularly by regular people.[15]

Emerging technologies are being introduced to increase the performance and productivity of skin patches by working in different directions, as follows: (a) producing innovative polymers for on-skin electronics, (b) formulating stable matrices for assembling electronics, (c) designing biodegradable flexible substrates that can assemble electronics and be easily attached to the skin and (d) dual-integrating dual systems, where the patch not only monitors the health but also works as a self-healing material and drug release system.[16]

The key parameters to consider in the design of a multifunctional skin patch are skin adaptability, mechanical durability, and capability to adapt to the complicated skin surface (Fig. 1a).[17]

Achieving skin-adaptability in electronic devices requires the incorporation of highly reconfigurable architectures with features such as high stretchability, shape moldability, and self-healing ability. Several reports are available on the fabrication of devices having organic or inorganic constituents on a wafer-thin substrate, which can lead to a small bending radius of micrometers even after using materials of relatively large elastic moduli.[19,20] Recently developed patches incorporate multiple key functions of medical devices into flexible substrates based on emerging biomaterials and electronic technologies. The incorporation of materials with high fracture resistance, such as carbon nanotubes, graphene oxide, polymers, metal oxides, and hydrogels, can be a practical approach to obtain mechanically strong devices.[21,22] For example, reduced graphene oxide acts as a sensing platform for many electroactive species, which helps in the immobilization of glucose oxidase and detection at low concentrations.[23] Many different types of functional skin adhesive patches with rigid bulk metal

Daniel Rybak

Daniel Rybak is a PhD student at the Institute of Fundamental Technological Research, Polish Academy of Sciences (IPPT PAN). He has a Master of Pharmacy (MPharm). During his master's research, he developed polyester nanoparticles with paclitaxel as a drug delivery system for cancer treatment. In his doctoral studies, his research focuses on electrospinning and 3D printing of stimuli-responsive biopolymer drug delivery systems for skin treatment.

Yang Li

Yang Li currently works at the College of Electronic and Optical Engineering and College of Flexible Electronics (Future Technology) in Nanjing University of Posts and Telecommunications. He obtained his B.S. and M.S. degrees from the University of Science and Technology Beijing in 2013 and 2016, respectively. In 2021, he received his PhD in Chemical Engineering from Polytechnique Montreal (affiliated with University of Montreal). His research interests focus on conducting polymers based stretchable and healable electronics, as well as wearable bioelectronics for health monitoring.

electrodes are regularly used in hospitals to monitor the condition of patients *via* ECG, EEG, and EMG.[24,25] Besides incorporating functional biomaterials, the structural and morphological design of the device also plays a crucial role in maintaining its mechanical stability.[26] Besides, electrical stimulation has been applied in wound treatment due to its superiorities in promoting cell growth and proliferation, collagen deposition, angiogenesis, *etc.*[3,27] Recently, Du *et al.*[28] developed self-powered and photothermal triboelectric nanogenerator (TENG) skin patches with polypyrrole/F127 hydrogels for wound healing. The developed e-skin patches effectively promoted angiogenesis, collagen deposition, accelerated tissue regeneration, and wound closure in a short period of ~9 to 11 days by combining photothermal heating and real-time electric stimulation.

Numerous wearable skin patches have been introduced to monitor blood glucose, blood lactate, uric acid, and creatinine levels from blood or biofluids such as sweat, saliva, and urine.[29–31] Recently, a functionalized poly(acrylamide)-based hydrogel was used to formulate a soft interface between wearable electronic devices and human skin,[32] *i.e.*, poly(3,4-ethylenedioxythiophene) (PEDOT)-reinforced laser-irradiated graphene as hetero-structured 3D transducers in a flexible skin patch biosensor.[33] Many advanced skin patches such as pulse oximetry sensing patches with ultralow power consumption,[34] multifunctional hybrid skin patches,[35] textile sensor patches for sweat analysis,[36,37] stress monitoring patches,[38] blood pressure sensing patches,[8] self-powered smart patches,[39] and optoelectronic skin patch[40] have been successfully produced. A PubMed® and EspaceNET search for the term "electronic skin patches" in the title/abstract of peer-review papers demonstrated the exponential increase in the research over the past ten years into the development of these versatile materials for biomedical applications (Fig. 1b).

Currently, many advanced technologies have provided enormous support to the health sector. However, the development of e-skin patches can be considered unique in many ways. It enables the prediction of physiological parameters and regulation of health conditions by regularly monitoring bioanalytes. An individual can detect, analyze or take some preliminary measures until they can be seen by a medical practitioner. Although recent reviews have presented the importance of skin-patchable electronics,[41–43] a comprehensive review that covers the simultaneous progress of different skin patches and biomaterials components, including sensors, substrates, and self-powered electronics and functional materials for fabricating skin patches is lacking.

In this review, we highlight the recent advances in skin patches, including the natural evolution of wearable materials starting from flexible substrates, leading to multi-functional emerging biomaterials, stretchable sensors, self-powered systems, and other nanomaterials utilized for building these systems.

2. Flexible substrates for SPs

2.1 Fabrication of substrates

Polymeric materials with flexibility are particularly of interest and useful for fabricating skin patches given that these materials can be bent into various shapes or compressed without rupture. In particular, flexible substrates with self-healing ability, suitable moisture, biodegradation, and biocompatibility are even more desirable for skin patch applications. It was also observed that flexible materials used for epidermal electronics showed enhanced sensitivity by improving the adhesion strength and compliance of the flexible substrates.[44,45] With the benefits of providing strain compatibility to human skin and proper compliance to human motion, flexible substrates can be involved in monitoring physical parameters (*e.g.*, temperature, heart rate, and wound monitoring) in real-time to improve diagnosis and facilitate preventative medicine.

Bin Ding

Bin Ding received his BS from Northeast Normal University (China) in 1998 and his MS from Chonbuk National University (Korea) in 2003. After that he earned his PhD at Keio University (Japan) in 2005. Currently, he is a Full Professor at the Innovation Center for Textile Science and Technology, Donghua University. His research mainly focuses on filtration materials, waterproof and breathable fabrics, oil–water separation materials, flexible ceramic nanofibers, and nanofiber aerogels.

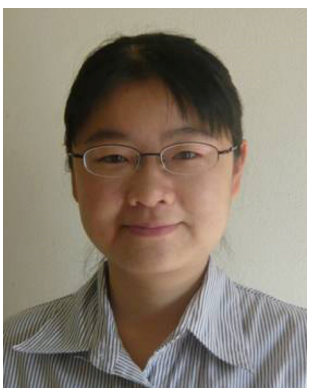

Yi-Cheun Yeh

Yi-Cheun Yeh is an Associate Professor at the Institute of Polymer Science and Engineering at National Taiwan University. She pursued her PhD in Chemistry at the University of Massachusetts at Amherst under the guidance of Prof. Vincent Rotello. Upon graduation, she moved to Philadelphia to perform her postdoctoral studies in the Polymeric Biomaterials Laboratory of Prof. Jason Burdick. Presently, her laboratory focuses on engineering the interface between materials and biology, and spans the areas of nanoparticles, biomaterials, and biofabrication.

In general, flexible substrates can be fabricated through the choice of elastomeric materials or the design of interfacial crosslinking mechanisms between polymer chains. Elastomeric materials with soft or tensile properties (*e.g.*, *cis*-polyisoprene, *cis*-polybutadiene, polysiloxane, styrene–butadiene copolymer, and ethylene–propylene copolymer) can be used to construct flexible substrates. For example, *cis*-polyisoprene is a well-known synthetic rubber that offers similar traits and physicochemical properties to natural rubber. *cis*-Polyisoprene polymer with high uniformity can be employed in various applications that require consistent quality and performance. For example, Ruangmak *et al.* applied porous *cis*-1,4-polyisoprene as a matrix in drug absorption and release due to its uniform porous structures and non-cytotoxicity to human cells.[46] The drug release time was regulated mainly by the concentration gradient. Simultaneously, the pore size of the matrix and external electric field was used to control the diffusion coefficient of drug release. Besides, owing to the corrosion resistance of polyisoprene, it maintains its original porous structure during the drug release process without decomposing.

Another popular elastomer used as a flexible substrate is polysiloxane, which is a hydrophobic polymer with low moisture retention. Polysiloxane has been widely used for medical applications due to its lower glass transition temperature, low viscosity, high gas permeability, and low surface tension. For example, Wu *et al.* developed a polydimethylsiloxane(PDMS)-based substrate with mechanical stretchability, softness, and adhesion to the human skin.[47] The mechanical properties of PDMS were strengthened by embedding polyethyleneimine (PEI), and the PDMS/PEI composites presented adhesiveness of ~1 N, Young's modulus of ~24 kPa, and elongation of >300%. Besides, PDMS/PEI composites were further fabricated as a film for biomedical applications, showing good repeatability and stability signals under high-frequency bending and expanding through fingers.

Various chemical interactions (*i.e.*, dynamic covalent bonds and noncovalent interactions) have been applied in developing flexible substrates. Dynamic covalent bonds include imine bonds, disulfide bonds, and diel-Alder reactions. The formation of imine bonds *via* the reaction between aldehydes and amines improves the stability and mechanical properties of flexible substrates.[48–51] For example, Chen *et al.* synthesized self-healing hydrogels *via* the imine bonds between aldehydes of oxidized sodium alginate (OSA) and amines of *N*-carboxyethyl chitosan (CEC) or adipic acid dihydrazide (ADH).[50] The CEC-OSA-ADH hydrogel displayed high elongation strength and self-healing properties, where the synthetic ratio of amine to aldehyde of 1 : 1 afforded a stress strength of up to ~30 kPa and healing efficiency of up to ~86%. Disulfide bonds can be formed from the oxidation of the sulfhydryl groups for the crosslinking of polymers.[52,53] For example, mesoporous silica nanocomposite (MSN) hydrogels were synthesized using composites of thiol surface-functionalized MSNs (MSN-SH) and thiol-functionalized 4-arm-polyethylene glycol (4-arm-PEG-SH).[53] In addition to self-healing abilities, the MSN hydrogels exhibited tunable mechanical properties by incorporating various amounts of MSNs in the functional PEG polymers. The composites with a lower content of MSNs showed a high equilibrium swelling degree (284%) in the network, suggesting the mechanical properties were improved at low MSN ratios. Diels–Alder reaction provides a chemical way to generate new six-membered rings by forming two new carbon–carbon bonds between a conjugated diene and alkene.[54–57] Yoshie *et al.* developed a novel self-mending polymer *via* the self-assembly of a copolymer *via* reversible Diels–Alder reaction, where the anthracene groups of the anthryl-telechelic poly(ethylene adipate) ($PEAA_2$) and the maleimide groups of tris-maleimide (M_3) were designed as the polymer blocks.[57] The $PEAA_2M_3$ polymer possessed elasticity and tensibility, which showed more than 1000% strain with the maximum stress of 26 kPa. The $PEAA_2M_3$ polymer could be stored under 100 °C for three days to recover its mechanical strength, with the tensile strength recovered up to 27% of the original mechanical strength.

In addition to dynamic covalent bonds, noncovalent bonds (*e.g.*, hydrogen bonds, metal–ligand interactions, and dipole–

Filippo Pierini

*Filippo Pierini is a Professor and the Head of the Pierini Research Group (**https://www.nanoprg.com**) at the Institute of Fundamental Technological Research (IPPT PAN). He received his M.Sc. in Advanced Chemical Methodologies with the highest grades and honors (110/110 summa* cum laude*) in 2009, and his PhD in Chemical Sciences at the University of Bologna (Italy) in 2013. His research interests include biomaterials, drug delivery, light–matter interaction, and the development of functional fibrous nanomaterials.*

Jagan Mohan Dodda

Jagan Mohan Dodda obtained his PhD in Chemistry from Bhavnagar University, India. Later, he carried out his postdoctoral research at Akita University (Japan), Korea Forest Research Institute (South Korea) and the University Sains Malaysia (Malaysia). He is currently a Senior Researcher at the New Technology Research Centre, University of West Bohemia, Czech Republic. His research focuses on multicomponent hydrogels, conducting hydrogels, and bioresorbable and nanocomposite films for biomedical applications.

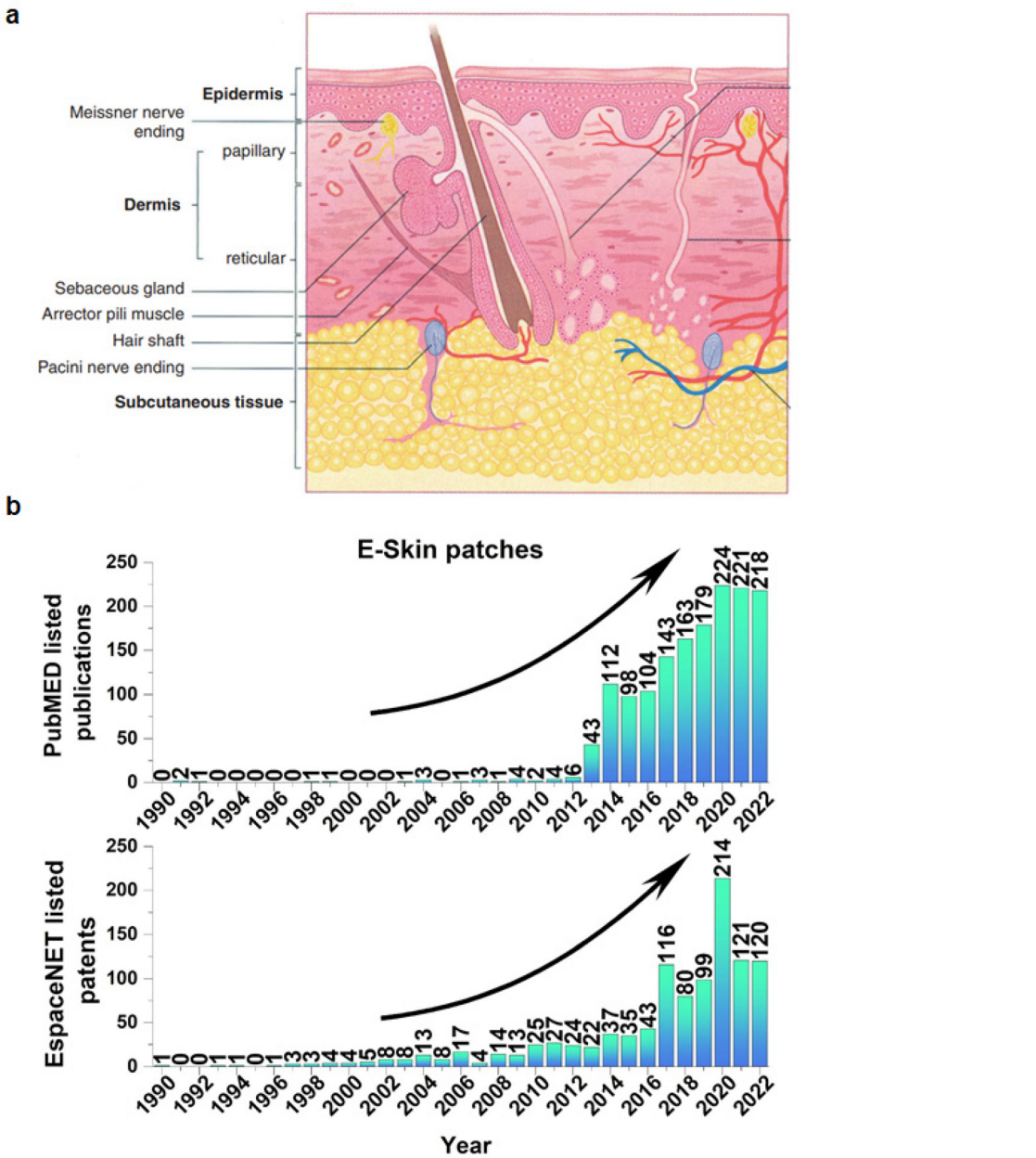

Fig. 1 (a) Multilayer structure of human skin tissue. Copyright 2006, Elsevier Saunders. Reprinted with permission.[18] (b) Rapid growth in the number of PubMed® publications and EspaceNET submitted patents on e-skin patches in the past two decades.

dipole interactions) can also be incorporated in the polymeric network to ameliorate the identities of the flexible substrates.[58–64] The hydrogel networks formed by hydrogen bonds possess outstanding high toughness, extremotolerant property, and self-healing capability. For example, an injectable hydrogel with hydrogen bonds was fabricated using a mixture of hydrazide-modified poly(*N*-isopropylacrylamide-*co*-acrylic acid) (poly(NIPAM-*co*-AA)-hdz), aldehyde-functionalized dextrin, and poly(*N*-acryloyl glycinamide) (PNAGA).[65] The maximum storage modulus of the PNIPAM-based hydrogel was promoted by 570% (from 90.2 to 517.0 kPa) by incorporating the intermolecular hydrogen bonding from PNAGA into the hydrogel network. Moreover, metal–ligand coordinated interaction was successfully introduced in the hydrogel polymer to endow the gel with improved mechanical strength. Based on the metal–ligand coordinated interaction of the first transition metal ions and *N*-isopropylacrylamide-based hydrogel, stimuli-responsive hydrogels were fabricated to explore their mechanical properties under the lower critical solution temperature.[66] The hydrogels embedded with metal ions exhibited better mechanical properties (*i.e.*, compressive stress, Young's modulus, and energy dissipation) than that without metal

ions. Especially the modified hydrogel with zinc ions presented the best compressive stress (4.64 MPa), modulus (44.2 kPa), and dissipation (350 kJ m^{-3}) among the hydrogels.

2.2 Types of flexible substrates

Here, several types of flexible substrates (*i.e.*, elastomers, hydrogels, and hydrogel-elastomer hybrids) used for the skin patches are illustrated with several representative examples.

2.2.1 Elastomers. The general characteristics of elastomers are both viscosity and elasticity. Owing to the property of elastomers to recover their original state after stretching, they (*e.g.*, styrene-ethylene-butadiene-styrene (SEBS) and poly(dimethylsiloxane) (PDMS)) have been applied in the construction of skin patches.

SEBS is a thermoplastic copolymer with excellent thermosensitivity, UV resistance, and ease of production. For example, a series of SEBS derivative materials with different butadiene-to-styrene ratios and carbon nanotubes presented well-order structures to resist UV radiation.[67] Besides, the drug release rate and skin permeability of the SEBS copolymer exhibited satisfactory properties (*i.e.*, viscoelasticity, permeability, and dissolution test) for skin patches.[68] Feng *et al.* utilized SEBS triblock copolymer as the starting material to fabricate conductive polymer composites *via* the introduction of graphite nanoplatelets (GNPs) (Fig. 2a).[69] Tensile tests were performed to evaluate the mechanical properties of the SEBS/GNP composites, showing that composites could be stretched to 125% with maximal stress (Fig. 2b). The relationship between GNP loading *versus* conductivity was plotted, as demonstrated in Fig. 2c, showing the electrical property of SEBS/GNP composites. A percolation threshold (ϕ_c) of SEBS/GNP composites was studied by fitting the variation in electrical conductivity (σ) with the content of GNPs through the equation $\sigma = \sigma_0(\phi - \phi_c)^{\tau}$. According to the results, the percolation threshold for the composites was 0.299%, indicating that the materials possessed high electrical conductivity at low filler contents. The SEBS/GNP composites were further applied to monitor instantaneous resistance variation from various human motions. All electrical signals were stable and replicable during the cycles, showing that the SEBS/GNP composites were highly promising for wearable sensors (Fig. 2d–g).

PDMS, one type of silicon-based polymer, is a promising elastomer in various practical applications due to its non-toxic, non-irritating, and non-sensitizing nature. Consequently, PDMS has been widely utilized to fabricate skin patches.[44,70–73] For example, Park and coworkers developed a new type of epidermal electronic by fabricating nanocomposites with PDMS and silver nanowires (AgNWs) (Fig. 3a and b).[44] A commercially available nonionic surfactant (Triton X) was added to the nanocomposites to improve their mechanical properties. The AgNW-embedded PDMS nanocomposite could be directly attached to human skin for use as strain and electrocardiogram (ECG) sensors, presenting good adhesiveness and stability following repeated bending of the wrist and forearm (Fig. 3c). Compared to the PDMS substrate without AgNWs, the PDMS substrate embedded with AgNWs presented better adhesiveness without delamination to the human skin after repetitive motions (Fig. 3d and e). Therefore, the PDMS-based nanocomposites possessed highly conformable, stretchable, transparent, and higher water vapor permeability, showing the promise of PDMS-based substrates for the design of e-skin devices.

2.2.2 Hydrogels. Hydrogels, which are three-dimensional networks of hydrophilic crosslinked polymers containing an ample amount of water, have been widely applied in different fields, especially in the biomedical area. Hydrogels have become extensively attractive for skin repair and regeneration due to their versatile properties and multiple stimuli-responsiveness. Lu *et al.* introduced polydopamine nanoparticles (PDA-NPs) in a poly(*N*-isopropylacrylamide) (PNIPAM) network to prepare PDA-NP/PNIPAM hydrogels (Fig. 4a).[75] It was observed that the self-healing and drug release of the PDA-NP/PNIPAM hydrogels could be regulated through near-infrared (NIR) irradiation (Fig. 4b and c), where methasone was released when the NIR laser was on. In contrast, the drug release was stopped once the NIR laser was off (Fig. 4d). Also, NIR irradiation successfully induced self-healable properties of PDA-NP/PNIPAM hydrogels. The ruptured materials containing 0.8 wt% and 0.15 wt% PDA-NPs almost healed upon NIR irradiation for one second. Alternatively, the PDA-NP/PNIPAM hydrogel with 0.8 wt% PDA-NPs could be suspended without breaking after NIR irradiation for 10 s (Fig. 4e). After 9 days of wound treatment, treatment with epidermal growth factor (EGF)-loaded hydrogel exhibited the highest healing ratio of up to 68.5%, compared with the healing ratio of PDA-NP-coated hydrogel was only 45.2% (Fig. 4f). Thus, EGF has been demonstrated to accelerate wound healing by introducing the PDA-NP/PNIPAM hydrogels. Other examples of using hydrogels as flexible substrates for skin repair include gelatin methacrylate/tannic acid hydrogels,[76] chitosan-*g*-polyaniline/benzaldehyde-based-functionalized poly(ethylene glycol)-*co*-poly(glycerol sebacate) hydrogels[77] and chitosan-based hydrogels.[78]

2.2.3 Hydrogel-elastomer hybrids. Hydrogel-elastomer hybrids have been recognized as promising materials because they combine the unique features of hydrogels (*e.g.*, high-water content, permeability, biocompatibility, and biodegradability) and elastomers (*e.g.*, sufficient mechanical strength and flexibility), providing superior properties to expand the potential uses in the biomedical industry. Chen *et al.* proposed an efficient mechanical interlock method to merge the merits of hydrogels and elastomers. The mechanical interlock of the hydrogel-elastomer hybrids was achieved by introducing polyacrylamide/Ca-alginate (PAM/Ca-Alg) hydrogels in porous thermoplastic polyurethane (TPU) networks after thermal curing (Fig. 5a).[79] The hybrids were formed through the interlock interactions between the hydrogels and elastomers, which enhanced the bonding strength without separation after peeling force (Fig. 5b–e). The bond strength between the hydrogel and elastomer was further evaluated, showing that the interlocked structure exhibited the highest adhesiveness (50.9 J m^{-2}). In comparison, the network and film composites

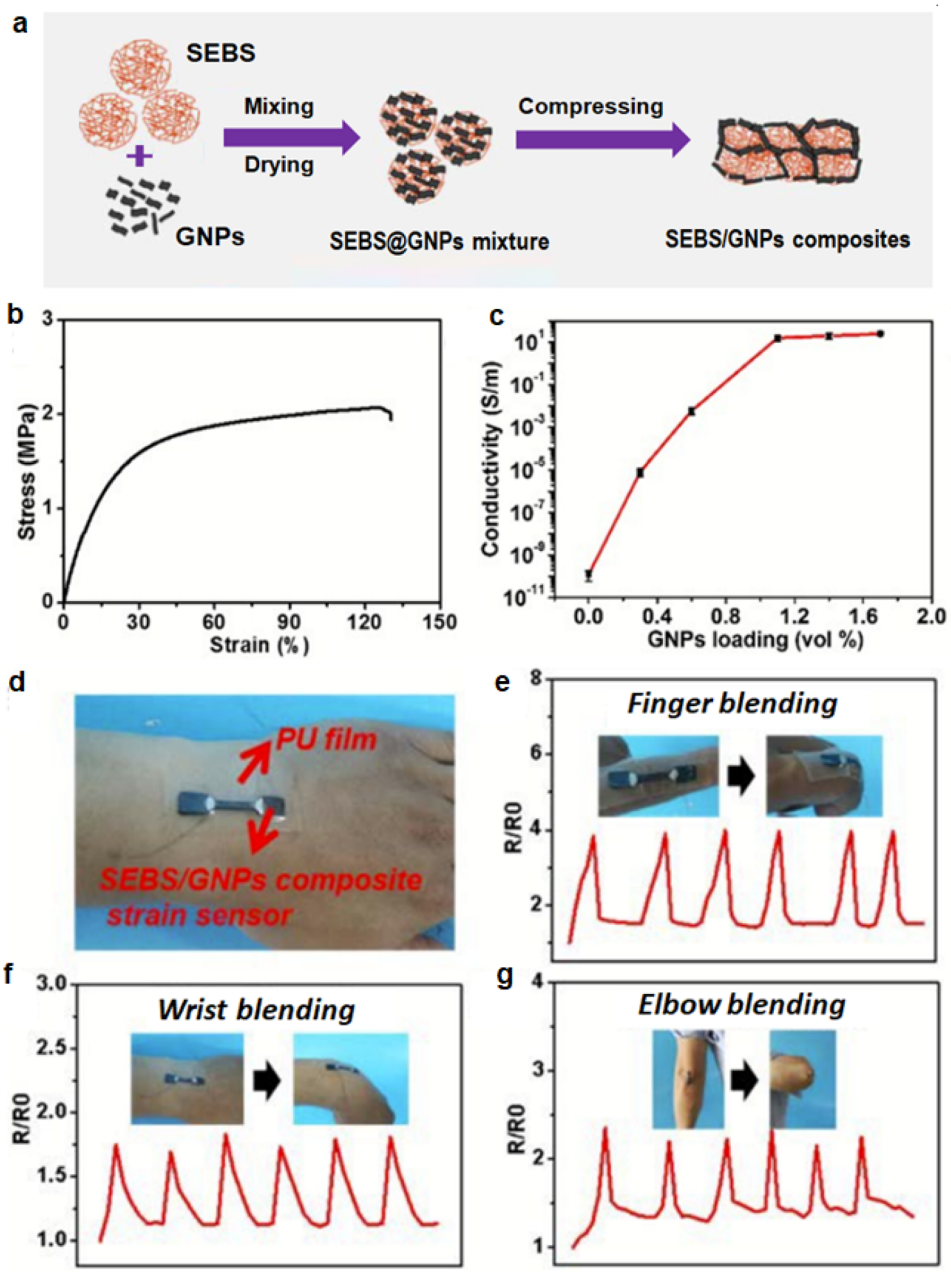

Fig. 2 (a) Schematic of the fabrication of SEBS-based composites. (b) Stress–strain curve of composites. (c) Electrical conductivities of SEBS-based composites with various GNP loadings. (d) Photo of a strain sensor attached to a wrist on polyurethane film. Electrical resistance sensors measuring the physical motion of (e) finger bending, (f) wrist bending, and (g) elbow bending. Reproduced with permission.[69] Copyright 2019, The Royal Society of Chemistry.

showed poor interaction of 5.10 and 3.56 J m^{-2}, respectively. Furthermore, the interlocked hybrids possessed a Young's modulus of 11.5 kPa, and the stress–strain curves showed that the hybrids could be stretched to 557% with a maximum stress of 28.7 kPa. A breaking point appeared in the stress–strain curve due to the rupture of the TPU networks during the stretching process. Most importantly, the hybrids presented remarkable skin adherence with an adhesive strength of ~30 N m^{-1}, which is comparable to that of commercial polyimide tape (Fig. 5f).

2.2.4 Other biocompatible synthetic polymers. Recently, biocompatible and biodegradable polymers have attracted interest for application in drug delivery skin patches and wound repair. Polylactide (PLA), polyglycolide (PGA), and their derivatives have been studied thoroughly to meet the diverse requirements of skin patches. For example, the solvent casting method was employed to synthesize a patch material incorporating PLA as a matrix and phycocyanin-alginate composites as the active ingredient.[80] Also, the patch material could act as a

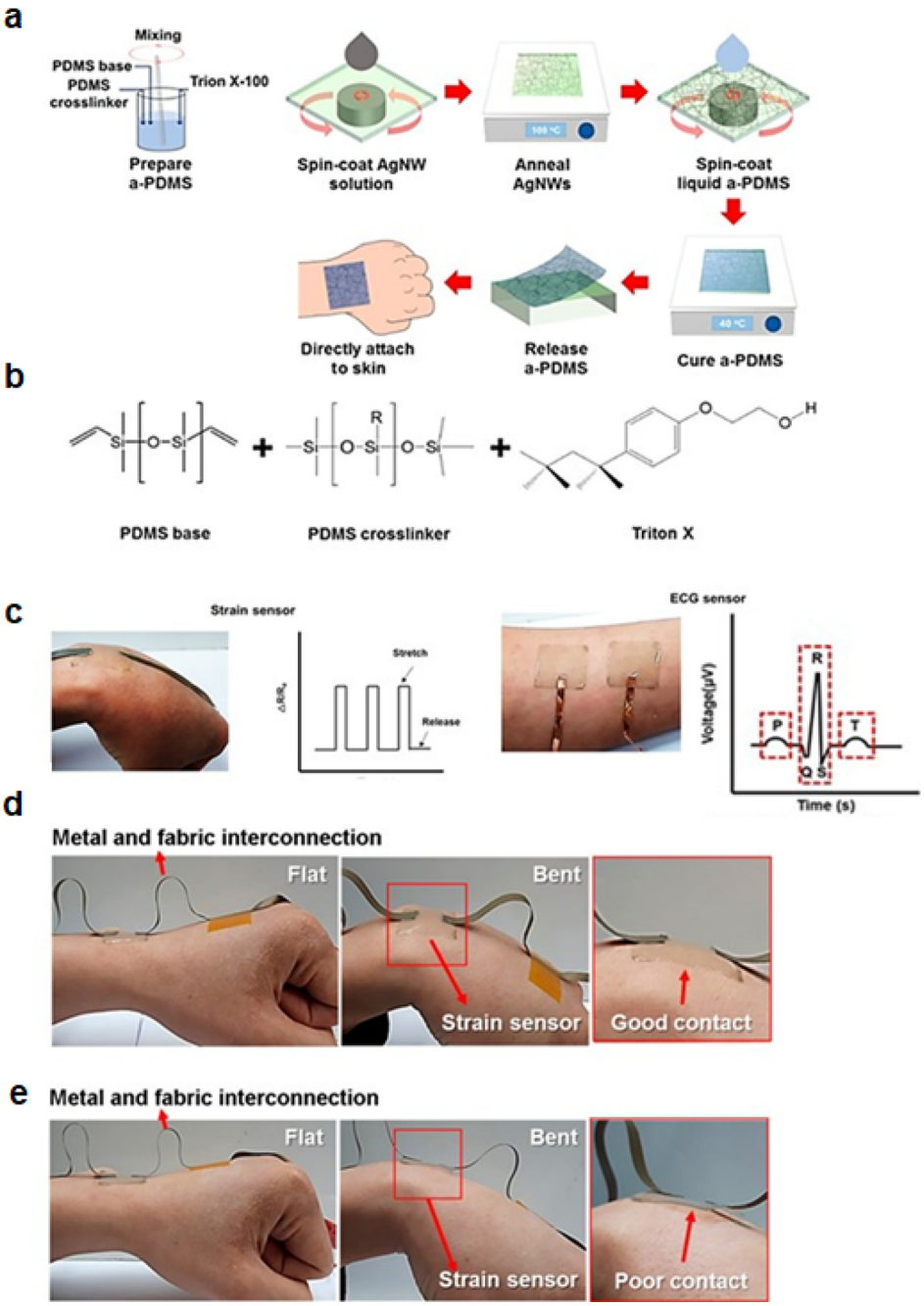

Fig. 3 (a) Schematic images of the fabrication processes of modified PDMS materials. (b) Modified polydimethylsiloxane (PDMS) was fabricated using PDMS-base, PDMS cross-linker and Triton X. (c) Flexible electrode was fixed on the wrist and forearm for monitoring strain and the ECG sensor, respectively. (P wave: atrial depolarization; QRS complex: ventricular depolarization; and T wave: ventricular repolarization). (d) Photographs of PDMS-based flexible strain sensors with AgNWs. (e) Photographs of PDMS-based flexible strain sensors without AgNWs. Reproduced with permission from Reference.[74] Copyright 2018, the American Chemical Society.

drug carrier with tunable mechanical properties *via* various phycocyanin/alginate ratios, where phycocyanin and alginate in the ratio of 40 : 60 exhibited the highest elongation (33.3%), and drug release rate was increased when the phycocyanin content was decreased. In another example, a PCL-PGA composite containing the drug ciprofloxacin (CPFX) was covered on the surface of PLA material, where the ratio of PCL and PGA was adjusted to control the drug release time on PLA networks by tuning the degradation ratio of PCL-PGA composites.[81] With an increase in the PCL content in the drug carrier, the breaking strength and elongation both increased; conversely, the degradation rate and drug-release rate decreased.

Recent studies have explored various sensing materials by introducing functional nanomaterials in polymer-based sub-

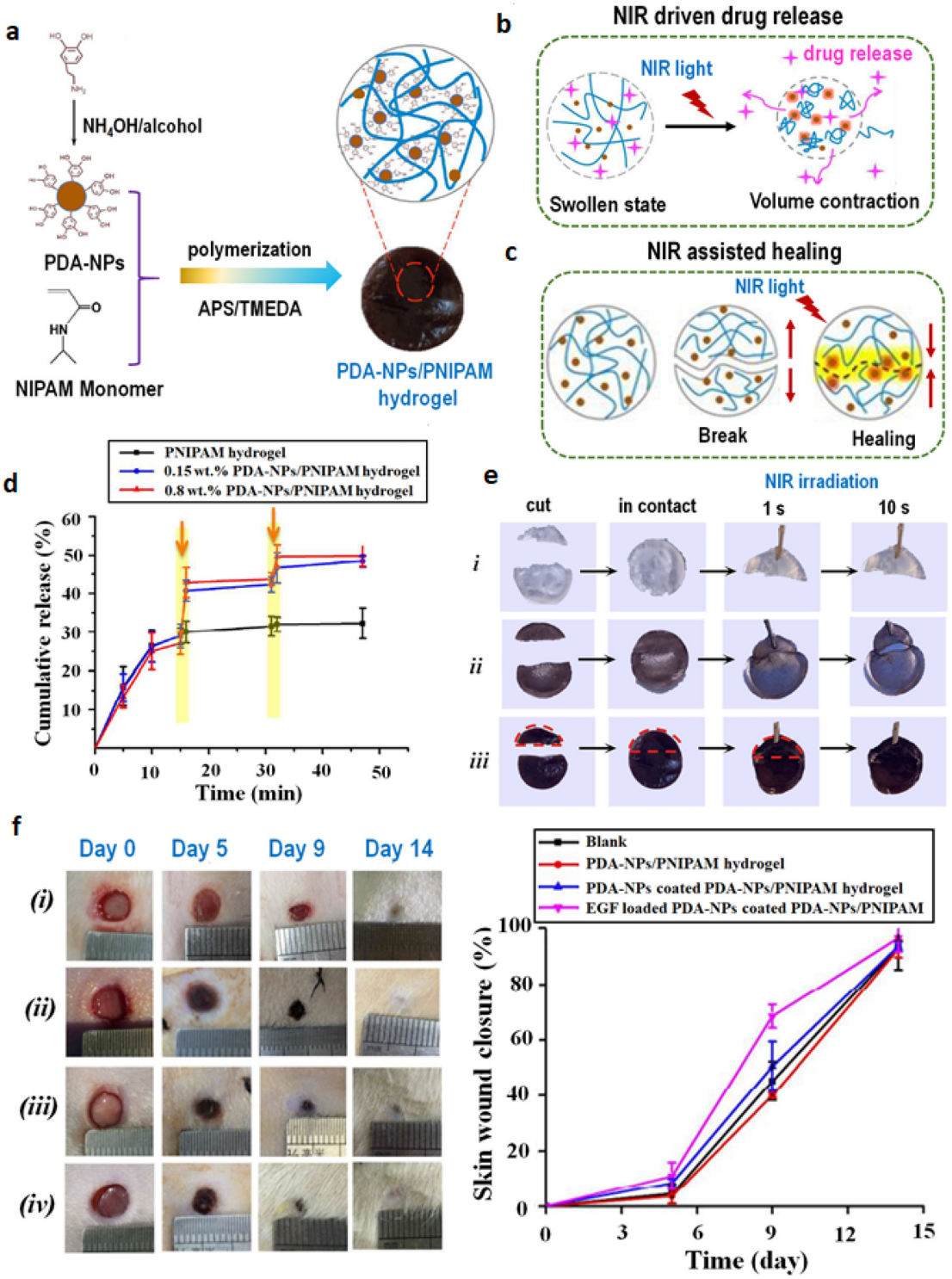

Fig. 4 (a) Schematic of the PDA-NP/PNIPAM hydrogel fabrication. (b) NIR-controlled pulsatile drug release. (c) NIR-assisted wound healing. (d) Dexamethasone cumulative release from PNIPAM-based hydrogels under NIR laser irradiation and without laser irradiation. (e) As NIR-irritated for 1 and 10 s, PNIPAM hydrogels (i), hydrogels with 0.15 wt% PDA-NPs (ii) and 0.8 wt% PDA-NPs (iii) heal themselves. The hydrogels were hung under gravity. (f) Representative photos of the gross appearance of defects treated with PNIPAM (i), 0.8 wt% PDA-NPs/PNPAM (ii), PDA-NPs-coated-PDA-NPs/PNIPAM hydrogels (iii), and EGF-loaded PDA-NPs-coated-PDA-NPs/PNIPAM hydrogels (iv) at days 0, 5, 9, and 14. Reproduced with permission.[75] Copyright 2016, the American Chemical Society.

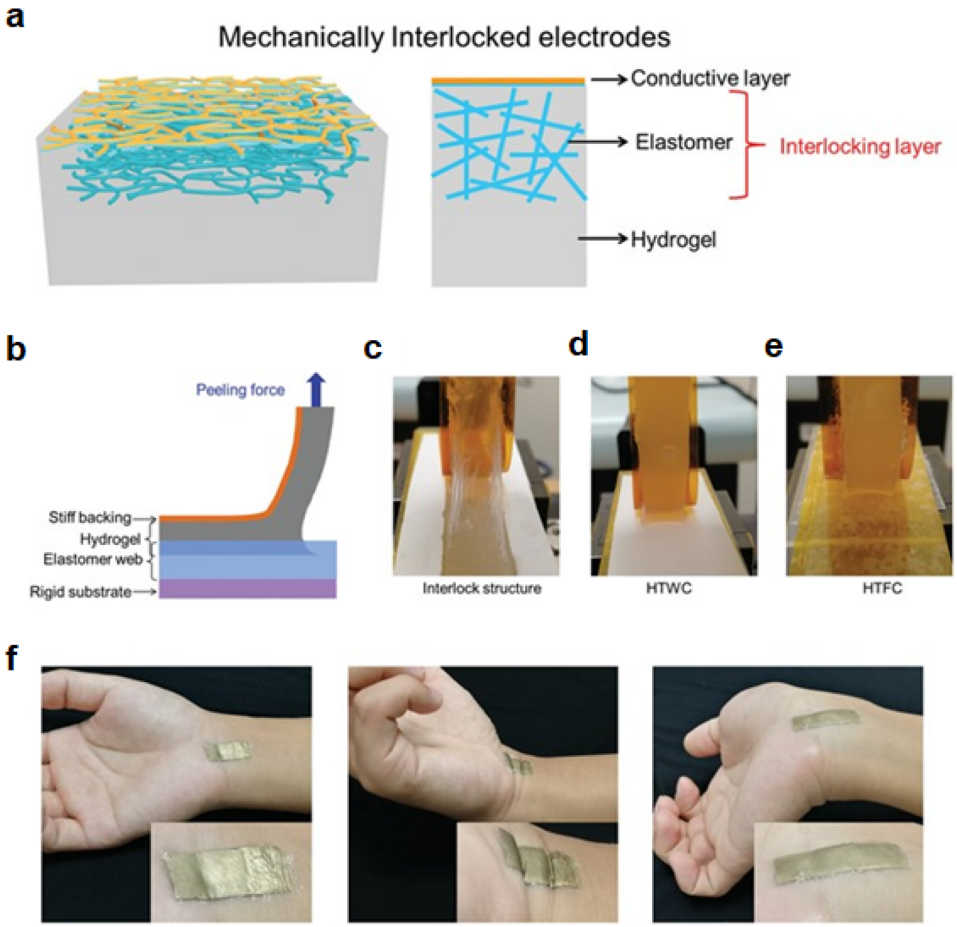

Fig. 5 (a) Schematic of interlocked hydrogel-elastomer hybrids. A hybrid structure is formed by embedding the hydrogel in a porous elastomer web. (b) Diagrammatic representation of the peeling test for bonding strength. (c–e) Optical images of the peeling process for (c) interlocking hybrids, (d) hydrogel–TPU web composites (HTWC), and (e) hydrogel–TPU film composites (HTFC). (f) Interlocked hybrid as skin electrodes for monitoring EMG signals. Reproduced with permission.[79] Copyright 2020, Wiley-VCH.

strates with explicit micro or nano-structure design.[82,83] Besides these unique structures, stretchable electronics with biomimetic structure design are also efficient in detecting multiple mechanical forces *via* innovative material design strategies.

3. Emerging functional biomaterials as SPs

Functional nanostructured materials have attracted increasing attention in several scientific fields, including biosensors[84] and biomaterials.[85] The rapid growth of this scientific area profoundly influenced the effective development of devices that require activation to perform specific activities.[86] Considering this, the progress in the fabrication of novel skin patches capable of fulfilling different tasks (*e.g.*, healing skin damage,[87] eradicating pathogen infections,[88] and sensing specific molecules/activities[89]) led to significant advancements in the technological in the last few years.[90]

The efficiency of skin patches has been profoundly enhanced using nano- and micro-structured materials in the last few decades.[91] From the beginning of the nanotechnology-driven breakthrough in skin treatment, it was clear that basic requirements such as biocompatibility[92] and physical and chemical compatibility of the material with both body tissue[93] and possible bioactive molecules present in the developed biomaterials[94] should be fulfilled. Additionally, it is worth remembering that the skin is a vast organ, with various and very dynamic activities over time, which makes the development of materials with multiple properties such as the possibility to perform different functions and to control them by endogenous[95] or external stimuli necessary.[96]

Scientists working in the field of chemistry have recently devoted enormous efforts to synthesizing polymer functional biomaterials with smart features, delivering excellent results.[97] Specifically, effective biomaterials were obtain with the potential to be used in applicative medicine, combining novel chemical paths with intelligent materials, where the hierarchical structuration of nano- and micro-platforms plays a crucial role.[98] Therefore, stable responsive nanoagents such as plas-

monic nanoparticles[99] and fabrication techniques with great adaptability aimed at producing fine-tuned fibrous polymer-based biomaterials (*e.g.*, 3d printing[100] and electrospinning[101]) are giving a fresh outlook to biopolymers for skin treatment.

In this section, we present a detailed overview of the forefront functional biomaterials for novel skin patch development, focusing on crucial aspects such as the impact of gradient-structured scaffolds,[102] the opportunity to furnish novel features provided by the inclusion of inorganic materials, the enhanced effects given by biologics as bioactive molecules[103] as well as the possibility to develop advanced smart multi-responsive and multifunctional skin patches.[104]

3.1 Gradient scaffolds for skin regeneration

Many tissues, *e.g.*, skin, have various physicochemical gradients with arranged transitional zones that build distinct functional regions in the tissue.[85] Three main layers can be distinguished in the skin, *i.e.*, epidermis, dermis and hypodermis.[105] The epidermis is composed of different sublayers of keratinocytes, and its primary role is to provide a barrier to the external environment. The dermis is composed of fibroblasts, collagen, and inflammatory and immune cells, providing structural support and elasticity to the skin. The deepest hypodermis layer contains fat cells, collagen and sensory nerves and provides support, temperature control and mass transport of nutrients through vessels. It also connects skin tissue and underlying inner organs. The function of these layers is determined by their physicochemical properties, especially the gradual changes in various physical characteristics deep in the skin, such as stiffness, porosity, and architecture.[106,107]

Due to the multi-layer nature of the skin, gradient-based strategies have gained substantial attention as promising candidates for mimicking the skin tissue environment.[85] Consequently, many research groups have designed biomaterials with different physicochemical gradients that can be directly combined during the synthesis or postprocessing of biomaterials. The techniques used to produce novel scaffolds commonly include rapid prototyping, electrospinning and more traditional techniques such as freeze-casting and selective irradiation. Moreover, these methods are also employed to form more advanced solutions. However, there are many considerations in the design of biomaterials for wound healing. One is selecting the type of gradient that can be formed in biomaterials, including chemical signal gradients and physical gradients such as pore size and compound gradients. In the following subsections, we present specific examples of gradient materials that can be employed in the design of cellular scaffolds that can improve wound healing processes.

3.1.1 Physical gradients. Gradient-containing biomaterials with different physical and mechanical cues are needed to control cell migration and provide a suitable cell niche. One biomaterial factor governing cell migration is porosity, which enables the transportation of nutrients and waste products. It also influences cell function and interactions with the scaffold such as binding and spreading. In skin layers, different cells and their organization can be found; therefore, the specific pore sizes of each layer should be considered in the design of biomaterials.

3.1.2 Pore size. Niu *et al.* reported the preparation of a full-thickness skin scaffold with a gradient pore structure and the construction of the epidermis and dermis layer by 3d printing different ratios of bio-inks.[108] Their hypothesis was that a dense layer without a macroporous structure protects the wound surface and maintains a moist environment on the wound surface. By optimizing the material composition (proportion of sodium alginate/gelatin/collagen) and printing parameters for each layer, suitable hydrogel bioink formulations were achieved, which simulated the physiological structure of the skin. The printed scaffold with uniform microscopic pores on the surface and inside provided cell adhesion and growth. Moreover, in the *in vivo* model of a porcine full-thickness wound, the scaffold accelerated wound healing, reduced skin wound contraction, and re-epithelialization after four weeks from operation. Furthermore, the collagen fibers and blood vessels were more prominent due to the presence of interconnected macroscopic channels. The authors expect that the developed pore gradient scaffold can enable the rapid and economical production of skin scaffolds for future clinical applications.

Pore-size gradients in electrospun mats can be formed by tuning the expansion of 2D membranes in different layers by introducing various amounts of surfactant during the gas-foaming process. Chen *et al.* fabricated 3D electrospun scaffolds with different fiber organizations by expanding 2D nanofibrous membranes composed of multiple regions.[109] The generated areas had a different fiber distribution produced by varying mandrel rotating speeds. The aligned area expanded the most, creating the prominent pores in the scaffold, while the randomly oriented fibers created a more compact structure with smaller pores. Finally, dual gradients in pore sizes and fiber organizations from random to partially aligned and aligned were prepared, enabling the better reproduction of the skin structure. Moreover, the compositional gradients on 3D nanofiber assemblies were introduced by transforming the electrospun mat into a 3D scaffold consisting of radially aligned nanofibers. Then, after dripping the model substance at the center of the scaffold, radial spreading was observed due to the radially aligned pores in the scaffold. This method enabled to fabrication of compositionally graded scaffolds with graded essential fibroblast growth factors. The *in vitro* study showed that more fibroblasts were detected on the bFGF gradient scaffold compared to the scaffolds without and with an equivalent dose of free bFGF after 4 and 8 days of incubation. Also, the total number of fibroblasts inside the scaffold was markedly higher due to the migration of cells into the scaffolds at varying depths. The authors concluded that 3D nanofiber assemblies with porosity and multiple composition gradients can be produced based on this strategy. This method allows for spatial control of various signaling molecules and can lead to the effective regulation of the cell response.

3.1.3 Stiffness. The mechanical properties of scaffolds in which cells reside have emerged as an essential regulator of

cell fate. The role of substrate stiffness on cell fate decisions is still under investigation; however, their responses to the mechanical environment are well-characterized and often complex. Many research groups developed gels and hydrogels with stiffness gradients and evaluated the migratory behavior of cells. Kidoaki *et al.* used a photocurable styrenated gelatin to produce gels with a gradient elastic modulus in the range of 10 to 400 kPa.[110] According to the 3T3 cell movement trajectory analysis, cells migrated favorably from the soft base region of 10 kPa toward regions with a high elastic jump of 80 kPa. The same pattern of cell migration from soft to stiffer areas could also be found in other cells. However, although several important *in vitro* studies have been reported on the effect of material stiffness on cell behavior, there are no examples in the literature of biomaterials that exploit this phenomenon to rebuild injured skin tissue.

Milojević *et al.* developed a hybrid hydrogel-thermoplastic polymer scaffold with tunable structural and chemical properties.[111] By alternating the deposition of PCL and alginate/carboxymethylcellulose gel filaments, scaffolds with the desired architecture and viscoelasticity were prepared. Several types of scaffolds with different filament thicknesses and overall macroporosity were developed. The authors proposed that the controlled degradability of the hydrogel layer depends on the crosslinking and permeability of the hydrogel component used in controlled drug delivery. However, although the concept of combining a stiff PCL with a soft hydrogel is interesting, the cellular studies in this work were only concerned with testing the biocompatibility of the fabricated biomaterial.

Ha, *et al.* developed skin-inspired hierarchical biomaterials with gradient stiffness and interlocked micro-ridge structures.[112] The proposed material worked as a triboelectric sensor (TES), which effectively transmitted external stress from stiff to soft layers, resulting in a susceptible signal capable of detecting human movement and vital signs. The epidermis layer was made of poly(vinylidene fluoride-*co*-trifluoroethylene) polymer P(VDF-TrFE), while the dermis was based on poly(dimethylsiloxane) (PDMS). The P(VDF-TrFE) layer had a hierarchical structure with nanofiber-like morphology and inner pores. PDMS exhibited open porous networks with a pore size of 2.2–5 μm. Moreover, the developed micro ridges in the interlocked polymers effectively modified the gap distance between the layers without using the bulk spacer to form ultrathin and flexible skin sensory receptors.

3.1.4 Scaffold composition. The composition selection and design of scaffolds are critical for developing skin-mimicking biomaterials that should have various physicochemical gradients in different layers. Most research groups focused on mapping the two structures of the skin, *i.e.*, the epidermis and dermis. However, achieving continuous composition gradients to better mimic tissues requires precise material dosing or techniques that can form hybrid biomaterials.

Ghosh *et al.* prepared a functionally graded electrospun scaffold produced in a single step.[113] Gradation of the scaffold was performed by changing the PCL-collagen solutions with different PCL-to-collagen ratios and electrospinning parameters (Fig. 6a). The structure of the epidermis layer was mapped using pure PCL fibers. The subsequent layers contained an increasing proportion of collagen in their structure. It was observed that an increase in the collagen concentration resulted in an increase in the porosity of each layer. Co-culture of dermal fibroblasts (PCS-201) and keratinocytes (HaCaT) on the scaffold resulted in cellular proliferation, differentiation and organization of the skin tissue. Moreover, the *in vivo* study on the excision model of rat skin revealed that the scaffold displayed more incredible wound healing, measured as wound closure time and tissue regeneration, compared to the standard treatment. Thus, the proposed multi-layer scaffolds may fit the existing complex gradients in various sublayers of this tissue.

Zhang *et al.* prepared an asymmetric bilayer dressing that mimicked the gradient structure of the epidermis and dermis by using electrospinning and 3D printing.[114] The scaffold design was aimed at fabricating a material with different properties, including surface hydrophilicity and hydrophobicity, porosity, and mechanical and antibacterial properties. The outer layer mimicked the epidermal layer and was prepared by electrospinning polycaprolactone/polylactic acid (PCL/PLA). The electrospun mat was water-repellent and did not allow for bacterial penetration. The 3D-printed hydrogel was based on sodium alginate/polyvinyl alcohol/chitosan and quaternary ammonium salt. The authors performed an *in vitro* study using human dermal fibroblasts (HFBS) and showed that the produced biomaterial is not cytotoxic. Simultaneously, the mechanical properties of the scaffold, including tensile strength, Young's modulus, and elongation at break, were similar to natural human skin.

Moakes *et al.* developed a continuous tri-layered implant using suspended layer additive manufacturing.[115] By controlling the bio-ink composition, the authors could form chemical and cellular gradients throughout the printed construct. The first epidermis layer was pectin mixed with collagen (2 : 1) gel and contained 2 × 106 keratinocytes. The papillary dermis was prepared from pectin–collagen (2 : 1) gel and contained 3 × 106 dermal fibroblasts, while the reticular dermis contained 1.5 × 106 dermal fibroblasts. The last layer was comprised of pectin–collagen gel (1 : 1) and contained adipose-derived stem cells (5 × 105 cells). As a suspension medium, agarose gel was used. Low-viscosity bio-inks exerted minimal stress on the cells during processing. The *ex vivo* study on human skin showed great integration of the construct in simulated skin wounds. Moreover, the cellular components played a crucial role in the scaffold with observable mobilization of adipose tissue in the construct, making it a great candidate for full-thickness wound healing.

3.2 Chemical signal gradients

Chemical signal gradients enable the formation of continuous concentration gradients of signalling molecules such as growth factors or cell adhesion peptides.[116] Molecules can be immobilized at the biomaterial surface or have a soluble form

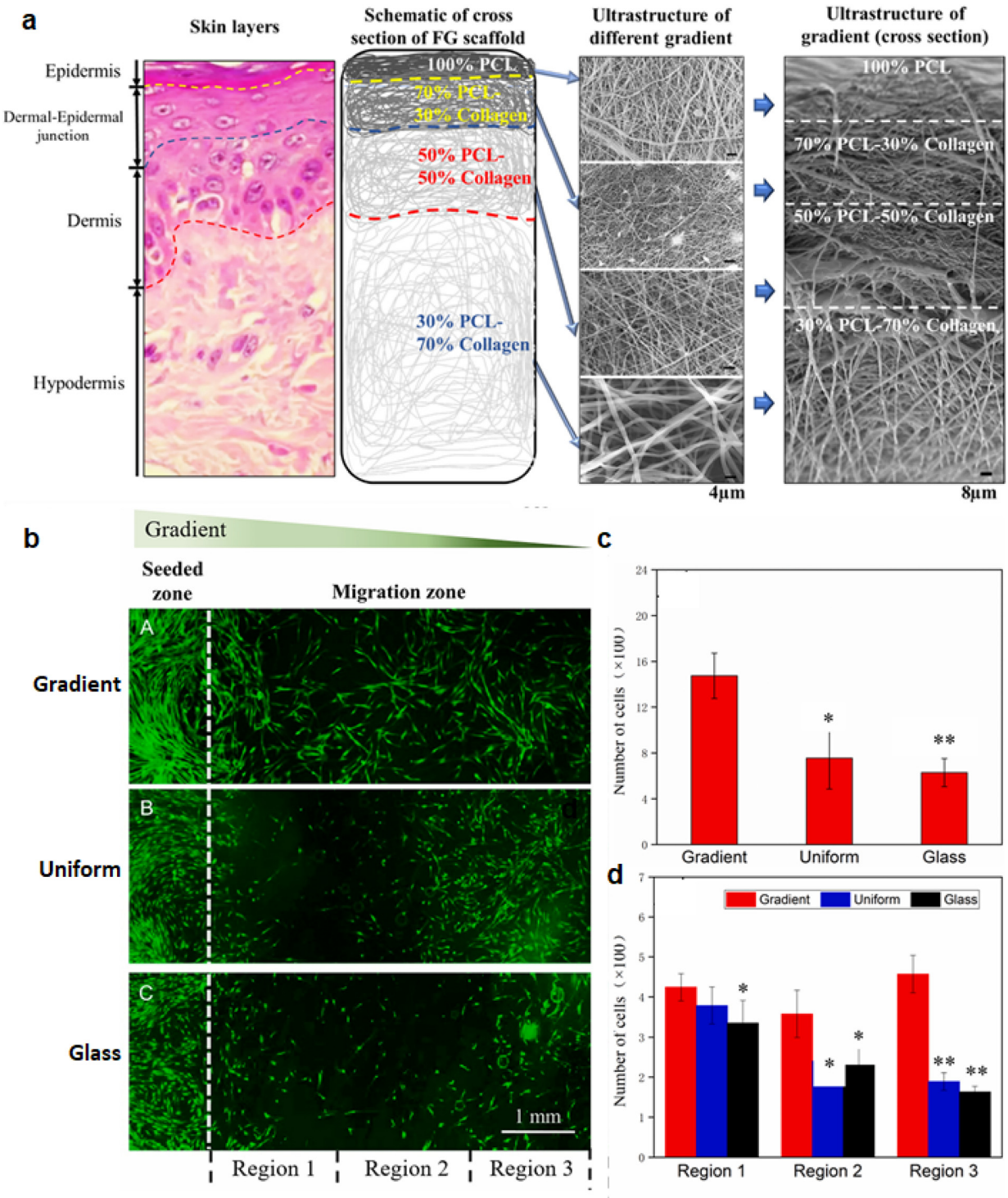

Fig. 6 Schematic representation of different gradients of functionally graded scaffolds: (a) Hematoxylin–Eosin (H&E)-stained skin sections and representative SEM images of each layer with top views and transverse sections.[113] (b) Fluorescence micrographs showing the migration of human skin fibroblasts from the seeded zone on the glass slides covered by a gradient and uniform layer of fibronectin and blank glass slides after 3 days of culture. The actin cytoskeleton of cells was stained by phalloidin (green). Reproduced with permission. Copyright 2022, Elsevier. (c) Number of human skin fibroblasts in the migration zones on the glass slides coated by a graded or uniform layer of fibronectin and blank glass slide after 3 days of incubation. (d) Number of human skin fibroblasts in the different regions of the migration zone. *$p < 0.05$ and **$p < 0.01$ compared to the glass slide coated by graded fibronectin. Reproduced with permission.[118] Copyright 2022, Elsevier.

that is released in a predefined manner. Spatial and temporal concentration difference is especially required in designing a biomimetic wound healing approach.

He *et al.* designed a precise gold nanoarray with a nanospacing gradient of adhesion peptide arginine–glycine–aspartate (RGD).[117] The authors employed block copolymer micelle nanolithography to prepare gold nanoarrays with a nanospacing gradient. Endothelial cells (ECs) and smooth muscle cells (SMCs) were used to analyze the cell behavior. The authors found that SMCs exhibited significant orientation and directed migration along the nanospacing gradient. In the case of ECs, weak spontaneous anisotropic migration was observed. The observed response of both cell types to the peptide nanospacing gradient provides new ideas for designing cell-instructive nanomaterials that can be used in wound healing.

Zhou *et al.* developed a method to generate linear and circular gradients of proteins or drug-releasing polymeric microparticles on planar surfaces by controlling the electrostatic field distribution during electrohydrodynamic jet printing.[118] Circular gradients were formed using cylindrical magnets and changing their diameter from 4 to 8 and 12 mm. With the use of fibronectin as a model protein, they generated a circular gradient of fibronectin (Fig. 6b). They investigated its effect on accelerating fibroblast migration mimicking wound closure processes and found that more cells were present in all the regions of the gradient of fibronectin (Fig. 6c and d). Another example included the preparation of linear gradients using bar magnets and forming unidirectional and bidirectional patterns of laminin, respectively. The generated gradations significantly promoted the migration of human fibroblast cells from the peripheral to the central area. Moreover, the unidirectional and bidirectional gradients of laminin enhanced the proliferation and migration of cells with an increase in laminin content.

Amagat *et al.* developed programmed dual-electrospun 3D scaffolds with customizable biomolecule gradients.[119] Initially, different customized fluorescent (rhodamine and fluorescein) gradients and patterns were obtained in PCL fibers. Further, using a coagulation bath collector filled with ethanol, wet electrospun PCL fibers were fabricated with a tailored gradient of PCL functionalized with benzophenone-4-isothiocyanate (BPITC). BPITC is a heterobifunctional crosslinker capable of inserting primary amine-binding sites in PCL. Using horseradish peroxidase (HRP) antibody as the target molecule, a colorimetric assay was used to quantify the obtained PCL-HRP gradient. According to the authors, any desired primary amine-containing molecule can be introduced in the scaffold in a gradient manner by post-conjugation of molecules with the dressing.

Motealleh *et al.* prepared step-gradient nanocomposite (NC) scaffolds by 3D printing different layers of NC hydrogels containing increasing concentrations (from bottom to top) of bifunctional nanomaterials (NMs).[120] The bifunctional NMs were synthesized by functionalizing periodic mesoporous organosilica (PMO) with dexamethasone (Dex) and poly-D-lysine (PDL). The synthesized bifunctional NMs were stimuli (pH)-responsive and enabled the sustained release of dexamethasone. The authors demonstrated that bifunctional NMs used in vertically increasing concentrations influenced the migration of fibroblasts in the XZ plane toward higher concentrations of PMO-Dex-PDL.

3.3 Inorganic/organic composites for better wound healing management

The combination of inorganic bio-actives and organic matrices exhibits excellent potential for improving skin regeneration. Accordingly, the organic–inorganic combination approach has become a promising opportunity in cutaneous wound healing due to its antibacterial and mechanical properties, biocompatibility, and biodegradability.[120] Also, it has attracted enormous interest because of its hemostatic and angiogenetic properties and immunoregulation ability.[121] Based on the material complexity, they it be divided into simple polymeric fibrous/hydrogel networks loaded with inorganic micro- and nanoparticles, inorganic/organic composite biomaterials or advanced inorganic particles based on living cellular systems. Given that bacterial infections are the most challenging factors in wound healing, introducing antibacterial agents in some polymeric networks can be greatly beneficial. According to previous research, some metal nanoparticles show the above-mentioned properties.

Gold nanoparticles (AuNPs) are used in many biomedical applications as an inorganic filler due to their intrinsic antibacterial and antioxidant properties, which help wound healing by regulating inflammatory processes and hemostasis. Moreover, they are known for their biocompatibility and angiogenic function.[122] AuNP composites are not only used in the fields of antibiotics and gene delivery but also in laser-activated wound healing, which uses their photo-thermal properties.[123] In one report, Huang *et al.* demonstrated that plasmonic gold nanorods combined with elastin-like polypeptides could be used in ruptured intestinal tissue. The photo-thermal properties of AuNPs contributed to the generation of heat (light-heat conversion), significantly enhanced tissue healing and demonstrated antibacterial properties.[124] The adhesion properties of skin patches play a crucial role in their useability.[123] Sun *et al.* investigated the adhesive properties of a chitosan-based platform combined with AuNPs. They demonstrated that the anisotropy and concentration of Au in the chitosan matrix dictate the adhesive strength of the nanoplatform. The nanocomposite with Au showed much higher tissue adhesion compared with chitosan alone. The adhesion strength of pure chitosan was around 260 kPa for all reaction times, while all the nanocomposites with AuNPs exhibited significantly increased adhesion strength over time. Interestingly, the middle concentrated composite showed an adhesion strength of 927 kPa (2.5-times that of the reference chitosan) after 3 days. The lowest and the highest concentrated samples showed a similar adhesion strength around 520 kPa.[125] One major challenge in novel medicine and wound healing is the increasing rate of multi-drug resistant (MDR) bacteria. Thus, Yang *et al.* developed a PCL/gelatin scaffold doped with (6-aminope-

nicillanic acid)-coated AuNPs (Fig. 7), which exhibited remarkable activity upon exposure to MDR bacteria.[126] The *in vitro* and *in vivo* resulted proved that the matrix can treat MDR bacteria wound infections. It showed an almost 100% bacteriostatic rate *in vitro* against *E. coli* and MDR *E. coli*. It was also highly efficient in *E. coli*, MDR *E. coli*, *P. aeruginosa* and MDR *P. aeruginosa* growth inhibition compared to gauze and PCL/gelatin as a reference.

Silver nanoparticles (AgNPs) are widely used in biomedical applications due to their anti-microbial activity. AgNP/organic matrices are the most viable in current market-approved medical devices, hydrogels, dressings and ointments.[41] AgNPs exhibit surface plasmon resonance, and thus also used in biosensing and laser-activated applications. In the report by Haidari *et al.*, they showed that a thermo-responsive composite of AgNP and Pluronic F-127 hydrogel had antibacterial effects in conjunction with wound healing promotion *in vitro* and in a wound-infected mouse model.[127] In a recent report by Makvandi *et al.*, they prepared an injectable hydrogel based on hyaluronic acid, corn silk extract and AgNPs. The nanocomposite possessed good rheological properties and gelation time close to the body temperature. Furthermore, the *in vitro* study exhibited antibacterial activity and faster wound closure and repair.[128] However, one of the main drawbacks of AgNPs is their capability to produce ROS, which can be used as an antibacterial additive but also cause cytotoxicity and DNA damage. In the report by Rigo *et al.*, they noted that ROS production is mostly size- and concentration-dependent.[129] It can lead to mitochondrial dysfunction and cellular shrinkage in different cell lines.[130] Recently, Ninan *et al.* presented an innovative plasma 3D printing approach for the preparation of PCL scaffolds immobilized with AgNPs. The scaffolds showed inhibition of bacteria associated with wound infections, good biocompatibility, and reduced pro-inflammatory cytokines.[131]

Composites containing CuNPs are applied in wound repair considering not only their antibacterial properties due to their photo-thermal performance but also their ability to promote the vascularisation process through hypoxia, upregulation of vascular endothelial growth factor (VEGF) and upregulation of the integrin expression. In the report by Gopal *et al.*, they applied a chitosan-based copper nanocomposite topically in a wound rat model to evaluate its healing properties. The composite enhanced cutaneous wound healing by regulating different cells, cytokines and growth factors. The chitosan-based copper nanocomposite also showed higher fibroblast proliferation and re-epithelialization in the treated rats compared to the reference chitosan and acetic acid.[132] Recently, a photo-thermal active CuNP composite hydrogel was prepared in the study by Tao *et al.* The composite was made using methacrylate-modified gelatin (GelMA) and *N,N*-bis(acryloyl) cystamine (BACA)-chelated CuNPs *via* radical polymerization with a photoinitiator. The CuNPs could convert NIR laser light (808 nm wavelength) into heat *via* surface plasmon resonance. The NIR irradiation and release of copper ions led to the tremendous antibacterial activity of the composite. The *in vitro* wound-healing process using the *S. aureus* model was accelerated, showing the great antibacterial activity of the composite.[133] Sen *et al.* investigated

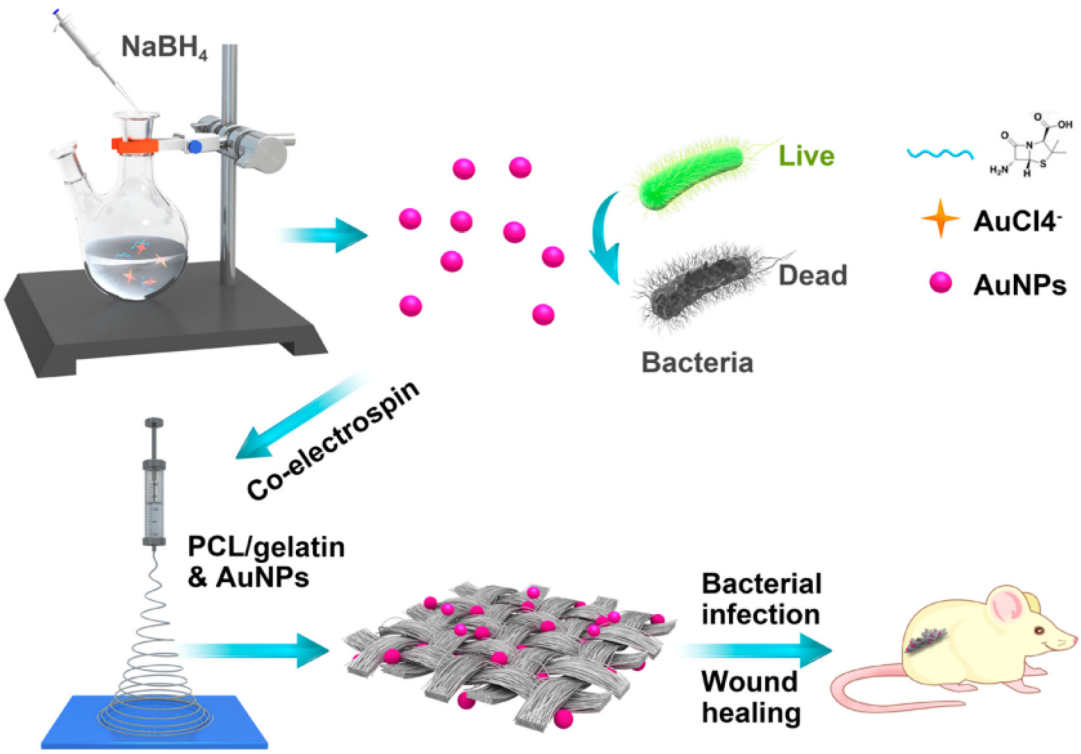

Fig. 7 Scheme of preparation and application of matrix in wound healing. Reproduced with permission.[126] Copyright 2017, the American Chemical Society.

the induction of hypoxia-inducible factor-dependent pathways by copper ions. They were found to be effective in wound healing applications as an improving wound closure agent with a higher cell density in the granulation layer of tissue.[134]

Zinc oxide nanoparticles (ZnONPs) have been reported in many wound healing patches due to the significant contribution of zinc to growth and development in human body processes and its role in wound healing.[123] During wound healing, zinc levels can increase by over 20% in the first phase and up to 30% during the proliferation and granulation phases.[123] Augustine *et al.* reported the fabrication of an electrospun polycaprolactone scaffold with incorporated ZnO and tested it *in vivo* using a guinea pig model. The membrane showed enhanced cell adhesion and wound healing without scar formation. The improved wound healing abilities were possibly due to the increased cell migration and proliferation. No sign of inflammation up to 2 wt% of ZnNPs was observed. PCL with 1 wt% ZnNPs showed the best cell migration, proliferation and fibroblast attachment.[135] In a recent study, Zhu *et al.* reported a new route for skin wound closure by developing a zinc-doped bioactive glass/succinyl chitosan/oxidized alginate composite hydrogel. The composite showed excellent antibacterial properties and cell compatibility. Furthermore, macroscopic growth promotion and stimulation of the cells to secret angiogenic factors (CD31 and a-SMA) were observed.[136] Furthermore, Raguvaran *et al.* developed sodium alginate/gum acacia/ZnOP hydrogels and evaluated their wound-healing properties, which exhibited dose-dependent effectiveness and *in vitro* healing effect on fibroblast cells. The cytotoxicity of ZnOPs was reduced due to the sustained release of particles from the hydrogels.[136]

Silicon has been incorporated in many silicon-based biomaterial composites, such as silicate-based glasses and silicon nanoparticles. Silicon in complex inorganic/organic devices enhances angiogenesis and collagen deposition.[137] Wu *et al.* synthesized an effective ROS-scavenging adhesive nanocomposite by immobilizing ceria nanocrystals on the surface of mesoporous SiNPs. The composite was proven to have strong adhesion and ROS-scavenging effect. MSN-ceria closed the wound bed quickly, promoting skin regeneration in the injured area, and thus can find application in cutaneous wound healing.[138] BG composites proved to have antibacterial, anti-inflammatory and hemostatic properties. They are used with polymeric matrices to obtain flexible wound dressings. Silica nanocomposites were developed in a recent report, combining polyvinylpyrrolidone and nano-silica aggregates. The authors prepared wet and freeze-dried dressing materials and tested their wound healing properties in a mouse *in vivo* model. They proved that the materials could release nanosilica, enhancing wound contraction and re-epithelization.[139]

Graphene oxide (GO) is a single-layered carbon-based structure that has recently gained popularity in various biomedical applications.[107] Complex platforms containing GO have been exploited in multiple applications such as drug delivery, imaging, biosensors and composite dressings for wound healing.[123] In one report, Xue *et al.* prepared a hierarchical and porous structure made of GO-chitosan-calcium silicate. The matrix was proven to possess good tensile strength, breathability and water absorption. Moreover, the material showed photothermal properties with antibacterial and antitumor effects. The structure positively affected wound healing in *in vitro* and *in vivo* diabetic mouse models.[140] Recently, Adepu and Ramakrishna *et al.* reported the development of an injectable self-healing hydrogel with perfect thermo-responsive properties and tissue adhesion. The hydrogel consisted of an antibacterial component, *i.e.*, quaternized chitosan, conductive element polydopamine-coated reduced GO, and thermo-responsive component poly(*N*-isopropyl acrylamide) (PNIPAm). Due to its composition, the hydrogel exhibited similar conductivity to human skin tissue, good swelling ratio and photothermal antibacterial properties. Moreover, its antioxidant ability improved wound healing. Testing the full-thickness skin defect model showed faster wound closure and total collagen level. Furthermore, introducing antibacterial doxycycline in the healing platform improved these properties.[141]

3.4 Composites with biologics as a wound healing approach

During skin regeneration, the cascade interactions between different types of cells, growth factors (GFs), and cytokines are determinants for regulating the phases of the healing process. In this frame, the local administration of biologics has been explored to mimic the physiological system and modulate wound closure.[142] However, the poor *in vivo* stability and enzymatic degradation of the bioactive molecules, together with their low absorption through the skin tissue limit the use of this practice.[143] Additional disadvantages are related to the excessive levels of biologics at the target site and their undesirable dispersion. To protect biologics from *in vivo* degradation and to guarantee suitable local concentrations in the long term, recent efforts have been devoted to the design of bioactive composite materials incorporating growth factors.[144]

Growth factors (GFs) and cytokines are biologically active molecules involved in all phases of the wound-healing process by regulating cell metabolic activities, proliferation, migration, and differentiation. Among them, epidermal growth factor (EGF), platelet-derived growth factor (PDGF), transforming growth factor-β (TGF-β), fibroblast growth factor (FGF), and vascular endothelial growth factor (VEGF) play critical roles in wound healing. Hence, promising results show that the delivery of biological signaling molecules at the wound site significantly accelerates skin regeneration. Specifically, EGFs and VEGFs are involved in the angiogenesis process and granulation tissue formation.[145] Accordingly, Denkbas *et al.* proposed an optimized chitosan sponge loaded with EGFs to recapitulate the skin tissue properties, while avoiding electrolyte and water loss from the wound and promoting fibroblast cell growth.[146] The combination of EGFs and FGFs has also been considered to modulate the epithelialization and synthesis of ECM molecules. A multi-layered system composed of electrospun nanofibrous polymer matrices providing a middle layer loaded with EGFs and basic FGFs was designed and produced.[147] Improved epithelialization and angiogenesis in the presence of GFs were reported, together with faster skin remo-

deling and wound closure (Fig. 8a). Furthermore, VEGFs have been incorporated into systems to promote angiogenesis and accelerate wound healing. Mohandas *et al.* fabricated a composite sponge made of chitosan and hyaluronic acid embedded with fibrin nanoparticles loaded with VEGFs, highlighting the formation of capillary-like tubes of seeded endothelial cells.[148]

Alternatively, PDGFs play a crucial role in regulating fibroblast cell migration. Thus, PDGF-BB-loaded chitosan nanoparticles were incorporated in a polycaprolactone electrospun mesh to improve the chemotaxis behaviour of fibroblasts.[149]

Additionally, granulocyte-macrophage colony-stimulating factor (GM-CSF) has been employed in the design of skin patches for wound healing. Specifically, GM-CSF was loaded in chitosan nanoparticles and embedded in a nanocrystalline cellulose hyaluronic acid composite material to promote granulation tissue, facilitate wound closure, and favor the re-epithelization process.[150]

Besides, cell-based therapy provides some important modulatory factors in the wound healing process, including the secretion of cytokines, attenuation of inflammatory reactions, regulation of immunological functions, and promotion of cell recruitment, thus enhancing epithelialization, angiogenesis, and formation of granulation tissue.[151] However, the local delivery of relevant cells often results in a short cell survival time, cell dispersion, and failure to penetrate the wound site. Therefore, researchers have recently designed systems for protecting cell survival and migration during the delivery process, while providing moisture and preventing fluid loss.[152] Revi *et al.* proposed the delivery of differentiated cells (*i.e.*, keratinocytes and fibroblasts) through a chitosan sponge, revealing the potential of the system to promote wound healing and reduce scar tissue formation.[153] In another study, human umbilical vein endothelial cells (HUVECs) were delivered through a poly (L-lactide-*co*-caprolactone) and human fibroblast-derived ECM (hFDM), resulting in faster cell proliferation and higher vascular morphogenesis. A chemoattractant effect on HUVECs and human dermal fibroblasts was also observed *in vitro*, while accelerated wound regeneration and neovascularisation were reported *in vivo*.[154] Additionally, materials loaded with stem cells have demonstrated outstanding potential for cell growth, self-renewal, and differentiation.[142] Human umbilical cord mesenchymal stem cells were loaded in a calcium alginate gel, showing suitable cell proliferation and enhanced VEGF expression, thus leading to faster wound healing and angiogenesis.[155] Moreover, Ha *et al.* proposed a novel skin patch by incorporating human mesenchymal stem cells (MSCs) in an hFDM/polyvinyl alcohol hydrogel.[156] The results evidenced the improved dermal fibroblast migration due to the paracrine factors expressed by MSCs, thus promoting tissue regeneration and wound closure. MSCs were also encapsulated in microneedle arrays made of a shell of poly(lactic-*co*-glycolic) acid and a core of gelatin methacryloyl for the local delivery of cells with minimal invasiveness.[157] Furthermore, adipose-derived stem cells (ASCs) were introduced in a skin patch made of poly(3-hydroxybutyrate-*co*-hydroxyvalerate) (PHBV) for enhancing the skin tissue regeneration and neovascularisation with reduced scarring.[158] Indeed, the presence of ACSs led to a lower level of myofibroblast differentiation, thus preventing the formation of scars.

Besides, it has been proven that exosomes (EXOs) secreted by stem cells can increase the paracrine effect in skin regeneration. EXOs were isolated from ASCs and MSCs and loaded in a composite system containing alginate (Fig. 8b) and methacrylated hyaluronic acid, respectively.[159] The results showed the effective acceleration of collagen deposition, angiogenesis, and wound closure.[160]

Advances in nucleic acid research have enormously increased the potential of gene therapy for wound healing.[103] Specifically, the delivery of ribonucleic acids (RNAs) has been demonstrated to strongly regulate the healing phases by promoting or inhibiting key signaling pathways,[161] thus favoring the formation of improved quality of neo-skin tissue.[162] However, the administration of RNAs at the target site suffers from significant limitations, including nuclease degradation, impermeability of cell membranes, and off-target effects.[163] In this case, incorporating RNAs in composite materials is one of the safest options for maintaining RNA functionalities and guaranteeing their successful and effective delivery.[164] Koh *et al.* loaded messenger RNA (mRNA) in a microneedle patch made of polyvinylpyrrolidone (PVP) and reported the maintained functionality of mRNA for up to 2 weeks with no *in vitro* degradation effect.[165] Furthermore, the incorporation of RNA-loaded silica nanoparticles in a hyaluronic acid microneedle system allowed the transdermal delivery of short interfering RNA (siRNA), evidencing resistance to degradation as well as suitable penetration and diffusion of siRNA through the skin (Fig. 8c).[166] The results indicated that the successful silencing of the target mRNA prevented excessive scar tissue formation. Lan *et al.* introduced a specific siRNA for inhibiting the expression of matrix metalloproteinase 9 (MMP-9), which could prevent wound healing.[167] Specifically, siRNA was complexed with Gly-TETA and loaded in a Pluronic F-127 and methylcellulose hydrogel, showing sustainable siRNA release over time and significant knockdown of MMP-9. Effective improvements in wound closure were also reported. Similarly, siRNA was delivered to silence interferon regulatory factor 5 (irf5) for tuning macrophage polarisation, thus reducing the inflammatory response at the wound site. siRNA remained stable and protected, while embedded in selenium-based layer-by-layer nanocomplexes with an additional layer of polyethyleneimine.[168] The appropriate release of siRNA led to successful reprogramming toward pro-healing M2 macrophages, reducing inflammation and promoting the healing process.

3.5. Smart multi-responsive skin patches for drug delivery

The popularity and progress of developing smart materials are increasing annually.[126] These materials can intelligently respond to external or internal chemical, physical or biological stimuli. Considering wound healing and the type of helpful stimulus, the materials can be divided into groups, including pH-, light-, thermo-, electromagnetic- and multi-responsive platforms.

There are two primary methods to control drug release from biomaterial matrices. The first is stimuli-activated nanocarriers (*e.g.*, nanoparticles, nanofibers, hydrogels, and nanoemulsions), which increase/decrease the drug release in

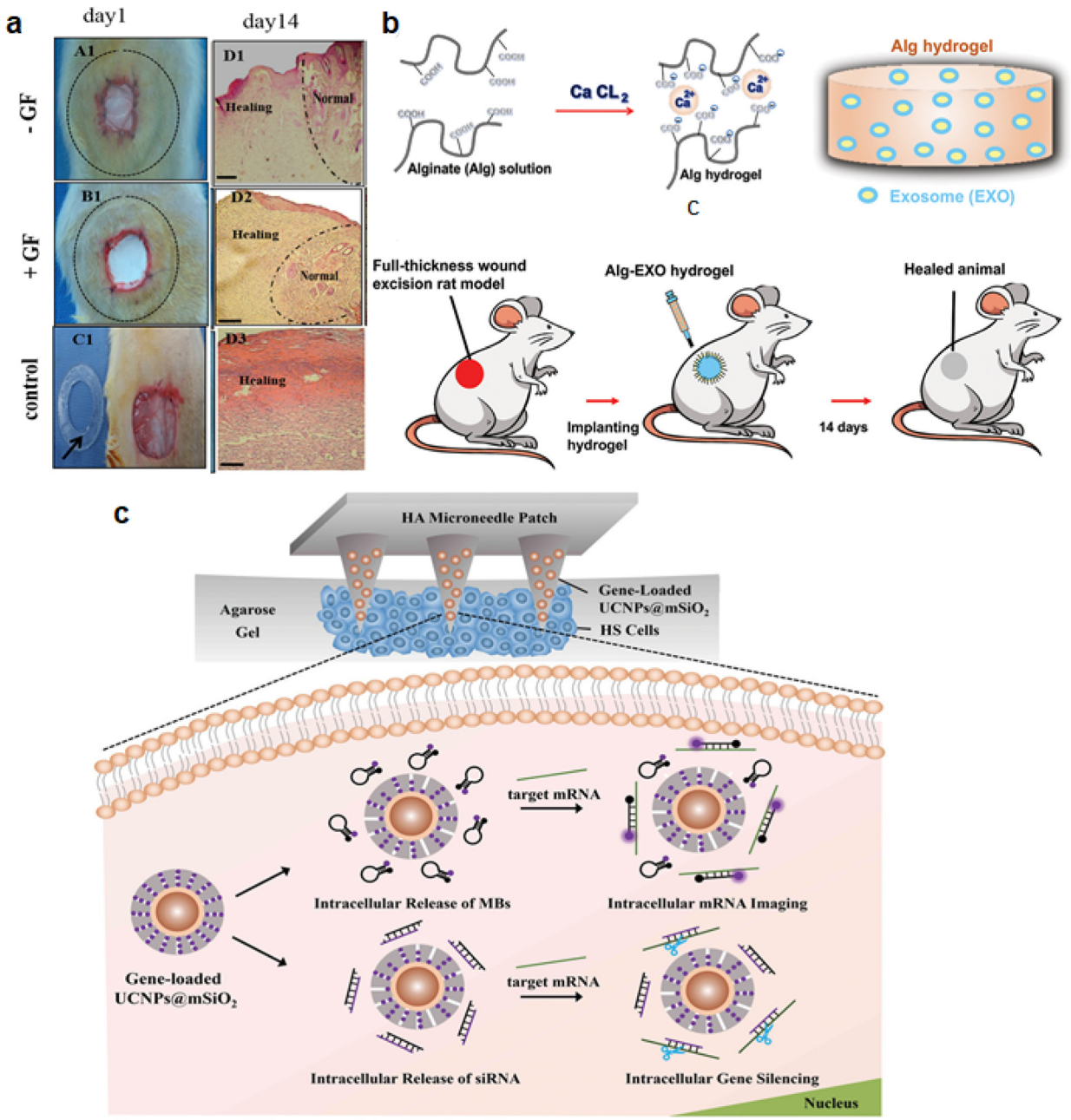

Fig. 8 Biologic approaches for wound healing. (a) *In vivo* investigation of wound healing up to day 14 for wound dressings with and without embedded EGFs and FGFs. Reproduced with permission.[147] Copyright 2018, Wiley Periodicals, Inc. (b) Schematic representation of ASC exosomes incorporated in an alginate hydrogel for healing full-thickness skin defects in a rat model.[160] Copyright 2019, Wiley Periodicals, Inc. (c) Representative illustration of hyaluronic acid-based microneedles incorporating silica particles loaded with siRNAs for reducing inflammation during wound healing. Reproduced with permission.[166] Copyright 2019, WILEY–VCH.

response to specific stimuli. The second is polymers with a charged surface targeted to particular regions or cells, which can be internalized by them.[141] The change in their chain structure triggers the release of the drug. It responds to the stimulation in a controlled cascade-like manner, giving material functionalities such as on/off switching of active substance delivery. The crucial property that allows this type of material to be achieved is the reversible change in structure. Poly-(*N*-isopropyl acrylamide) (PNIPAM) is an example of a thermo-responsive hydrogel with a lower critical solution temperature (LCST) of around 32 °C. Exceeding the LCST, PNIPAM reversibly changes from a hydrophobic to hydrophilic state, increasing the drug release.[169] In the study by Blacklow *et al.*, PNIPAM was combined with other functional materials to develop active adhesive wound dressings.[170] Besides PNIPAM, the platform consisted of alginate, AgNPs, chitosan and carbodiimide. Because the platform was double-layered, it proved to adhere firmly to the skin and actively contract wounds in

response to the body temperature. The bottom chitosan-carbodiimide layer ensured tissue adhesion, while the upper PNIPAM-alginate network with AgNPs exhibited thermo-sensitive and antibacterial activity. *In vitro* and *in vivo* mouse studies showed its supporting influence on wound healing by significantly improving wound closure after 7 days compared to the control groups. It also helped granulation tissue formation and re-epithelization with no severe immune response and good biocompatibility. The detection of pathogenic infections and on-demand drug delivery at the wound site are crucial advantages in advanced patient care. In a recent study, Mirani *et al.* developed GelDerm, which is an advanced multifunctional dressing, enabling the colorimetric measurement of pH, which varies in infections, and release of antibiotics.[171] The patch was built using an alginate fiber-based pH sensor loaded with drug-eluting scaffolds. The 3D printing method was used to fabricate alginate-loaded resin beads doped with pH-responsive dye and gentamicin-loaded alginate scaffolds. Measuring the pH is an excellent opportunity to control wound condition. The *in vitro* and *ex vivo* tests showed the ability to detect bacterial infections with less than ±5% error compared to the commercially available pH strips. The patch on the infected wound site changed color over time, indicating the sensation of bacteria. Alternatively, when the drug-loaded patch was placed on the wound site, the color change was significantly reduced, showing the possibility of sustained antibiotic delivery. Injectable polymeric hydrogels with adhesive properties can attach and bond damaged tissues, which is crucial in stopping the bleeding process and fluid leakage. Liang *et al.* developed an adhesive hydrogel based on hyaluronic acid-*graft*-dopamine and reduced GO as a skin patch.[172] The hydrogel not only showed highly similar properties to human skin, but also polydopamine endowed it with antioxidant activity, tissue adhesiveness, hemostatic ability, self-healing ability, conductivity, and NIR photothermal activity. The platform showed sustained antibiotic delivery (doxycycline) *in vivo* and antioxidant properties with a hemostatic effect in the free radical scavenging test and mouse liver injury model. It also showed a better healing effect *in vivo* than the commercially available Tegaderm film (Table 1).[173–179] Several multiresponsive composite hydrogels have been utilized as matrix for the drug delivery systems.[180–183] An interesting pH/redox-responsive 5-layered system of thiolated chitosan and thiolated chondroitin sulfate was recently fabricated by Esmaeilzadeh *et al.*[182] This platform was crosslinked by alkaline pH or chloramine-T, leading to a change in mechanical and surface properties and also cell adhesion and spreading. Alternatively, reducing the disulfide bonds reversed the cross-linking and lowered the cell adhesion. The reduction also induced the release of bioactive factors from the platform. The authors considered that this material is beneficial for future wound healing applications (Table 1).

Table 1 Examples of smart stimuli-responsive composites used in drug delivery[169]

Type of stimulus	Example of material	Application	Stimuli-responsive agent	Role of stimuli	Ref.
Light-responsive	Hydrogel composite made of catechol-functionalized chitosan	Cancer treatment, antibacterial	MnO_2 nanosheets	NIR light triggered the release of anticancer doxorubicin and degraded internal hydrogen peroxide into oxygen, resulting in reduction of hypoxic tumor microenvironment and cancer cell elimination	173
	PNIPAM hydrogel coated with PDA-NPs	Wound healing	PDA	NIR laser irradiation caused pulsatile release of drugs and triggered 1 min quick healing after unfavorable damage	174
	Bioadhesive hydrogel made of dodecyl-modified chitosan and WS_2 nanosheets	Wound healing	WS_2 nanosheets	Under NIR laser irradiation, nanosheets generate heat and trigger antibiotic drug release to the wound site	175
	PNIPAM hydrogel coated with polydopamine nanoparticles	Wound healing	Polydopamine nanoparticles	NIR laser irradiation allows release of the drug from the matrix in a pulsatile manner and fast healing after tissue damage	174
Thermo-responsive	Pluronic® F127 and hydroxypropyl methylcellulose are used in burned wound infections	Wound healing, infections	Pluronic® F127	Increasing gel stiffness by exceeding the temperature of 32 °C from 4 °C. Platform showed suitable antibacterial therapy and anti-inflammatory activity	176
	Electrospun PMMA fibers attached to the flexible PET, covered with cross-linked PNIPAAm hydrogel sheets	Transdermal drug delivery	PNIPAAm	Heating of composite resulted in an increase in model drug (methylene blue) release ratio	177
	Crosslinked P(NIPAAm-*co*-NIPMAAm) containing AuNR hydrogel encapsulated between two nanofibrous PLLA + rhodamine B layers	Photothermal therapy, Transdermal drug delivery	P(NIPAAm-*co*-NIPMAAm)	Platform showed on-demand drug model (rhodamine B) penetration in pig tissue. Moreover, platform demonstrated efficiency in the rapid and controlled release of molecules	178
	Self-healing hybrid supramolecular hydrogel made of GO nanosheets and quadruple hydrogen bonding ureidopyrimidinone moieties to PNIPAm	Local cancer treatment, transdermal drug delivery	PNIPAm	The bioadhesive proved to be a good candidate for local drug delivery with rapid self-healing behavior and good adhesion to biological tissues. The doxorubicin release profiles revealed the dual thermo- and pH-responsive properties of the hydrogel	179

Table 1 *(Contd.)*

Type of stimulus	Example of material	Application	Stimuli-responsive agent	Role of stimuli	Ref.
Multi-responsive	Bioadhesive alginate-boronic acid conjugate hydrogels	Drug delivery	pH and glucose/boronic acid-diol complexation	Hydrogel showed pressure-sensitive bioadhesive to biological tissues, self-healing ability and multi-responsiveness	180
	Bioadhesive dopamine-functionalized 4-armed PEG and phenylboronic acid	Drug delivery in tissue engineering	pH, glucose, and dopamine triple-responsive/dopamine and modified PEG	Good adhesiveness to biological tissues and the disintegration rate of the hydrogel increased by decreasing the pH from 9 to 3	181
	Multilayered system made of thiolated chitosan and thiolated chondroitin sulfate	Wound healing, tissue engineering	pH and redox/amino groups, carboxyl and sulfate groups	Drug delivery system showed controlled release of bioactive molecules, crosslinking in alkaline pH or reduction of disulfide bonds changed mechanical and surface properties and cell function	182
	Composite hydrogels composed of PAA, oligo(ethylene glycol) methacrylate, 2-(2-methoxyethoxy) ethyl methacrylate, chitosan	Drug delivery, cancer treatment	pH and thermal/PAA (pH-sensitive) and oligo(ethylene glycol) methacrylate and 2(2-methoxyethoxy) ethyl methacrylate (thermal sensitive)	The drug release was significantly accelerated in a neutral environment in comparison with acidic pH. *In vitro*, hydrogel loaded with 5-fluorouracil had lower cell growth inhibition efficiency for normal cells and higher for cancer cells than the pure 5-fluorouracil reference	183
	Hybrid hydrogel made of lignin/poly (ionic liquids)/3-butyl-1-isopropyl-1*H*-imidazol-3-ium bromide/ 1-vinylimidazole and bromobutane	Drug delivery, cancer treatment	pH and thermo-responsive	Drug release occurred at intracellular acidic pH, resulting in the death of malignant cancer cells	184
	Multilayered platform developed on thiolated chitosan and thiolated chondroitin sulfate	Drug delivery	pH and redox-responsive amino, carboxyl and sulfate groups	Alkaline pH triggered cross-linking, and the reduction of disulfide bonds changed the mechanical and surface properties, tuned cell contact and control of release kinetics	182
pH-responsive	Collagen and PEG	Diabetic wound healing	Collagen	Collagen was found to be effective in drug release rate in diabetic wound repair	185
	Injectable dopamine-conjugated HA/ mesoporous silica	Tumor treatment, drug delivery	Dopamine	Bioadhesive showed high therapeutic efficiency against tumor, simultaneously avoiding damage to healthy organs. The composite showed faster release rate at 5.0 pH than 7.4	186
	Bioadhesive hydrogel PAA and PAAm	Drug delivery	PAA and PAAm	Platform showed ability to release lipophilic and hydrophilic drugs based on the environment pH. In alkaline or acid conditions, the bioadhesive can conduct programmable and bidirectional bending by shrinking anionic and cationic networks and asymmetric swelling	187
	Membrane made of chitosan and pectin	Drug delivery, tissue regeneration	Chitosan	Platform exhibited on-demand release behavior in a pH-controlled manner	188
	Injectable chitosan-grafted-dihydrocaffeic acid/oxidized pullulan	Drug delivery	Chitosan-*g*-dihydrocaffeic acid	Injectable hydrogel showed good gelation time and pH-dependent equilibrated swelling ratio. Under acidic conditions, hydrogel had larger swelling and pore size, which accelerated the drug release	189
	Hybrid material made of carbon nanotubes and GO/tectomers	Tissue engineering, cancer treatment	Tectomer	Composite showed controlled release from a pH-dependent coating, and can be used as a pH-switchable bioadhesive coating and scaffold for tumor treatment	190
Electromagnetic-responsive	Adhesive hydrogel made of acrylamide and PEG dimethacrylate with GO and gelatin	Wound healing	GO	The application of external electric stimulation was found to modulate the release kinetics of drugs	191
	Injectable, self-healing hydrogel made of phenylboronic acid and *cis*-diol-modified PEG	Drug delivery	Modified PEG	Adhesive hydrogel showed the size-dependent controlled release of protein encapsulated in the network, and also showed the glucose-responsive release of larger proteins	192
	PAA grafted with gum ghatti	Transdermal drug delivery	Gum ghatti	Electric stimulus applied to the skin increased the drug release, which was examined by histopathology	193

Table 1 *(Contd.)*

Type of stimulus	Example of material	Application	Stimuli-responsive agent	Role of stimuli	Ref.
Smart patches in clinical applications	Bioadhesive hemostatic hydrogel – hyaluronic acid-graft-dopamine and reduced graphene oxide	Drug delivery, hemostatic	NIR responsiveness	Hydrogel showed sustained drug release properties and promising potential for full-thickness skin regeneration	172
	Bioadhesive hydrogel made of graphene aerogel/poly(*N*-isopropylacrylamide)/polydopamine nanoparticles	Drug delivery	Thermo- and NIR responsiveness	Correlation between drug release and resistance allowed the drug-release behavior of the bioadhesive hydrogels to be monitored using electrical signals	194
	Multi-responsive bioadhesive – poly (*N*-isopropylacrylamide) terminated with catechol/polypyrrole nanoparticles	Drug delivery	pH, temperature, and NIR light-responsiveness	Bioadhesive with multi-responsive behavior, especially NIR light response, can be beneficial in removable sealant materials and remotely controlled release systems	195

3.6. Multi-functional composites – therapeutics and diagnostics

Emerging composites can be designed to simultaneously provide various functions together with their main characteristic of mechanically supporting the tissue during the repair process. Additional features related to antibacterial, self-healing, and cellular ingrowth abilities have been recently addressed to accelerate wound closure and improve outcomes. Advanced functions have also been targeted, including the capability to respond to external changes in temperature, pH, and light, thus tuning the release of loaded drugs. In this frame, novel multi-functional systems have been demonstrated to prevent infections, while controlling the activation of drug release effectively.[196]

Hydrogels have been widely investigated for producing adhesive systems for wound healing given that their composition, water content, and physicochemical properties are comparable to that of the native ECM. Furthermore, to design materials with multi-functional properties, antimicrobial agents are often introduced and embedded in hydrogel-based adhesives to inhibit undesired infections. Annabi *et al.* conjugated an antibacterial polypeptide (*i.e.*, Tet213) in a hydrogel network composed of polymers derived from the ECM. The results showed its outstanding adhesive characteristics together with good biocompatibility *in vitro* in terms of 2D and 3D cell culture. Finally, *in vivo* degradability, restraint of infections, and enhancement of wound healing were also reported.[197] Effective antimicrobial properties were reported in silver nanoparticles formed *in situ* in a silk fibroin-based bioadhesive hydrogel[198] and triclosan complexed with beta-cyclodextrin and conjugated in methacrylated glycol chitosan hydrogel.[199] Besides, hydrogels containing polysaccharides and peptide dendrimers showed superior adhesiveness compared to commercially available systems, together with antimicrobial and hemostatic properties (Fig. 9a).[200] Strategies for providing hemostatic effects through these composites were also investigated by Zhang *et al.*, where they developed novel hydrogels made of serotonin and chondroitin sulfate. In the proposed system, serotonin acted as a hemostatic factor and crosslinker for the formation of an adhesive hydrogel, while chondroitin sulfate influenced the cell response, thus promoting wound repair.[201] In another study, injectable hydrogels containing gelatin and hyaluronic acid demonstrated potential for homeostasis and full-thickness wound closure.[202]

Besides, mussel or scallop adhesive proteins have inspired several multi-functional systems due to their outstanding performance.[203] Gallic acid-modified chitosan hydrogels,[204] chitosan oligosaccharide combined with polyethylene glycol diglycidyl ether,[205] dopamine-grafted gelatin,[206] and cellulose-based hydrogels[207] are great examples of mussel-inspired constructs with remarkable adhesive properties for effective wound closure. In this frame, Yang *et al.* designed a mussel-inspired injectable adhesive by introducing gallic acid in a collagen/ε-polylysine system (Fig. 9b). The authors reported antibacterial activity *in vitro* and suitable adhesive properties in a wet environment *in vivo*, accelerating wound repair, while avoiding scar tissue formation.[208] In another study, mussel adhesive proteins were employed for the fabrication of the shell of adhesive microneedles with a silk fibroin core, demonstrating superior adhesiveness and wound closure under wet and dynamic conditions.[209] Alternatively, Wang *et al.* developed a scallop-inspired adhesive system by grafting dopamine to a hyaluronic acid hydrogel. The resulting adhesive exhibited a significant hemostatic effect and formation of granulation tissue.[210]

Stimulus-responsive materials have been explored to create systems that can react to external stimuli and environment changes, thus tuning their therapeutic effects. Among them, pH-responsive and thermo-responsive materials have been the most investigated by researchers. Qu *et al.* prepared an injectable chitosan/Pluronic-based hydrogel that is responsive to pH stimuli, evidencing significant effects on the degradation rate and release profile of curcumin. This system showed matching mechanical characteristics with the skin tissue, together with suitable adhesion, hemostatic and biocompatible properties. *In vivo* tests on a full-thickness skin defect model revealed superior collagen deposition, vascularisation, and granulation tissue formation.[211] Alternatively, temperature responsiveness has also been introduced in materials for adhesive applications in wound healing.[104] Hydrogels composed of Pluronic and hydroxypropyl methylcellulose loaded with gold nano-

particles were developed as thermo-responsive adhesives for controlling drug release through temperature stimuli. The proposed system exhibited strong adhesion, biocompatibility, and antimicrobial properties.[176] Besides, chondroitin sulfate-based hydrogels were applied as multi-responsive adhesives to facilitate wound repair.[212]

Furthermore, strategies for loading nucleic acids in composites have been recently evaluated to deliver RNAs, hence regulating the wound healing process. Specifically, miR-223 microRNAs (miRNAs) were incorporated in hyaluronic acid nanoparticles embedded in an adhesive gelatin methacryloyl hydrogel for reprogramming macrophages to anti-inflammatory phenotype (Fig. 9c). This resulted in neo-vascularization, reduced inflammation, and accelerated wound healing.[213]

4. Stretchable sensors for SPs

On-skin flexible patch sensors are widely used in monitoring the vital signs of the human body to determine its health condition.[214–217] For example, face monitoring includes the collection of temperature and electromyography signals, which allows the detection and understanding of the expressions and underlying emotions.[218] The pulse signals gathered at the wrist can be used to monitor the heart rate and health condition of organs.[219] Depending on the usage and working principles, on-skin flexible sensors can be classified into two categories, as follows: (i) electromechanical sensors and (ii) electrochemical sensors.

4.1 Wearable electromechanical sensors

Generally, electromechanical sensors are directly attached to the human skin to monitor physiological signals *via* the change in resistance, capacitance, or conductivity.[220–222] The common electromechanical sensors include temperature sensors, strain sensors, and pressure sensors.

The continuous monitoring of body temperature is significantly meaningful for human health. Song *et al.* designed a flexible and costless temperature sensor by mixing conducting polymer poly(3,4-ethylenedioxythiophene):poly(styrenesulfonate) with polyaniline (PEDOT:PSS/PANI), and the sensor exhibited a temperature coefficient of resistance of −0.803%/°C, detection resolution of 0.1 °C and fast response time of 200 ms (Fig. 10a).[223] A conductive organohydrogel with a honeycomb structure was fabricated by integrating carbon black and carbon nanotubes in a poly(vinyl alcohol)/glycerol gel network (Fig. 10b). The temperature sensors designed from these organohydrogels exhibited a temperature coefficient of resistance of −0.935% $°C^{-1}$ and long-term durability (Fig. 10c).[224]

Strain sensors play a significant role in motion monitoring and the gauge factor (GF) of the sensors are determined by the sensitive materials. Most metal-based sensors possess a GF value in the range of 2 to 5, while the GF of semiconductors is usually higher than 100.[225] In addition, the GF of strain sensors also relies on the sensing mechanism, configuration of sensing materials, *etc*. Zhai *et al.* designed a "point to point" conductive network based on carbon black/polyaniline nanoparticles/thermoplastic polyurethane film (CPUF), which has a low detection limit of 0.03% strain, wide sensitivity range of up to 680% strain and high GF of ~3000, together with fast response/recovery time (<0.1 s) and good durability even after 10 000 stretching/releasing cycles, demonstrating its great potential in wearable strain sensors for human–machine interaction and environmental monitoring (Fig. 10d–f).[226] A freestanding ultrathin strain sensor with high gas permeability was also obtained by covalently grafting nanofibrous PANI on stretchable elastomer nanomesh, which can provide highly accurate and continuous recording of motions, while exerting minimal constraints and maintaining low interference with the body.[227]

Pressure sensors are the most common electromechanical sensors, which transform applied force into an electrical signal output. Lin *et al.* reported the preparation of a breathable and lightweight piezoresistive sensor based on polyvinylpyrrolidone nanofibers coated by polypyrrole (PVP@PPy).[228] Although piezoresistive sensors provide high-pressure sensitivity, multiple external power supplies are needed to maintain continuous monitoring.[229] Piezoelectric sensors can generate a variation in charge under mechanical strain and possess high sensitivity as well as fast response speed, which endow them with great advantage and potential in wearable sensors.[230] Zhong *et al.* demonstrated a sandwiched piezoelectric structure-based flexible patch, which exhibited a high equivalent piezoelectric coefficient of d_{33} at 4050 pC N^{-1} to selectively perform either actuating or sensing function (Fig. 10g).[231] As a sensor, the patch sensor exhibited both a pressure detection limit of 1.84 Pa for sensing resolution and excellent stability of less than 1% variations in 6000 cycles (Fig. 10h).

4.2 Wearable electrochemical sensors

Wearable electrochemical sensors based on transforming chemical signals into electrical signals to detect human health conditions, such as glucose sensors, blood oxygen sensors, and ion sensors, are gaining significant attention and have advanced in the past few years.[232–234] Generally, wearable electrochemical sensors rely on photolithography and printing to fabricate electrodes on flexible substrates (*e.g.*, polydimethylsiloxane (PDMS), polyethylene terephthalate (PET), and cellulose paper), and adopt Bluetooth or near-field communication (NFC) to transfer signals to mobile phones, achieving the real-time monitoring of biomarkers in body fluids (*e.g.*, sweat, saliva, blood, and tear). Javey's group in UC Berkeley is the pioneer in this field and they integrated ion sensors and lactate as well glucose sensors on PDMS, realizing the real-time monitoring of bio-signals for the first time.[235] Afterwards, they adopted the iontophoresis method for periodic sweat extraction combined with *in situ* analysis capability, enabling the continuous and noninvasive monitoring of individuals.[236–240] For instance, they integrated hydrophilic fillers with wearable electrochemical sensors for rapid sweat uptake in the sensing channel towards pH, Cl^-, and levodopa monitoring, and demonstrated patch functionality for dynamic sweat analysis related to routine activities, stress

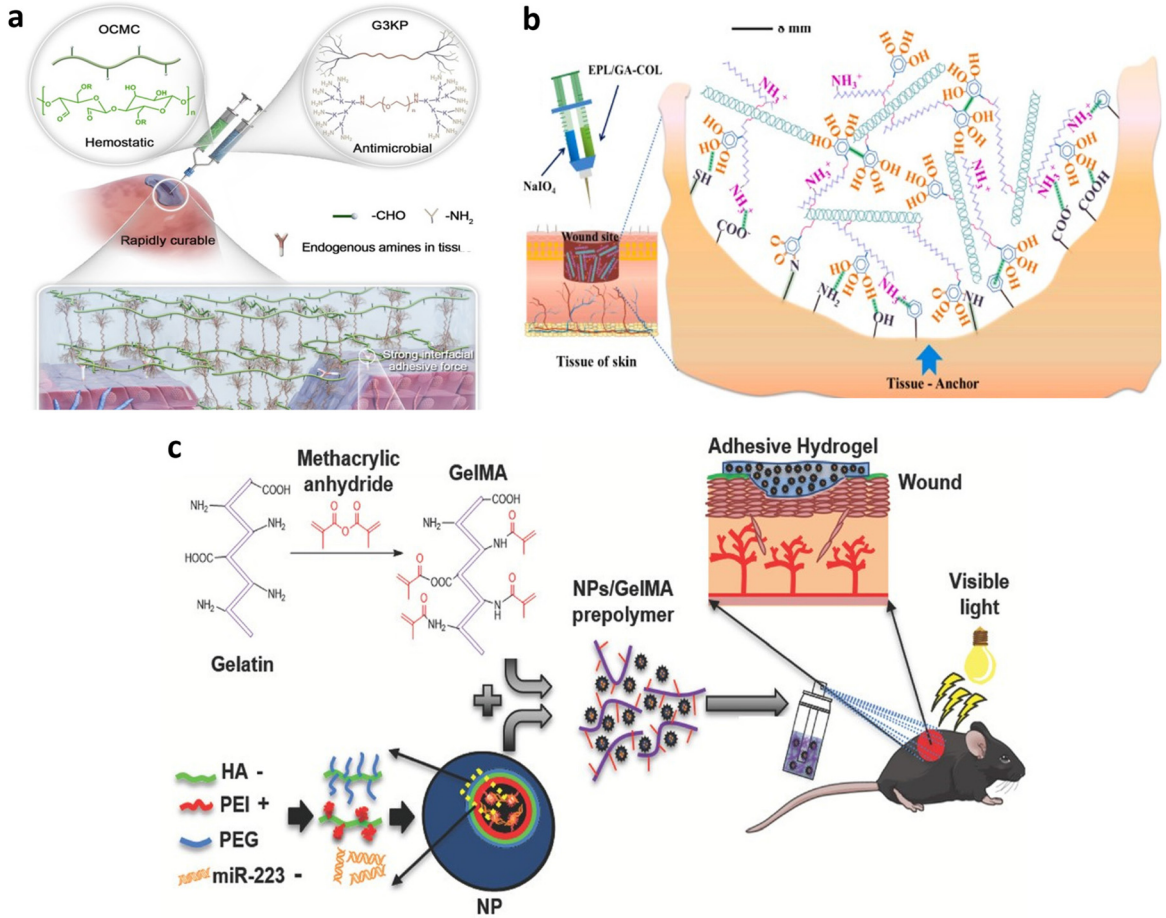

Fig. 9 Multi-functional bio-adhesives for wound healing. (a) Representative illustration of polysaccharide/peptide dendrimer bio-adhesive hydrogel for providing hemostatic and antibacterial functions during wound healing. Reproduced with permission.[200] Copyright 2019, the American Chemical Society. (b) Schematic representation of mussel-inspired collagen/ε-polylysine bio-adhesive injected at the wound site and related molecular mechanisms between hydrogel and tissue surfaces. Reproduced with permission.[208] Copyright 20202, Elsevier B.V. (c) Representative scheme of gelatin methacryloyl hydrogel incorporating hyaluronic acid/miRNA nanoparticles and its application as adhesive in wound healing mouse model. Reproduced with permission.[213] Copyright 2019, WILEY–VCH.

events, hypoglycemia-induced sweating, and Parkinson's disease.[240] Furthermore, other groups also performed thorough research on this topic. Rogers's group fabricated a series of wearable microfluidic devices and integrated them with a biomarker detector, enabling the continuous monitoring of chemicals inside sweat *via* electrochemical and colorimetric sensing, solving the deviation induced by the mixing of fresh and old sweat.[241–245] Given that complex biological matrices affect the sensing process, integration of diverse sensors is necessary to reduce the disturbance of different signs and achieve multi-modal sensing. Wang's group also developed various integrated epidermal tattoo sensors, realizing the real-time detection of glucose, lactate, and other ions.[246–250] For example, towards dynamic and comprehensive health self-monitoring, they presented an integrated, conformal, and stretchable wearable sensor consisting of ultrasonic transducers to monitor blood pressure and the heart rate, and electrochemical sensors to measure the levels of biomarkers (*i.e.*, glucose, lactate, caffeine and alcohol).[250]

5 Self-powered SPs

Recently, electronic skin patches have become more than skin adhesive patches with wound dressings for damaged tissue treatment and prevention of wound infections, but also comprehensive integrated systems with electrostimulation (ES) and health monitoring properties.[251,252] There are two main types of electronic skin patches, *i.e.*, implantable and wearable. Electronic skin patches with multiple functions require the integration of numerous electronic/sensing components on conformal and soft substrates. This is attributed to the growing trend of high-quality requirements of electrostimulation therapies and real-time physiological signals detections,[28,253–255] consequently leading to a higher demand for power supply. Electronic skin patches rely heavily on external power supply units, especially bulky batteries, to meet the power consumption requirements, which severely hampers the portability and feasibility of skin patch systems. This can be attributed to the fact that batteries with limited power capacities need regular replacement or disposal maintenance,

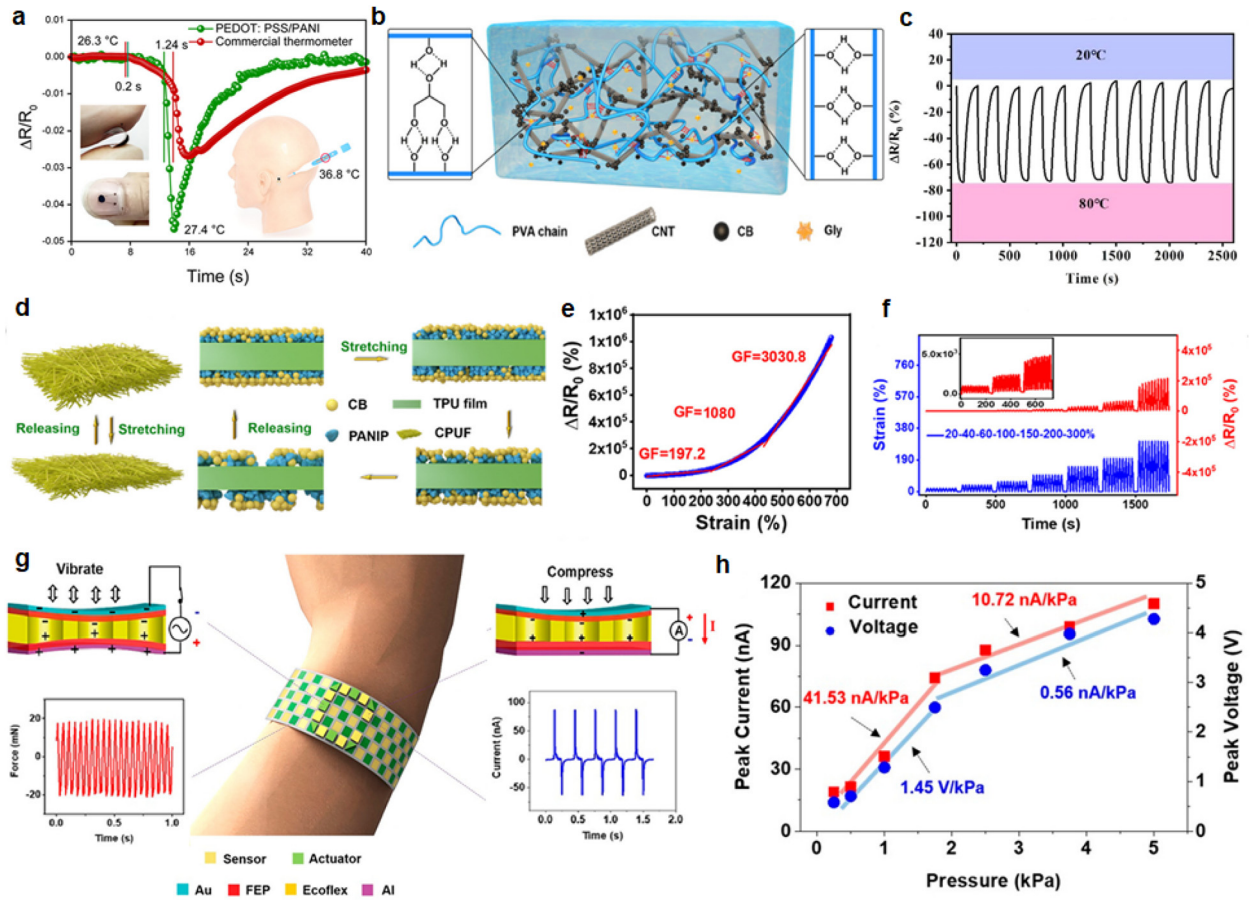

Fig. 10 Summary of wearable electromechanical sensors. (a) Change in the electrical signal of PEDOT:PSS/PANI temperature sensor and commercial thermometer when the heat source approached them. Inset image: optical photograph of the PEDOT:PSS/PANI temperature sensor. Reproduced with permission. Copyright 2022,[223] the American Chemical Society. (b) Synthetic mechanism illustration of organohydrogel sensor. (c) Reproducible temperature-discrimination capacity of the sensor during repetitive approaches of cold (30 °C) and heat (80 °C) sources. Reproduced with permission. Copyright 2020,[224] the American Chemical Society. (d) Mechanism of CPUF composites in a tensile test. (e) $\Delta R/R_0$ of CPUF *vs.* strain. (f) $\Delta R/R_0$ under a step strain of 20–300% in 10 cyclic stretching/releasing tests. Reproduced with permission. Copyright 2022,[226] the American Chemical Society. (g) Schematic diagram depicting the piezoelectric actuator/sensor structures as a wearable, flexible device for mechanical human–machine interfaces for applications such as real-time feedback and long-distance haptics communications and working mechanism of a sensor by generating electrical current outputs due to the mechanical deformation under external forces (bottom) for a prototype device under a stimulating pressure of 2.5 kPa. (h) Peak short-circuit currents and open-circuit voltages under varying applied pressure magnitudes at a constant frequency of 3 Hz. Reproduced with permission. Copyright 2019,[231] the American Chemical Society.

and recycling traditional batteries has proven cumbersome and challenging to achieve comprehensively.[256] Additionally, most batteries probably pose a health hazard to the human body due to possible leakage of the battery electrolyte and the risk of overheating.[257]

Energy harvesting technologies, especially nanogenerators that can scavenge sufficient energy from the surrounding environment, have brought novel design concepts and enabled the fabrication of self-powered electronic skin patches. Energy harvesters have become versatile power sources for electronic devices, considering their wide material section and flexible configurations.[258] These self-powered devices convert solar, heat, and mechanical energy from the ambient environment into electric power with impressive efficiencies by exploiting photovoltaics, thermo/pyroelectricity, and piezo/triboelectricity effects.[259,260] Among these routes, mechanical energy harvesters possess unique advantages over solar energy harvesters and thermal energy harvesters because the human body has limited access to light sources, and the amount of heat provided is much less. Various body motions and physiological movements, including muscle stretching, joint motions, heart beating, and breathing, can be adopted as energy sources for wearable and implantable electronic skin patches.

The past decade has witnessed an impressive surge in self-powered electronic skin patches, which can be divided into two main categories. The first serves as an electrical energy source that provides complementary power for batteries or capacitors to prolong the lifespan of electronic devices. However, the limited size of self-powered electronic patches, especially for implantable usage and the growing energy

volume density mismatch of energy harvesters present tremendous challenges for this type of self-powered system. On the contrary, directly providing biomedical functions such as ES and sensing, and simultaneously generating electricity to power themselves have become a powerful alternative for electronic applications that distinguish them from battery-driven systems.

5.1 Electrostimulations enabled by self-powered e-SPs

Self-powered electronic skin patches that can provide electrostimulations (ES) without integrating additional power supply components can simplify the device structure and have significant potential for therapeutic applications. Luigi Galvani first discovered internal electricity in biological systems in 1794.[261] Since then, significant efforts have been devoted to understanding the effects of bioelectricity on the human body for their wide applications in clinic. Besides, bioelectrical signals have proven to be a vital element that individuals utilize to control various physiological functions. Taking the brain as an example, it relies on electrical signals to process and transmit information and interact with the ambient environment with the assistance of the nervous system, which can ensure the well-coordinated operation of the entire biological system. It is believed that the endogenous electric potential plays a critical role in organ regeneration and tissue healing.[262]

Various clinical purposes have been achieved through ES, such as wound healing, pain relief, nerve stimulation, and organ regeneration.[263] These therapeutic methods enabled by ES conventionally use short-duration and high-frequency electrical pulses produced by bioelectronics powered by batteries or supercapacitors. Alternatively, considering the availability and effectiveness of energy, self-powered electronic skin patches that may generate more effective ES for targeted physiological functions to achieve therapeutic purposes possess distinct and perhaps the most irreplaceable advantages. ES have been proven to be extraordinarily successful in regulating cell proliferation and migration, reducing inflammation and accelerating wound bed closure by modulating the effect of the endogenous electric field of the wound associated with sodium (Na^+) and potassium (K^+) ions.[264,265] For example, a self-powered electronic skin patch based on a piezoelectric nanogenerator (PENG) was reported, which consisted of ZnO NP-modified PVDF /sodium alginate as the functional materials.[266] The fabricated self-powered electronic skin patch relied on a dual-response-model piezoelectric effect, namely, horizontal friction and vertical swelling, to simulate the endogenous bioelectricity effect to accelerate wound healing. It was also proven effective in preventing the scar tissue formation in a rat wound, as shown in Fig. 11a. Besides, the TENG-powered electronic skin patch with a hydrogel embedded between a double-layer PDMS membrane could also enhance the endogenous electric field and promote wound healing.[267]

Self-powered skin patches with ES property are not limited to wound healing but can be used for other functions. As shown in Fig. 11b, a self-powered skin patch based on a triboelectric nanogenerator was successfully employed for muscle and electrical nerve stimulation in a rat, which are critical and desirable for prosthesis control and movement facilitation in the future.[268]

The self-powered skin patch could automatically provide ES that is synchronized to corresponding human motions, and temperature fluctuations or gradients, thus imposing practical therapeutic effects without any rectification and external manipulations.[268] A self-powered skin patch comprised of a flexible and biocompatible TENG was adhered to the surface of the stomach, which could generate biphasic electrical pulses corresponding to stomach peristalsis.[269] As schematically shown in Fig. 11c, the induced electric pulses could stimulate the vagal afferent fibers, and eventually control the desire to eat, thus achieving weight control.

5.2 Health monitoring enabled by self-powered e-SPs

Electronic skin patches can be mounted on the surface of the skin, wound, heart or spine to acquire real-time and high-fidelity essential bio-signals, including human motion, body temperature, blood pressure, electrophysiological signals, and cardiac mapping, for human healthcare and augment the natural sensory capability to enhance rehabilitation.[270] Energy harvesting technology enables electronic skin patches to collect biometric information in a convenient and non-invasive way.

Electrophysiological signals are critical bio-signs of biological activities, mainly including ECG, EMG, and EEG. Long-term and continuous monitoring of these signs can offer vital clinical cues of the health status of an individual *via* attachable bioelectronics.[271] Taking ECG as an example, it can capture electrical signals that can directly reflect the heartbeat process. As shown in Fig. 12a, an electrochemical wearable electronic platform was developed for continuous ECG monitoring based on biocompatible Prussian blue (PB)-coated PET/CNT fiber materials.[272] Besides, the mechanical-electrochemical device exhibited a high power generation of up to 3.8 μW cm^{-2} at low frequencies. Great endeavours have been devoted to developing ECG sensors for cardiac health monitoring. However, the recently commercialized wearable ECG sensors are rigid and require adhesive tape to connect to the human body. Meanwhile, the employment of batteries or capacitors requires them to be periodically replaced or recharged. Alternatively, conformable self-powered electronic skin patches allow for long-term and continuous ECG monitoring, which is conducive to the early diagnosis and treatment of cardiovascular disease.[273]

Biophysical sensors integrated into self-powered electronic skin patches mainly include pressure, strain, temperature, and optical sensors. Self-powered biomechanical sensors that detect pressure or strain variations of human motions, heart beating, pulse, and respiration usually rely on piezoelectric and triboelectric effects. As shown in Fig. 12b, using core–shell structured piezoelectric fibers, a highly conformable electronic skin was demonstrated for tactile sensing and human joint motion monitoring.[274] Temperature is another vital indicator

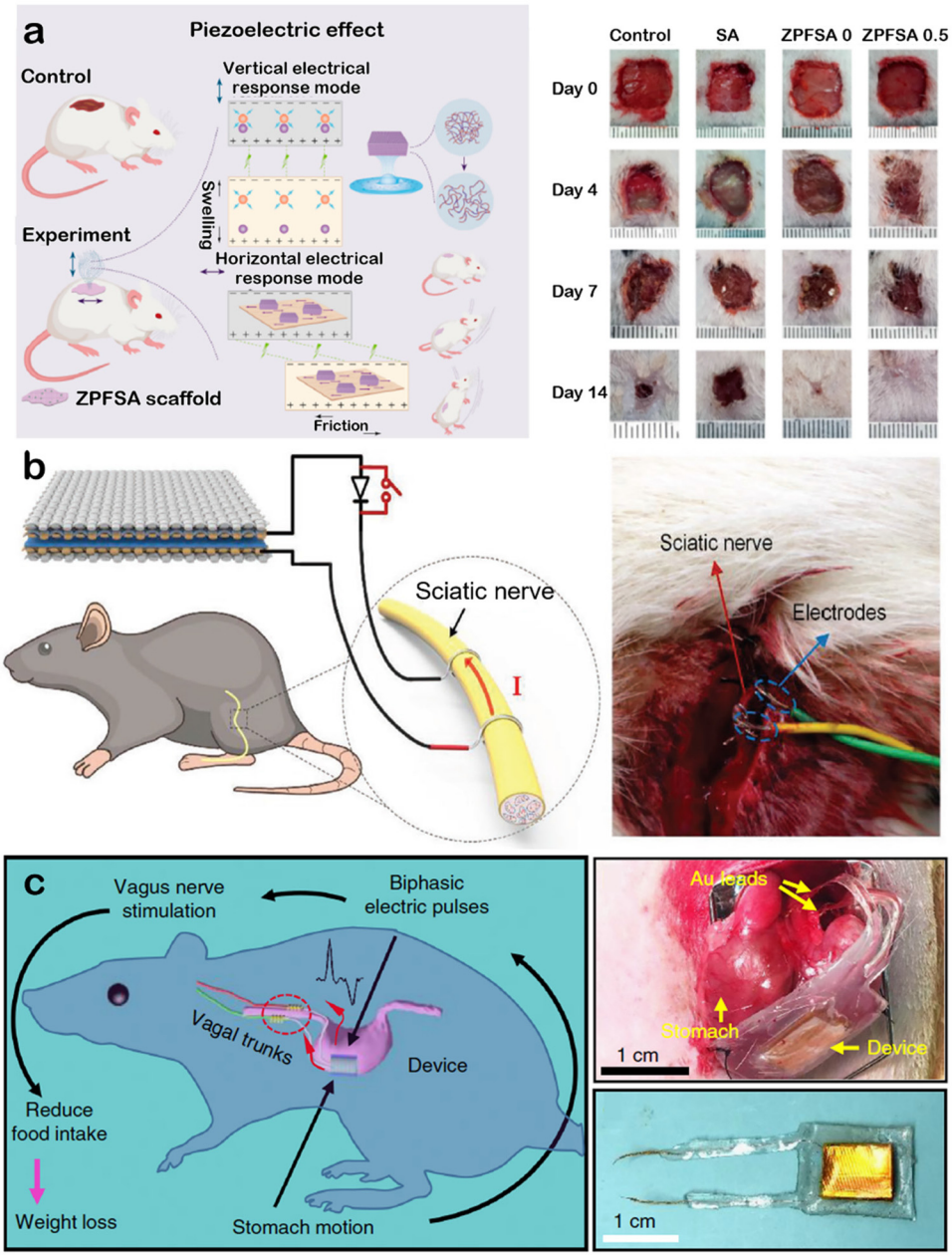

Fig. 11 Electrostimulations enabled by self-powered electronic skin patches. (a) Piezoelectric electronic skin patch for wound healing. Reproduced with permission.[266] Copyright 2022, the American Chemical Society. (b) Triboelectric electronic skin patch for sciatic nerve stimulation. Reproduced with permission.[268] Copyright 2019, Wiley-VCH. (c) Triboelectric electric skin patch for electric stimulation of vagal afferent fibers to control weight. Reproduced with permission.[269] Copyright 2018, Springer Nature.

for the medical diagnosis and evaluation of an individual, especially during the current COVID-19 pandemic. Besides relying on power supply unit-integrated self-powered systems for continuous temperature detection, self-powered electronic skin patches that can harvest heat energy into electricity based on thermoelectric and pyroelectric effects have also attracted wide attention. Thermoelectric materials can generate electrical power from temperature gradients, whereas pyroelectric materials can convert temperature gradients into electrical energy through the Seebeck effect.[275]

5.3 Integrated self-powered e-SPs with multiple functions

The booming demand for improved quality of daily life and comprehensive monitoring of human health conditions has accelerated the rapid evolution of electronic devices that can be attached to biological skin or organs to collect various information and trigger proper treatment measures. Integrated self-powered electronic skin patches that integrate diversified sensors, capacitors, flexible batteries, signal processing modules, and data transmission unit into a complete system

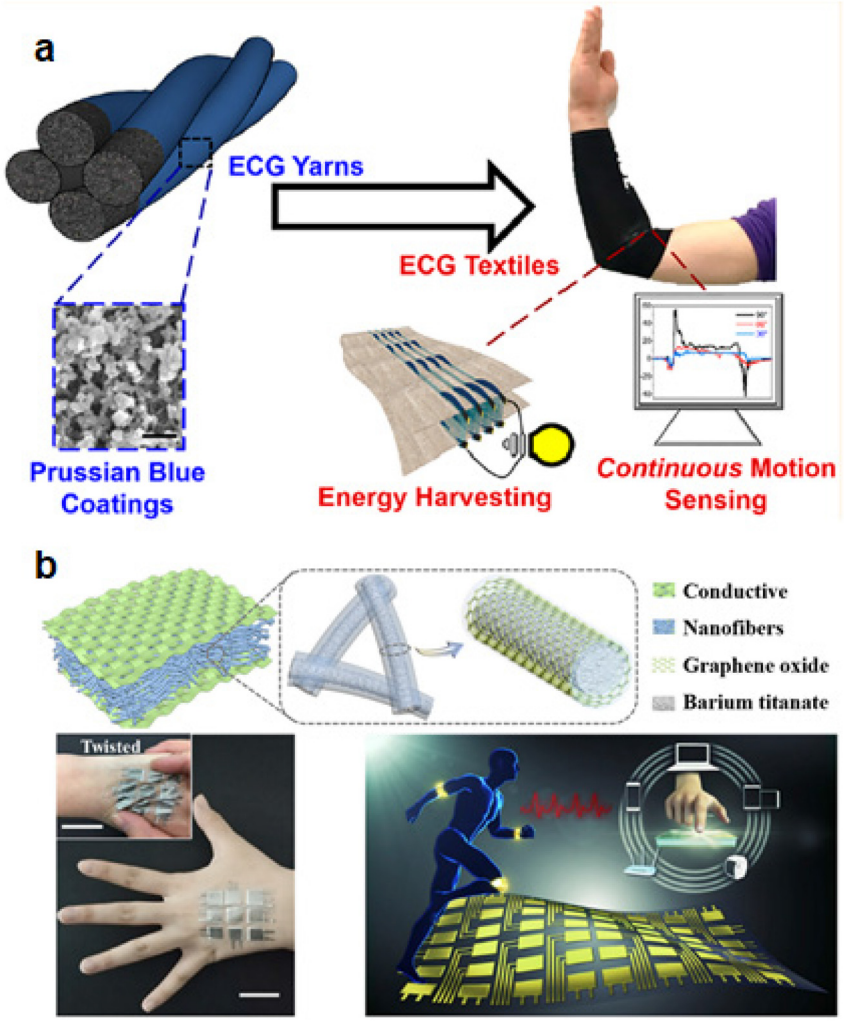

Fig. 12 Self-powered electronic skin patches enable health monitoring. (a) Wearable electronic skin patch for continuous ECG monitoring.[274] Copyright 2020, the American Chemical Society. (b) Core–shell piezoelectric fiber-based electronic skin patch for health monitoring. Copyright 2022, Elsevier.

have become desirable for advances in ubiquitous-healthcare systems. Further development in continuous and real-time monitoring of diversified physical and electrophysiological signals has allowed the employment of biomedical information to trigger or induce appropriate and timely therapy treatments. In addition, a self-powered electronic skin patches that can provide complementary power to batteries or capacitors have also exerted great potential in continuous and long-term implantable bioelectronics. Self-powered electronic skin patches assembled with microneedle patches and thermo-responsive or electro-responsive biomaterials can allow for controllable drug delivery through diagnostic feedback. Therefore, technologies that combine full-fledged diagnostic systems with drug-loaded structures have significant potential for point-of-care and personalized therapy. Integrated self-powered electronic skin patches with multiple functions will be reviewed in this section for their wide applications in health surveillance and disease treatment.

Self-powered electronic skin patches are expected to possess multimode sensing capabilities to truly mimic the nature of biological skin. With the continuous development in recent years, self-powered electronic skin patches integrated with dual or multiple sensing units have been reported for wearable electronic devices. For instance, a dual-mode electronic skin patch was fabricated by vertically assembling pressure-sensing and temperature-sensing units into one fiber-based device (Fig. 13a).[276] The integrated self-powered electronic skin patch obtained precise pressure-temperature sensing capabilities *via* flexible PVDF/ZnO nanofibrous membranes and thermal-resistance carbon nanofibers, respectively. Temperature, pressure, and strain are crucial parameters for wound diagnosis and healing. In another similar study, a temperature and strain electronic skin patch was obtained using a thermoelectric and strain-sensitive material.[277] This self-powered patch could achieve wound monitoring and optimize the conditions for better healing, which are crucial for patients with chronic wounds, especially pressure ulcers. Besides, the coating and printing techniques provide self-powered patches with great potential for large-scale applications.

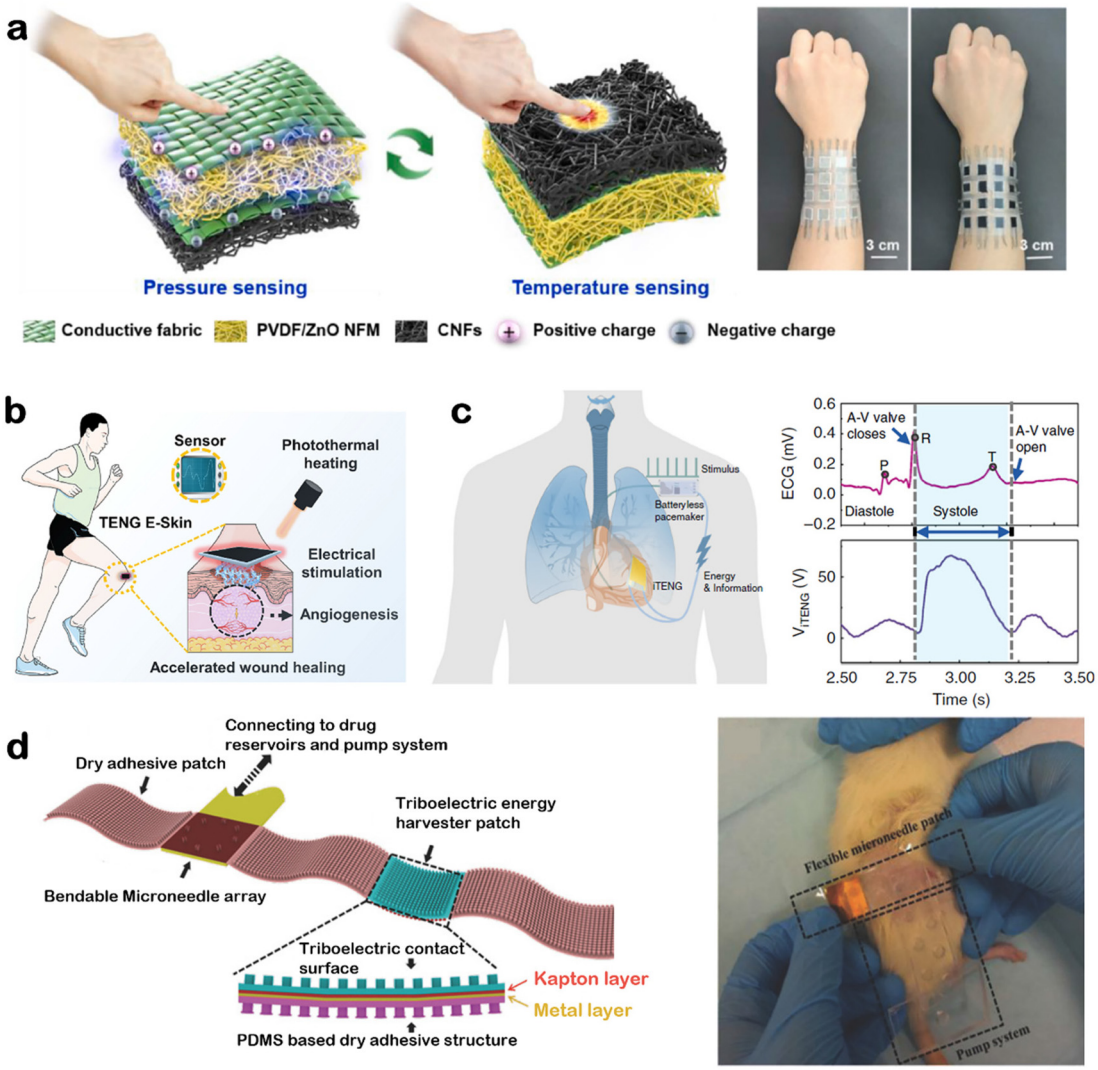

Fig. 13 Integrated self-powered electronic skin patches with multiple functionalities. (a) Dual-mode self-powered electronic skin patch for temperature and pressure detection. Reproduced with permission.[276] Copyright 2021, Elsevier. (b) Triboelectric and photothermal electronic skin patch for wound healing and health monitoring. Reproduced with permission.[278] Copyright 2022, Elsevier. (c) Triboelectric electronic skin patch serving as a symbiotic cardiac pacemaker. Reproduced with permission.[279] Copyright 2019, Springer Nature. (d) Self-powered microneedle patch for controllable drug delivery. Reproduced with permission.[282] Copyright 2016, Wiley-VCH.

Providing appropriate care and support therapy based on idiographic circumstances for chronic wound patients is necessary. Various self-powered electronic skins with integrated sensing functions and combined therapeutical strategies have been developed for integrated, synergistic treatment. As shown in Fig. 13b, a single-electrode triboelectric electronic skin patch was constructed to detect body motions and accelerate wound healing.[278] The employment of conductive and photothermal polypyrrole/Pluronic F127 hydrogels endowed this bioelectronic with remarkable light-to-heat conversion efficiency, which could warm the wound and improve the blood microcirculation. Considering its efficient electrical stimulation and photothermal heating, the self-powered electronic skin patch presents significant potential for wound healing applications, enabling wound closure within less than 9 days. Moreover, the device can function as a biomechanical sensor for health monitoring, such as breathing monitoring and finger motion detection, which can compensate for partial loss of biological sensation.

Compared to battery-driven devices, self-powered implantable electronic skin patches do not require periodic replacement through invasive and complex surgery, which can improve the lives of patients and reduce infection risks. A symbiotic cardiac pacemaker was obtained based on a TENG-powered electronic skin patch.[279] As shown in Fig. 13c, the self-powered device adhered to the surface of the heart and ingested energy from cardiac motion to maintain regular operation. Meanwhile, the heart received ES from the implantable device for regulating cardiac physiological activity. Thus, the self-powered symbiotic pacemaker successfully achieved cardiac pacing. It corrected sinus arrhythmia on a large-animal scale, which may revolutionize clinical cardiopathy

treatments by applying the self-powered pacemaker with a much smaller and simpler design configuration.

Additionally, electronic skin patches can be utilized to achieve feedback-regulated controlled drug delivery, such as collagen, insulin, chitosan, and gelatin. These well-integrated electronic skin patches can monitor the health condition of patients or wounds and provide professional advice or/and timely local treatment, offering alternative targeted therapies and improving health conditions according to individual differences. The integration of health monitoring, signal processing, and interfacing with external computing apparatus is inevitable to require a built-in energy source.[280,281] Consequently, self-powered electronic skin patches have become an unrivalled choice. A self-powered wearable electronic skin patch was constructed as a complete drug delivery system with a feedback control function.[282] As shown in Fig. 13d, the device was compromised of a microneedle patch that can non-invasively release insulin for people with diabetes and a triboelectric energy harvest patch for biomechanical energy conversion, assembled with adhesive patches to ensure that they could be attached to curvilinear skin. The self-powered electronic skin patch assembled with a microfluidic control system could control drug delivery, alert patients and offer guidance when it is time to deliver the appropriate dose of the drug.

5.4 Future challenges and prospectives of e-SPs

The integration of energy harvesters in self-powered electronic skin patches can provide abundant electrical power for monitoring biological signs and therapy processes. The application potential of self-powered electronic skin patches is far greater than that mentioned above. ES have also been widely used for the treatment of certain neurologic and psychiatric disorders. However, despite the impressive strides that have been achieved, a significant gap remains between self-powered electronic skin patches at the proof-of-concept stage and the final practical applications in real life. Nevertheless, the existing challenges offer tremendous opportunities for future developments. In this section, current challenges and prospects are systematically summarized (Fig. 14).

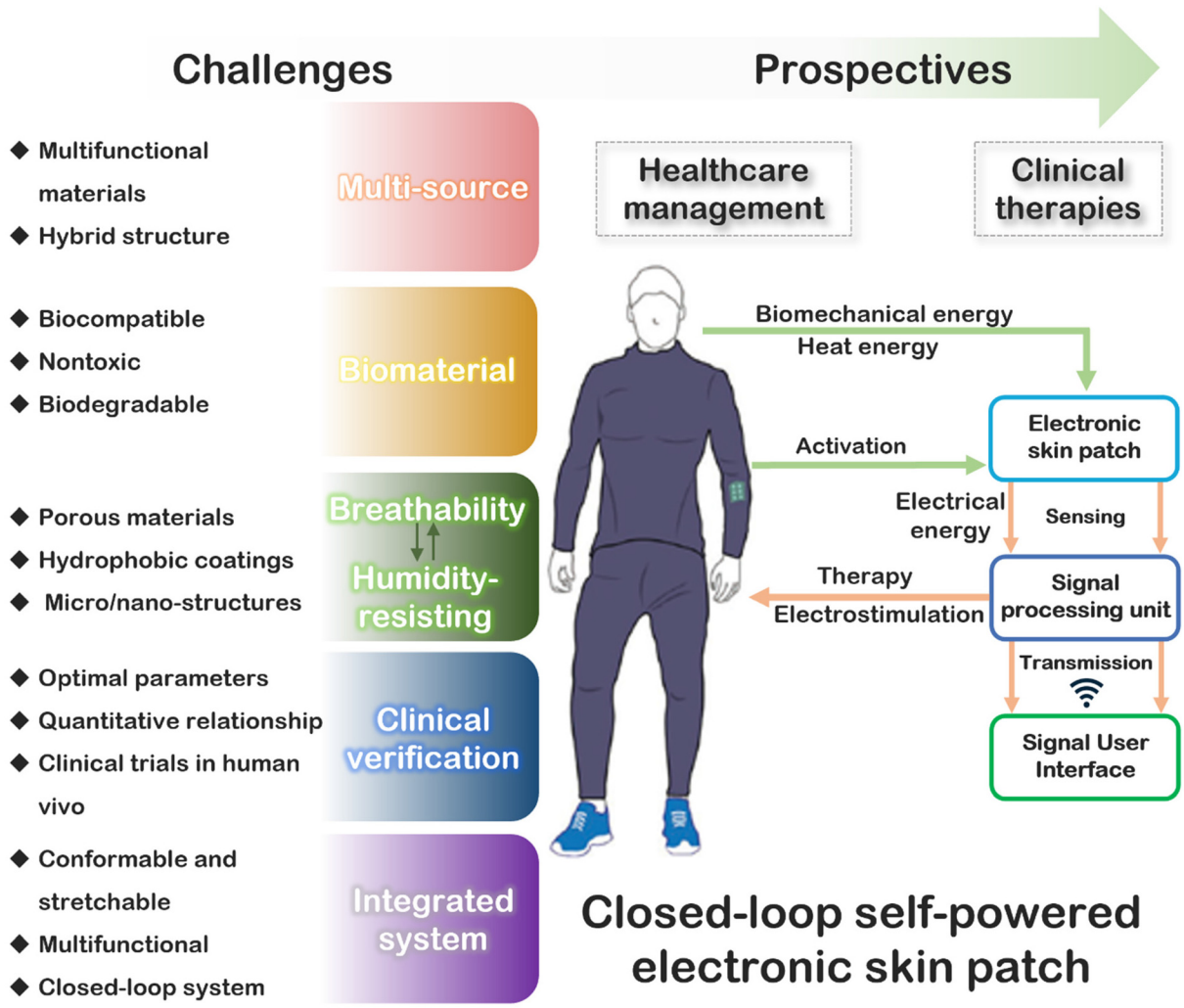

Fig. 14 Challenges and perspectives of self-powered electronic skin patches. Reproduced with permission.[283–285] Copyright 2019, Wiley-VCH.

The first critical challenge associated with self-powered electronic skin patches is generating sufficient and stable electrical power from small energy sources. Although self-powered electronic skin patches can harvest various energy from the human body, ranging from biomechanical energy to body temperature gradients and fluctuations, the input energy provided by humans is limited under some conditions. In the case of biomechanical energy harvesters, the inherent energy available *in vivo* is small, which impedes the further development of TENG/PENG-based implantable patches. Also, given that pyroelectric electronic skin patches with high power output usually require rapid temperature fluctuations, it is relatively difficult to find a proper application scenario for humans.[286] Besides, the increasingly smaller electronic devices and significant energy demands of the back-end data collection and signal processing units also present challenges for flexible self-powered electronic skin patches. Thus, to tackle this issue, the energy harvesting efficiency should be further enhanced. Additionally, self-powered electronic skin patches with multisource brings new design concepts to broaden their feasibility. These devices mainly rely on hybrid structures and/or multifunctional materials to harvest multisource energy. Especially, the coexistence of ferroelectricity and the photovoltaic effect in photoferroelectrics provides an opportunity for self-powered patches to demonstrate photovoltaic, piezoelectric, and pyroelectric effects in the same multifunctional material. This property has ignited great interest in exploring new science and enabled long-term, continuous health management and therapies.

In the particular case of wearable and implantable systems, the desirable biomaterials for self-powered electronic patches will require further investigation to reduce the immune reaction. Generally, the physicochemical prerequisites of biomaterials mainly include biocompatibility, mechanical stability, biodegradation, and capability of cell interaction. However, although various biomaterials, such as natural or synthetic polymers, with outstanding properties have been widely reported, it is still challenging to endow semiconductors and conductors with excellent biocompatibility for used *in vivo* for clinical purposes. An ideal approach that will allow the remarkable development of biocompatible devices is the combination of natural polymers with synthetic polymers. To realize the full potential of self-powered electronic skin patches, the device should be designed with conformable and stretchable configurations based on constructing materials to match the relevant movement patterns perfectly. Furthermore, bioelectronic devices are supposed to acquire self-healing properties owing to the inevitable damage caused by wear and tear during long-term use.

Effective moisture and gas management through breathable design is desirable for electronic patches to ensure thermal-moisture balance and a comfortable microenvironment between the skin/device interface. In addition, a breathable design is required to prevent sweat accumulation at the interactive interface, thus guaranteeing the initial adhesion for stable electric performance. Compared to dense and airtight film and rubber materials, the porous structure of sponges, smart fibers, textiles, and nanonetworks has aroused intense interest from researchers to enhance the air permeability of materials. A typical example is the application of nanofibrous membranes to construct self-powered electronic skin patches. An all-nanofiber structured electronic skin patch serving as a pressure sensor and energy harvester demonstrated high gas permeability with a water vapour transmittance rate of up to 10.26 kg m^{-2} d^{-1}.[287] Similarly, with flexible textiles as the substrate, a self-powered skin patch based on Ag-decorated laser-induced graphene foam provided long-term practical use and improved comfort.[288] Nevertheless, these porous structured electronic skin patches are easily affected by contamination and even induce a capillary effect, especially in highly humid or water vapour conditions, which result in low power generation and loss of electrical performance. Consequently, this contradictory relationship makes it urgent to develop new technology and novel device concepts. Combining porous structures with a superhydrophobic surface has proven to be an effective and promising approach to enable waterproofing and achieve gas exchange in electronic devices. Integrating hydrophobic and oleophobic coatings into self-powered electronic skin patches is conducive to modulating the surface wettability and realizing liquid repellency for the target application in varying humid environments. Besides, it is also appropriate to apply bioinspired micro/nano-hierarchical structures, such as lotus and leaves, to ensure hydrophobic surfaces and steady operating performances. However, these strategies are demanding and may not be suitable for large-scale applications. Novel design concepts are eagerly desirable for further self-powered electronic skin patch development.

Biologically, self-powered electronic skin patches can generate an electrical pulse to provide ES for therapeutic applications, such as wound healing, nerve stimulation, and pain relief. However, although they are approaching clinical trials, the electrical stimulation parameters remain controversial. Thus, it is imperative to determine standards for ES in various self-powered patches, which mainly include treatment regimens and optimal parameters, such as current amplitude, frequency, and duration, as well as the polarity of the treatment electrode. Besides, different from *in vitro* ES studies, where the voltage and current can be detected accurately, it is technically challenging to precisely measure induced electric fields and currents in wounds in clinical therapeutics. This results in a lack of verification of directly measured electric fields and currents in most clinical conditions. Consequently, technological advances are desperately required to acquire further in-depth understanding of the quantitative relationship between ES from self-powered electronic skin patches and the targeted biological treatment. Meanwhile, biological regulation and treatment generally require controllable ES to ensure therapeutic effects. In addition to coupling with current control elements, employing muscle movements associated with targeted tissues or organs as a power source is an ideal alternative to tune the stimulation intensity and frequency according to the physio-

logical movements. Moreover, most reported works are confined to small-animal and cell scales. Thus, it is still a long way to go to realize the practical application of self-powered electronic skin patches on human-scale animals for therapies.

The ultimate goal using electronic skin is to one day realize the practical application of a closed-loop system for healthcare management, diagnosis, and therapy in real-life situations. For this purpose, a sophisticated sensing modulus, power management, wireless signal acquisition, secure data processing and transmission together with machine learning and deep learning technologies should all considered for the fabrication of a comprehensive bioelectronic device. Miniaturized bioelectronics and integrated circuit chips provide huge opportunities for the rapid progress of conformable and stretchable electronic devices for feasible continuous healthcare monitoring. However, transforming laboratory prototypes into completely portable, multifunctional, and smart electronic skin patches with long-term, continuous sensing capabilities remains challenging, accompanied by numerous problems. Although electronic devices have evolved into flexible and miniaturized devices, it is still technically challenging to assemble various electronic elements with excellent mechanical flexibility and stretchability for skin-attachable electronic applications. Besides, many integration modules result in higher demand for electric power, far beyond that supported by self-powered devices. Additionally, the interference from multiple input signals urgently needs to be well-resolved in integrated systems, which may rely on strategies to design multimodal sensors with decoupled sensing mechanisms. Integrated electronic skin patches combined with advanced data processing techniques, such as machine learning, have shown potential healthcare management and therapy. However, this technique highly depends on big data related to involved users, caregivers, and doctors. Meanwhile, the comprehensive validation of the system is also essential. Nevertheless, based on the joint efforts from materials scientists, biologists, data engineers, and medical professionals, it is believed that the understanding of biology and technical progress will eventually lead to closed-loop skin patches for both health monitoring and therapeutic treatments with unprecedented effectiveness.

6. Conclusions and outlook

Progressive approaches in designing flexible substrates, multifunctional biomaterial skin patches, electronics, and integrated multi-sensor devices have significantly contributed to the development of e-skin patches. Promising strategies in designing force-sensitive flexible polymer substrates with excellent electronic-mechanical self-healing abilities have been developed.[289] With the continuous maturity of new technologies and biomaterial development progression, there are simpler and more convenient methods to prepare better intelligent patches.[290] Patches that can adhere to the skin surface for long periods are very desirable due to the possibility of sensitive health data detection. The most important role is integrating the multi-functionality of patches, such as monitoring the wound state and the response depending on the stimulus. Novel patches can fulfil different responses such as wound healing, bacteria eradication and sensing specific body parameters, leading to huge technological evolution and development of e-skin patches.[90] Biological 3D printing seems to be an effective one-step preparation method for more integrated patch systems.[291]

Significant progress has also been witnessed in the design of materials and integration of electronic systems. Various polymeric materials have been employed in the construction of electronic sensors. Among them, micro-structured PDMS is considered the most popular substrate due to its great elasticity and biocompatibility. Nevertheless, its practical application is still the most challenging aspect. The multi-signal and noisy background of the human body impedes the distinction of specific signals. Moreover, the weakness of the human body signaling causes the need to use more outstanding materials.[292] Modifying already known chemicals seems promising, *e.g.*, new methods of hydrogel crosslinking or combining different chemical groups with MXenes and metal–organic frameworks (MOFs) may lead to the preparation of more suitable materials for this application.[293] Recently, molecularly imprinted polymers (MIP) have attracted significant interest from scientists. MIPs are used in the development of affinity biosensors because of their ability to produce stable biological or biomimetic receptors that can detect biomolecules such as antibodies or nucleic acid sequences. One of the most desirable properties of biosensors is their short response time and utility for continuous monitoring. However, the dynamically changing environment of the human body creates significant challenges. Specifically, fluctuations in pH, temperature, and ionic strength may affect the molecule-receptor binding kinetics.[292] The past decade has witnessed a dramatically accelerated pace in the technological incorporation of energy harvesters and electronic skin patches due to the availability of new materials and novel design concepts. Interest in self-powered electronic skin patches has been driven by their significant potential to (1) generate electrical stimulation for wound healing, pain relief, nerve stimulation, and organ regeneration; (2) harvest bioenergy as an effective way to solve the problem of bulky batteries; and (3) perceive real-time, high-fidelity critical signals of an individual's status for continuous, long-term health monitoring applications with unprecedented diagnostic and treatment proficiency. In addition, by relying on machine learning and deep learning by pattern recognition and modeling, the collection of diverse environmental signals will allow the device to respond actively to these stimuli with timely disease warnings and corresponding therapy procedures. However, several challenges still exist in the fabrication and detection of e-skin patches, such as the instability of signals, poor mechanical stability of substrates, low repeatability of electrodes, low stability of electrode detection under bending or stretching, and long response time for sweat stimulation.[294–299] Current wearable patch sensors can only provide a working time of up to a few hours, which is far

below the goal of long-term monitoring. When integrated with batteries, supercapacitors, and triboelectric devices, the power supply units can be smaller and more durable. Wearability and biocompatibility are other concerns for on-skin sensor patches, given that they should not cause discomfort to the skin condition and other health problems after wearing.

Although certain challenges remain to be addressed, it is believed that self-powered electronic skin patches will achieve their full potential with the ongoing advancement of all the above-mentioned aspects. It is envisioned that integrated systems with innovative material design and configuration engineering will allow closed-loop self-powered electronic skin patches to a powerful toolset, which may revolutionize healthcare management and clinical treatments toward improved quality of human life. Further, approaches to enhance the portability of wearable devices by integrating detection and treatment devices still need to be developed before their commercialization.[300–305] Besides, sustainable and eco-friendly materials should be considered for fabricating e-skin patches to reduce costs and minimize waste.

Further, the widespread application of these skin patches is limited by their sophisticated fabrication processes, the use of expensive materials (graphene, AgNPs, AuNPs, *etc.*) and electronic components, which directly affect their commercial viability. We believe that a simple but efficient approach for the manufacture of e-skin patches will take us further towards designing low-cost multifunctional skin patches for biomedical applications. Efforts to integrate the next-generation multi-sensor systems to monitor a wide range of parameters simultaneously need to be explored further, considering advanced electronics, wireless communications, clinical medicine, and auto-medication facilities. Thus, future studies need to focus on lowering the cost of e-skin patches and improving the sensitivity and reliability of the sensors simultaneously, resulting in high-performance integrated and multimodal sensing patches, thus promoting the commercialization of flexible patch sensors for e-skin. 3D printing technology seems to be promising in reducing production costs, scaling-up processes, and commercialization. The device costs can also be reduced by using carbon- and polymer-based materials and simplifying the production process.[306] Overall, electronic skin sensing materials are promising alternatives for quick diagnosis and monitoring health-related issues (*e.g.*, blood pressure, temperature, pulse rate, and heartbeat). Integrating two or more sensors in one device is an ongoing research trend. Soft and flexible materials will play a critical role when combined in composites and hybrid materials that integrate multiple recognition functions, fulfilling the market demand and enabling further clinical application.[41]

In summary, owing to the significant breakthrough in medical technology, nanofabrication, configuration design, and biomaterials selection, skin patches have emerged as a critical player for various biomedical purposes, including wound healing, drug delivery, health monitoring, energy harvesting, and other complex multifunctions. Although there are unmet challenges, it is believed that well-integrated electronic skin patches with comprehensive and multiple functions will be realized to enable real-time health monitoring and provide timely professional advice or/and local treatment, which will enable targeted therapies and improve health conditions according to individual differences. We hope that this comprehensive review will provide multidisciplinary researchers with inspired insights into next-generation skin patches with multiple biomedical applications. It is believed that interdisciplinary joint efforts from materials scientists, biologists, data engineers, and medical professionals will speed up the process of closed-loop skin patch systems for healthcare management, disease diagnosis and therapy, which can be applied in real-life situations, eventually revolutionizing healthcare and clinical therapy.

Conflicts of interest

There are no conflicts to declare.

Acknowledgements

The work was supported within the framework of a European Regional Development Fund Project, under the title Application of Modern Technologies in Medicine and Industry (No. CZ.02.1.01/0.0/0.0/17_048/0007280), and the National Center for Research and Development (NCBiR) (grant: WPC2/NanoHealer/2021). C. R. P. N. and F. P acknowledge the financial support from the Polish Ministry of Science and Higher Education through scholarships for outstanding young scientists. Y.-C. S. and Y.-C. Y. would like to thank the funding support from the National Science and Technology Council, Taiwan (NSTC 111-2113-M-002-008 and NSTC 111-2811-M-002-114).

References

1 M. N. Pastore, Y. N. Kalia, M. Horstmann and M. S. Roberts, *Br. J. Pharmacol.*, 2015, **172**, 2179–2209.
2 V. Dhandapani, P. Saseedharan, D. Groleau and P. Vermette, *J. Biomed. Mater. Res., Part B*, 2022, **110**, 950–966.
3 Y. Long, H. Wei, J. Li, G. Yao, B. Yu, D. L. Ni, A. L. F. Gibson, X. L. Lan, Y. D. Jiang, W. B. Cai and X. D. Wang, *ACS Nano*, 2018, **12**, 12533–12540.
4 J. Zhu, H. L. Zhou, E. M. Gerhard, S. H. Zhang, F. I. P. Rodriguez, T. S. Pan, H. B. Yang, Y. Lin, J. Yang and H. Y. Cheng, *Bioact. Mater.*, 2023, **19**, 360–375.
5 D. T. Phan, C. H. Nguyen, T. D. P. Nguyen, L. Tran, S. Park, J. Choi, B. I. Lee and J. Oh, *Biosensors*, 2022, **12**, 139.
6 G. Manasa, R. J. Mascarenhas, N. P. Shetti, S. J. Malode, A. Mishra, S. Basu and T. M. Aminabhavi, *ACS Appl. Bio Mater.*, 2022, **5**, 945–970.
7 D. Holmes, *Nat. Rev. Endocrinol.*, 2016, **12**, 247.

8 S. R. Steinhubl and E. J. Topol, *Nat. Biomed. Eng.*, 2018, **2**, 633–634.
9 Y. Q. Qiu, H. Fang, J. J. Guo and H. Wu, *Nano Energy*, 2022, **98**, 107311.
10 S. H. R. Cheong, Y. J. X. Ng, Y. Lau and S. T. Lau, *Prev. Med.*, 2022, **162**, 107170.
11 T. Shimura, S. Sato, P. Zalar and N. Matsuhisa, *Adv. Electron. Mater.*, 2022, 2200512.
12 J. T. Reeder, J. Choi, Y. G. Xue, P. Gutruf, J. Hanson, M. Liu, T. Ray, A. J. Bandodkar, R. Avila, W. Xia, S. Krishnan, S. Xu, K. Barnes, M. Pahnke, R. Ghaffari, Y. Huang and J. A. Rogers, *Sci. Adv.*, 2019, **5**, eaau6356.
13 Z. Zou, C. Zhu, Y. Li, X. Lei, W. Zhang and J. Xiao, *Sci. Adv.*, 2018, **4**, eaaq0508.
14 Z. Jiang, M. O. G. Nayeem, K. Fukuda, S. Ding, H. Jin, T. Yokota, D. Inoue, D. Hashizume and T. Someya, *Adv. Mater.*, 2019, **31**, 1903446.
15 J. R. Sempionatto, M. Lin, L. Yin, E. De la Paz, K. Pei, T. Sonsa-Ard, A. N. de Loyola Silva, A. A. Khorshed, F. Zhang, N. Tostado, S. Xu and J. Wang, *Nat. Biomed. Eng.*, 2021, **5**, 737–748.
16 Y. Wang, M. Guo, B. He and B. Gao, *Anal. Chem.*, 2021, **93**, 4687–4696.
17 Y. Lee, J. Park, A. Choe, S. Cho, J. Kim and H. Ko, *Adv. Funct. Mater.*, 2020, **30**, 1904523.
18 G. C. Andrews, W. D. James, T. G. Berger and D. M. Elston, *Andrews' diseases of the skin: clinical dermatology*, ed. W. D. James, T. G. Berger and D. M. Elston. Saunders Elsevier, Phliadelphia, PA, 10th edn, 2006.
19 M. Kaltenbrunner, T. Sekitani, J. Reeder, T. Yokota, K. Kuribara, T. Tokuhara, M. Drack, R. Schwodiauer, I. Graz, S. Bauer-Gogonea, S. Bauer and T. Someya, *Nature*, 2013, **499**, 458–463.
20 G. A. Salvatore, N. Munzenrieder, T. Kinkeldei, L. Petti, C. Zysset, I. Strebel, L. Buthe and G. Troster, *Nat. Commun.*, 2014, **5**, 2982.
21 J. Lee, T. J. Ha, H. F. Li, K. N. Parrish, M. Holt, A. Dodabalapur, R. S. Ruoff and D. Akinwande, *ACS Nano*, 2013, **7**, 7744–7750.
22 S. J. Rowley-Neale, E. P. Randviir, A. S. A. Dena and C. E. Banks, *Appl. Mater. Today*, 2018, **10**, 218–226.
23 Y. D. Liu, X. H. Liu, Z. P. Guo, Z. G. Hu, Z. H. Xue and X. Q. Lu, *Biosens. Bioelectron.*, 2017, **87**, 101–107.
24 R. G. Haahr, S. B. Duun, M. H. Toft, B. Belhage, J. Larsen, K. Birkelund and E. V. Thomsen, *IEEE Trans. Biomed. Circuits Syst.*, 2012, **6**, 45–53.
25 E. M. Krueger, M. E. Cullum, T. R. Nichols, M. G. Taylor, W. L. Sexton and R. I. Murahata, *Sking Res. Technol.*, 2013, **19**, 398–404.
26 S. I. Park, D. S. Brenner, G. Shin, C. D. Morgan, B. A. Copits, H. U. Chung, M. Y. Pullen, K. N. Noh, S. Davidson, S. J. Oh, J. Yoon, K. I. Jang, V. K. Samineni, M. Norman, J. G. Grajales-Reyes, S. K. Vogt, S. S. Sundaram, K. M. Wilson, J. S. Ha, R. X. Xu, T. S. Pan, T. I. Kim, Y. G. Huang, M. C. Montana, J. P. Golden, M. R. Bruchas, R. W. Gereau and J. A. Rogers, *Nat. Biotechnol.*, 2015, **33**, 1280–1286.
27 S. Du, N. Y. Zhou, Y. J. Gao, G. Xie, H. Y. Du, H. Jiang, L. B. Zhang, J. Tao and J. T. Zhu, *Nano Res.*, 2020, **13**, 2525–2533.
28 S. Du, H. N. Suo, G. Xie, Q. Q. Lyu, M. Mo, Z. J. Xie, N. Y. Zhou, L. B. Zhang, J. Tao and J. T. Zhu, *Nano Energy*, 2022, **93**, 106906.
29 M. Bariya, H. Y. Y. Nyein and A. Javey, *Nat. Electron.*, 2018, **1**, 160–171.
30 P. H. Lin, S. C. Sheu, C. W. Chen, S. C. Huang and B. R. Li, *Talanta*, 2022, **241**, 123187.
31 Y. W. Liu, L. Zhong, S. B. Zhang, J. Wang and Z. H. Liu, *Sens. Actuators, B*, 2022, **354**, 131204.
32 C. Lim, Y. J. Hong, J. Jung, Y. Shin, S. H. Sunwoo, S. Baik, O. K. Park, S. H. Choi, T. Hyeon, J. H. Kim, S. Lee and D. H. Kim, *Sci. Adv.*, 2021, **7**, eabd3716.
33 L. Y. Meng, A. P. F. Turner and W. C. Mak, *ACS Appl. Mater. Interfaces*, 2021, **13**, 54456–54465.
34 H. Lee, E. Kim, Y. Lee, H. Kim, J. Lee, M. Kim, H. J. Yoo and S. Yoo, *Sci. Adv.*, 2018, **4**, eaas953.
35 S. Yoon, H. Yoon, M. Abu Zahed, C. Park, D. Kim and J. Y. Park, *Biosens. Bioelectron.*, 2022, **196**, 113685.
36 W. Y. He, C. Y. Wang, H. M. Wang, M. Q. Jian, W. D. Lu, X. P. Liang, X. Zhang, F. C. Yang and Y. Y. Zhang, *Sci. Adv.*, 2019, **5**, eaax0649.
37 Y. Song, J. H. Min, Y. Yu, H. B. Wang, Y. R. Yang, H. X. Zhang and W. Gao, *Sci. Adv.*, 2020, **6**, eaay9842.
38 S. Yoon, J. K. Sim and Y. H. Cho, *Sci. Rep.*, 2016, **6**, 23468.
39 L. Ortega, A. Llorella, J. P. Esquivel and N. Sabate, *Microsyst. Nanoeng.*, 2019, **5**, 3.
40 H. J. Kim, Y. X. Jin, S. Achavananthadith, R. Z. Lin and J. S. Ho, *Iscience*, 2021, **24**, 103284.
41 N. P. Shetti, A. Mishra, S. Basu, R. J. Mascarenhas, R. R. Kakarla and T. M. Aminabhavi, *ACS Biomater. Sci. Eng.*, 2020, **6**, 1823–1835.
42 C. Y. Wang, T. Yokota and T. Someya, *Chem. Rev.*, 2021, **121**, 2109–2146.
43 Y. Li, W. H. Chen and L. H. Lu, *ACS Appl. Bio Mater.*, 2021, **4**, 122–139.
44 J.-H. Kim, S.-R. Kim, H.-J. Kil, Y.-C. Kim and J.-W. Park, *Nano Lett.*, 2018, **18**, 4531–4540.
45 Q. Yan, M. Zhou and H. Fu, *Composites, Part B*, 2020, **201**, 108356.
46 K. Ruangmak, N. Paradee, S. Niamlang, P. Sakunpongpitiporn and A. Sirivat, *J. Biomed. Mater. Res., Part B*, 2022, **110**, 478–488.
47 S. H. Jeong, S. Zhang, K. Hjort, J. Hilborn and Z. Wu, *Adv. Mater.*, 2016, **28**, 5830–5836.
48 S. Lü, C. Gao, X. Xu, X. Bai, H. Duan, N. Gao, C. Feng, Y. Xiong and M. Liu, *ACS Appl. Mater. Interfaces*, 2015, **7**, 13029–13037.
49 D. Zhu, H. Wang, P. Trinh, S. C. Heilshorn and F. Yang, *Biomaterials*, 2017, **127**, 132–140.

50 Z. Wei, J. H. Yang, Z. Q. Liu, F. Xu, J. X. Zhou, M. Zrínyi, Y. Osada and Y. M. Chen, *Adv. Funct. Mater.*, 2015, **25**, 1352–1359.

51 Y. Zhang, C. Fu, Y. Li, K. Wang, X. Wang, Y. Wei and L. Tao, *Polym. Chem.*, 2017, **8**, 537–544.

52 L. He, D. Szopinski, Y. Wu, G. A. Luinstra and P. Theato, *ACS Macro Lett.*, 2015, **4**, 673–678.

53 A. Zengin, J. P. O. Castro, P. Habibovic and S. H. van Rijt, *Nanoscale*, 2021, **13**, 1144–1154.

54 Y.-L. Liu and T.-W. Chuo, *Polym. Chem.*, 2013, **4**, 2194–2205.

55 J. Zhao, R. Xu, G. Luo, J. Wu and H. Xia, *J. Mater. Chem. B*, 2016, **4**, 982–989.

56 K. C. Koehler, K. S. Anseth and C. N. Bowman, *Biomacromolecules*, 2013, **14**, 538–547.

57 N. Yoshie, S. Saito and N. Oya, *Polymer*, 2011, **52**, 6074–6079.

58 H. Zhang, H. Xia and Y. Zhao, *ACS Macro Lett.*, 2012, **1**, 1233–1236.

59 Z. Zhang, T. Li, B. Chen, S. Wang and Z. Guo, *J. Mater. Sci.*, 2017, **52**, 10614–10623.

60 G. Deng, F. Li, H. Yu, F. Liu, C. Liu, W. Sun, H. Jiang and Y. Chen, *ACS Macro Lett.*, 2012, **1**, 275–279.

61 X. Ye, X. Li, Y. Shen, G. Chang, J. Yang and Z. Gu, *Polymer*, 2017, **108**, 348–360.

62 Y. Shi, M. Wang, C. Ma, Y. Wang, X. Li and G. Yu, *Nano Lett.*, 2015, **15**, 6276–6281.

63 G. Ge, Y. Lu, X. Qu, W. Zhao, Y. Ren, W. Wang, Q. Wang, W. Huang and X. Dong, *ACS Nano*, 2020, **14**, 218–228.

64 J. M. Dodda, M. G. Azar, P. Belsky, M. Louf, A. Broz, L. Bacakova, J. Kadlec and T. Remis, *Cellulose*, 2022, **29**, 6697–6717.

65 D. Wang, Y. Xia, D. Zhang, X. Sun, X. Chen, S. Oliver, S. Shi and L. Lei, *ACS Appl. Polym. Mater.*, 2020, **2**, 1587–1596.

66 Y. Guo, Z. Gao, Y. Liu, Z. Huang, C. Chai and J. Hao, *ACS Appl. Polym. Mater.*, 2019, **1**, 2370–2378.

67 D. Garcia-Garcia, J. E. Crespo-Amorós, F. Parres and M. D. Samper, *Polymer (Basel)*, 2020, **12**, 862.

68 C. G. M. Gennari, G. M. G. Quaroni, C. Creton, P. Minghetti and F. Cilurzo, *Int. J. Pharm.*, 2020, **575**, 118975.

69 Z. Shen and J. Feng, *J. Mater. Chem. C*, 2019, **7**, 9423–9429.

70 W. Qian, X. Hu, W. He, R. Zhan, M. Liu, D. Zhou, Y. Huang, X. Hu, Z. Wang, G. Fei, J. Wu, M. Xing, H. Xia and G. Luo, *Colloids Surf., B*, 2018, **166**, 61–71.

71 N. Varshney, A. K. Sahi, K. Y. Vajanthri, S. Poddar, C. K. Balavigneswaran, A. Prabhakar, V. Rao and S. K. Mahto, *Cytotechnology*, 2019, **71**, 287–303.

72 J. Kim, J. Park, U. Jeong and J.-W. Park, *J. Appl. Polym. Sci.*, 2016, **133**, DOI: **10.1002/APP.43830**.

73 S. Yoon, M. Seok, M. Kim and Y.-H. Cho, *Sci. Rep.*, 2021, **11**, 938.

74 J. H. Kim, S. R. Kim, H. J. Kil, Y. C. Kim and J. W. Park, *Nano Lett.*, 2018, **18**, 4531–4540.

75 L. Han, Y. Zhang, X. Lu, K. Wang, Z. Wang and H. Zhang, *ACS Appl. Mater. Interfaces*, 2016, **8**, 29088–29100.

76 B. Liu, Y. Wang, Y. Miao, X. Zhang, Z. Fan, G. Singh, X. Zhang, K. Xu, B. Li, Z. Hu and M. Xing, *Biomaterials*, 2018, **171**, 83–96.

77 X. Zhao, H. Wu, B. Guo, R. Dong, Y. Qiu and P. X. Ma, *Biomaterials*, 2017, **122**, 34–47.

78 Y. Li, X. Wang, Y.-n. Fu, Y. Wei, L. Zhao and L. Tao, *ACS Appl. Mater. Interfaces*, 2018, **10**, 26046–26055.

79 S. Pan, F. Zhang, P. Cai, M. Wang, K. He, Y. Luo, Z. Li, G. Chen, S. Ji, Z. Liu, X. J. Loh and X. Chen, *Adv. Funct. Mater.*, 2020, **30**, 1909540.

80 S. A. Adli, F. Ali, A. S. Azmi, H. Anuar, N. A. Nasir, R. Hasham and M. K. Idris, *Polymers*, 2020, **12**, 1669.

81 S. Liu, J. Yu, H. Li, K. Wang, G. Wu, B. Wang, M. Liu, Y. Zhang, P. Wang, J. Zhang, J. Wu, Y. Jing, F. Li and M. Zhang, *Polymers (basel)*, 2020, **12**, 288.

82 J. L. Cui, B. Z. Zhang, J. P. Duan, H. Guo and J. Tang, *Materials*, 2017, **10**, 1439.

83 H. R. Lim, H. S. Kim, R. Qazi, Y. T. Kwon, J. W. Jeong and W. H. Yeo, *Adv. Mater.*, 2020, **32**, 1901924.

84 W. Wang, S. Yang, K. Ding, L. Jiao, J. Yan, W. Zhao, Y. Y. Ma, T. Y. Wang, B. W. Cheng and Y. H. Ni, *Chem. Eng. J.*, 2021, **425**, 129949.

85 M. Rahmati, J. J. Blaker, S. P. Lyngstadaas, J. F. Mano and H. J. Haugen, *Mater. Today Adv.*, 2020, **5**, 100051.

86 F. Pierini, P. Nakielski, O. Urbanek, S. Pawlowska, M. Lanzi, L. De Sio and T. A. Kowalewski, *Biomacromolecules*, 2018, **19**, 4147–4167.

87 M. Farahani and A. Shafiee, *Adv. Healthcare Mater.*, 2021, **10**, 2100477.

88 S. Q. Zhang, J. W. Ye, X. Liu, G. Y. Wang, Y. Qi, T. L. Wang, Y. Q. Song, Y. C. Li and G. L. Ning, *Chem. Eng. J.*, 2022, **446**, 136994.

89 Y. Ziai, F. Petronella, C. Rinoldi, P. Nakielski, A. Zakrzewska, T. A. Kowalewski, W. Augustyniak, X. R. Li, A. Calogero, I. Sabala, B. Ding, L. De Sio and F. Pierini, *NPG Asia Mater.*, 2022, **14**, 18.

90 Z. J. Krysiak and U. Stachewicz, *Wiley Interdiscip. Rev.: Nanomed. Nanobiotechnol.*, 2023, **15**, e1829.

91 I. Hwang, H. N. Kim, M. Seong, S. H. Lee, M. Kang, H. Yi, W. G. Bae, M. K. Kwak and H. E. Jeong, *Adv. Healthcare Mater.*, 2018, **7**, 1800275.

92 S. Baik, J. Kim, H. J. Lee, T. H. Lee and C. Pang, *Adv. Sci.*, 2018, **5**, 1800100.

93 D. Kim, H. Kim, G. T. Hwang, S. B. Cho, S. H. Jeon, H. W. Kim, C. K. Jeong, S. Chun and C. Pang, *ACS Energy Lett.*, 2022, **7**, 1820–1827.

94 H. Jung, M. K. Kim, J. Y. Lee, S. W. Choi and J. Kim, *Adv. Funct. Mater.*, 2020, **30**, 2004407.

95 S. Pawlowska, C. Rinoldi, P. Nakielski, Y. Ziai, O. Urbanek, X. R. Li, T. A. Kowalewski, B. Ding and F. Pierini, *Adv. Mater. Interfaces*, 2020, **7**, 2000247.

96 P. Nakielski, S. Pawlowska, C. Rinoldi, Y. Ziai, L. De Sio, O. Urbanek, K. Zembrzycki, M. Pruchniewski, M. Lanzi, E. Salatelli, A. Calogero, T. A. Kowalewski, A. L. Yarin and F. Pierini, *ACS Appl. Mater. Interfaces*, 2020, **12**, 54328–54342.

97 D. L. Cao, X. Chen, F. Cao, W. Guo, J. Y. Tang, C. Y. Cai, S. Q. Cui, X. W. Yang, L. Yu, Y. Su and J. D. Ding, *Adv. Funct. Mater.*, 2021, **31**, 2100349.

98 S. Baik, H. J. Lee, D. W. Kim, J. W. Kim, Y. Lee and C. Pang, *Adv. Mater.*, 2019, **31**, 1803309.

99 Y. Ziai, C. Rinoldi, P. Nakielski, L. De Sio and F. Pierini, *Curr. Opin. Biomed. Eng.*, 2022, **24**, 100413.

100 N. Elahpour, F. Pahlevanzadeh, M. Kharaziha, H. R. Bakhsheshi-Rad, S. Ramakrishna and F. Berto, *Int. J. Pharm.*, 2021, **597**, 120301.

101 A. Dodero, M. Alloisio, M. Castellano and S. Vicini, *ACS Appl. Mater. Interfaces*, 2020, **12**, 31162–31171.

102 J. Y. Li, Y. Y. Zhou, J. B. Yang, R. Ye, J. Gao, L. Ren, B. Liu, L. Liang and L. L. Jiang, *Mater. Sci. Eng., C*, 2019, **96**, 576–582.

103 C. Rinoldi, S. S. Zargarian, P. Nakielski, X. R. Li, A. Liguori, F. Petronella, D. Presutti, Q. S. Wang, M. Costantini, L. de Sio, C. Gualandi, B. Ding and F. Pierini, *Small Methods*, 2021, **5**, 2100402.

104 A. Liguori, S. Pandini, C. Rinoldi, N. Zaccheroni, F. Pierini, M. L. Focarete and C. Gualandi, *Macromol. Rapid Commun.*, 2022, **43**, 2100694.

105 *Br. Med. J.*, 1949, **2**, 82–83.

106 J. L. Cai, J. J. Wang, C. X. Sun, J. W. Dai and C. Zhang, *Biomed. Mater.*, 2022, **17**, 064103.

107 S. Haldar, A. Sharma, S. Gupta, S. Chauhan, P. Roy and D. Lahiri, *Mater. Sci. Eng., C*, 2019, **105**, 110140.

108 C. Niu, L. Wang, D. Ji, M. Ren, D. Ke, Q. Fu, K. Zhang and X. Yang, *Cell Regener.*, 2022, **11**, 10.

109 S. X. Chen, A. McCarthy, J. V. John, Y. J. Su and J. W. Xie, *Adv. Mater.*, 2020, **32**, 2003754.

110 A. Kidoaki and T. Matsuda, *J. Biotechnol.*, 2008, **133**, 225–230.

111 M. Milojević, G. Harih, B. Vihar, J. Vajda, L. Gradisnik, T. Zidaric, K. S. Kleinschek, U. Maver and T. Maver, *Pharmaceutics*, 2021, **13**, 564.

112 M. Ha, S. Lim, S. Cho, Y. Lee, S. Na, C. Baig and H. Ko, *ACS Nano*, 2018, **12**, 3964–3974.

113 S. Ghosh, S. Haldar, S. Gupta, S. Chauhan, V. Mago, P. Roy and D. Lahiri, *Biomater. Adv.*, 2022, **139**, 212980.

114 T. Zhang, H. Xu, Y. G. Zhang, S. R. Zhang, X. Yang, Y. Wei, D. Huang and X. J. Lian, *Mater. Des.*, 2022, **218**, 110711.

115 R. J. A. Moakes, J. J. Senior, T. E. Robinson, M. Chipara, A. Atansov, A. Naylor, A. D. Metcalfe, A. M. Smith and L. M. Grover, *APL Bioeng.*, 2021, **5**, 046103.

116 M. Singh, C. Berkland and M. S. Detamore, *Tissue Eng., Part B*, 2008, **14**, 341–366.

117 J. He, R. Shen, Q. Liu, S. Zheng, X. Wang, J. Gao, Q. Wang, J. Huang and J. Ding, *ACS Appl. Mater. Interfaces*, 2022, **14**, 37436–37446.

118 Z. Y. Zhou, N. Liu, X. P. Zhang, X. C. Ning, Y. X. Miao, Y. Wang, J. H. Sun, Q. Wan, X. F. Leng and T. Wu, *Colloids Surf., B*, 2022, **209**, 112185.

119 J. Amagat, M. L. Jorgensen, Z. Y. Zhang, R. D. Xu and M. L. Chen, *Mater. Today Commun.*, 2021, **26**, 102066.

120 A. Motealleh and N. S. Kehr, *Biomater. Sci.*, 2020, **8**, 5628–5637.

121 M. Luo, K. Shaitan, X. Y. Qu, A. P. Bonartsev and B. Lei, *Appl. Mater. Today*, 2022, **26**, 101304.

122 M. Berthet, Y. Gauthier, C. Lacroix, B. Verrier and C. Monge, *Trends Biotechnol.*, 2017, **35**, 770–784.

123 S. K. Nethi, S. Das, C. R. Patra and S. Mukherjee, *Biomater. Sci.*, 2019, **7**, 2652–2674.

124 H. C. Huang, C. R. Walker, A. Nanda and K. Rege, *ACS Nano*, 2013, **7**, 2988–2998.

125 L. M. Sun, S. J. Yi, Y. Z. Wang, K. Pan, Q. X. Zhong and M. J. Zhang, *Bioinspiration Biomimetics*, 2014, **9**, 016005.

126 X. L. Yang, J. C. Yang, L. Wang, B. Ran, Y. X. Jia, L. M. Zhang, G. Yang, H. W. Shao and X. Y. Jiang, *ACS Nano*, 2017, **11**, 5737–5745.

127 H. Haidari, R. Bright, X. L. Strudwick, S. Garg, K. Vasilev, A. J. Cowin and Z. Kopecki, *Acta Biomater.*, 2021, **128**, 420–434.

128 P. Makvandi, G. W. Ali, F. Della Sala, W. I. Abdel-Fattah and A. Borzacchiello, *Carbohydr. Polym.*, 2019, **223**, 115023.

129 C. Rigo, L. Ferroni, I. Tocco, M. Roman, I. Munivrana, C. Gardin, W. R. L. Cairns, V. Vindigni, B. Azzena, C. Barbante and B. Zavan, *Int. J. Mol. Sci.*, 2013, **14**, 4817–4840.

130 C. Carlson, S. M. Hussain, A. M. Schrand, L. K. Braydich-Stolle, K. L. Hess, R. L. Jones and J. J. Schlager, *J. Phys. Chem. B*, 2008, **112**, 13608–13619.

131 N. Ninan, B. Joseph, R. M. Visalakshan, R. Bright, C. Denoual, P. Zilm, Y. B. Dalvi, P. V. Priya, A. Mathew, Y. Grohens, N. Kalarikkal, K. Vasilev and S. Thomas, *Mater. Adv.*, 2021, **2**, 6620–6630.

132 A. Gopal, V. Kant, A. Gopalakrishnan, S. K. Tandan and D. Kumar, *Eur. J. Pharmacol.*, 2014, **731**, 8–19.

133 B. L. Tao, C. C. Lin, Y. M. Deng, Z. Yuan, X. K. Shen, M. W. Chen, Y. He, Z. H. Peng, Y. Hu and K. Y. Cai, *J. Mater. Chem. B*, 2019, **7**, 2534–2548.

134 C. K. Sen, S. Khanna, M. Venojarvi, P. Trikha, E. C. Ellison, T. K. Hunt and S. Roy, *Am. J. Physiol.: Heart Circ. Physiol.*, 2002, **282**, H1821–H1827.

135 R. Augustine, E. A. Dominic, I. Reju, B. Kaimal, N. Kalarikkal and S. Thomas, *RSC Adv.*, 2014, **4**, 24777–24785.

136 J. Y. Zhu, G. H. Jiang, G. Song, T. Q. Liu, C. Cao, Y. H. Yang, Y. J. Zhang and W. J. Hong, *ACS Appl. Bio Mater.*, 2019, **2**, 5042–5052.

137 A. M. Brokesh and A. K. Gaharwar, *ACS Appl. Mater. Interfaces*, 2020, **12**, 5319–5344.

138 H. B. Wu, F. Y. Li, S. F. Wang, J. X. Lu, J. Q. Li, Y. Du, X. L. Sun, X. Y. Chen, J. Q. Gao and D. S. Ling, *Biomaterials*, 2018, **151**, 66–77.

139 F. Ori, R. Dietrich, C. Ganz, M. Dau, D. Wolter, A. Kasten, T. Gerber and B. Frerich, *J. Cranio-Maxillofac. Surg.*, 2017, **45**, 99–107.

140 J. M. Xue, X. C. Wang, E. D. Wang, T. Li, J. Chang and C. T. Wu, *Acta Biomater.*, 2019, **100**, 270–279.

141 S. Adepu and S. Ramakrishna, *Molecules*, 2021, **26**, 5905.

142 J. Koehler, F. P. Brandl and A. M. Goepferich, *Eur. Polym. J.*, 2018, **100**, 1–11.

143 S. P. Miguel, R. S. Sequeira, A. F. Moreira, C. S. D. Cabral, A. G. Mendonca, P. Ferreira and I. J. Correia, *Eur. J. Pharm. Biopharm.*, 2019, **139**, 1–22.

144 S. Saghazadeh, C. Rinoldi, M. Schot, S. S. Kashaf, F. Sharifi, E. Jalilian, K. Nuutila, G. Giatsidis, P. Mostafalu, H. Derakhshandeh, K. Yue, W. Swieszkowski, A. Memic, A. Tamayol and A. Khademhosseini, *Adv. Drug Delivery Rev.*, 2018, **127**, 138–166.

145 S. P. Miguel, D. R. Figueira, D. Simoes, M. P. Ribeiro, P. Coutinho, P. Ferreira and I. J. Correia, *Colloids Surf., B*, 2018, **169**, 60–71.

146 E. B. Denkbas, E. Ozturk, N. Ozdemir, K. Kececi and M. A. Ergun, *J Bioact Compat Pol.*, 2003, **18**, 177–190.

147 F. Nejaddehbashi, M. Hashemitabar, V. Bayati, M. Abbaspour, E. Moghimipour and M. Orazizadeh, *Artif. Organs*, 2019, **43**, 413–423.

148 A. Mohandas, B. S. Anisha, K. P. Chennazhi and R. Jayakumar, *Colloids Surf., B*, 2015, **127**, 105–113.

149 M. Piran, S. Vakilian, M. Piran, A. Mohammadi-Sangcheshmeh, S. Hosseinzadeh and A. Ardeshirylajimi, *Artif. Cells, Nanomed., Biotechnol.*, 2018, **46**, S511–S520.

150 N. K. Dehkordi, M. Minaiyan, A. Talebi, V. Akbari and A. Taheri, *Biomed. Mater.*, 2019, **14**, 035003.

151 M. L. Xue, R. L. Zhao, H. Y. Lin and C. Jackson, *Adv. Drug Delivery Rev.*, 2018, **129**, 219–241.

152 X. L. Chen, J. F. Wu, X. M. Cao, H. Jiang, Z. R. Wu, Z. D. Zeng, H. Chen and J. Zhang, *Am. J. Transl. Res.*, 2021, **13**, 13261–13272.

153 D. Revi, W. Paul, T. V. Anilkumar and C. P. Sharma, *J. Biomed. Mater. Res., Part A*, 2014, **102**, 3273–3281.

154 P. Du, C. Casavitri, M. Suhaeri, P. Y. Wang, J. H. Lee, W. G. Koh and K. Park, *ACS Biomater. Sci. Eng.*, 2019, **5**, 900–910.

155 S. Wang, H. C. Yang, Z. R. Tang, G. Long and W. Huang, *Stem Cells Int.*, 2016, **2016**, 3269267.

156 S. S. Ha, E. S. Song, P. Du, M. Suhaeri, J. H. Lee and K. Park, *ACS Biomater. Sci. Eng.*, 2020, **6**, 4266–4275.

157 K. Lee, Y. M. Xue, J. Lee, H. J. Kim, Y. W. Liu, P. Tebon, E. Sarikhani, W. J. Sun, S. M. Zhang, R. Haghniaz, B. Celebi-Saltik, X. W. Zhou, S. Ostrovidov, S. Ahadian, N. Ashammakhi, M. R. Dokmeci and A. Khademhosseini, *Adv. Funct. Mater.*, 2020, **30**, 2000086.

158 A. Zonari, T. M. M. Martins, A. C. C. Paula, J. N. Boeloni, S. Novikoff, A. P. Marques, V. M. Correlo, R. L. Reis and A. M. Goes, *Acta Biomater.*, 2015, **17**, 170–181.

159 L. Ferroni, C. Gardin, U. D'Amora, L. Calza, A. Ronca, E. Tremoli, L. Ambrosio and B. Zavan, *Biomater. Adv.*, 2022, **139**, 213000.

160 S. Shafei, M. Khanmohammadi, R. Heidari, H. Ghanbari, V. T. Nooshabadi, S. Farzamfar, M. Akbariqomi, N. S. Sanikhani, M. Absalan and G. Tavoosidana, *J. Biomed. Mater. Res., Part A*, 2020, **108**, 545–556.

161 E. Kolanthai, Y. F. Fu, U. Kumar, B. Babu, A. K. Venkatesan, K. W. Liechty and S. Seal, *Wiley Interdiscip. Rev.: Nanomed. Nanobiotechnol.*, 2022, **14**, e1741.

162 O. Tezgel, N. DiStasio, V. Laghezza-Masci, A. R. Taddei, A. Szarpak-Jankowska, R. Auzely-Velty, F. P. Navarro and I. Texier, *J. Drug Delivery Sci. Technol.*, 2020, **55**, 101421.

163 Y. P. Zhuang and W. G. Cui, *Adv. Drug Delivery Rev.*, 2021, **176**, 113885.

164 J. J. Chou, A. G. Berger, S. Jalili-Firoozinezhad and P. T. Hammond, *Acta Biomater.*, 2021, **135**, 331–341.

165 K. J. Koh, Y. Liu, S. H. Lim, X. J. Loh, L. F. Kang, C. Y. Lim and K. K. L. Phua, *Sci. Rep.*, 2018, **8**, 11842.

166 M. Wang, Y. Y. Han, X. J. Yu, L. L. Liang, H. Chang, D. C. Yeo, C. Wiraja, M. L. Wee, L. B. Liu, X. G. Liu and C. J. Xu, *Adv. Healthcare Mater.*, 2020, **9**, 1900635.

167 B. Y. Lan, L. M. Zhang, L. Q. Yang, J. F. Wu, N. Li, C. L. Pan, X. Y. Wang, L. X. Zeng, L. Yan, C. Yang and M. Ren, *J. Nanobiotechnol.*, 2021, **19**, 130.

168 M. Sharifiaghdam, E. Shaabani, Z. Sharifiaghdam, H. De Keersmaecker, B. Lucas, J. Lammens, H. Ghanbari, L. Teimoori-Toolabi, C. Vervaet, T. De Beer, R. Faridi-Majidi, S. C. De Smedt, K. Braeckmans and J. C. Fraire, *Nanoscale*, 2021, **13**, 15445–15463.

169 E. Khadem, M. Kharaziha, H. R. Bakhsheshi-Rad, O. Das and F. Berto, *Polymers*, 2022, **14**, 1709.

170 S. O. Blacklow, J. Li, B. R. Freedman, M. Zeidi, C. Chen and D. J. Mooney, *Sci. Adv.*, 2019, **5**, eaaw396.

171 B. Mirani, E. Pagan, B. Currie, M. A. Siddiqui, R. Hosseinzadeh, P. Mostafalu, Y. S. Zhang, A. Ghahary and M. Akbari, *Adv. Healthcare Mater.*, 2017, **6**, 1700718.

172 Y. P. Liang, X. Zhao, T. L. Hu, B. J. Chen, Z. H. Yin, P. X. Ma and B. L. Guo, *Small*, 2019, **15**, 1900046.

173 S. Q. Wang, H. Zheng, L. Zhou, F. Cheng, Z. Liu, H. P. Zhang and Q. Y. Zhang, *Biomaterials*, 2020, **260**, 120314.

174 L. Han, Y. N. Zhang, X. Lu, K. F. Wang, Z. M. Wang and H. P. Zhang, *ACS Appl. Mater. Interfaces*, 2016, **8**, 29088–29100.

175 N. Yang, M. Zhu, G. C. Xu, N. Liu and C. Yu, *J. Mater. Chem. B*, 2020, **8**, 3908–3917.

176 M. G. Arafa, R. F. El-Kased and M. M. Elmazar, *Sci. Rep.*, 2018, **8**, 13674.

177 A. Evanghelidis, M. Beregoi, V. C. Diculescu, A. Galatanu, P. Ganea and I. Enculescu, *Sci. Rep.*, 2018, **8**, 17555.

178 P. Nakielski, S. Pawlowska, C. Rinoldi, Y. Ziai, L. De Sio, O. Urbanek, K. Zembrzycki, M. Pruchniewski, M. Lanzi, E. Salatelli, A. Calogero, T. A. Kowalewski, A. L. Yarin and

F. Pierini, *ACS Appl. Mater. Interfaces*, 2020, **12**, 54328–54342.
179 Y. H. Chen, W. H. Cheng, L. J. Teng, M. Jin, B. H. Lu, L. Ren and Y. J. Wang, *Macromol. Mater. Eng.*, 2018, **303**, 1700660.
180 S. H. Hong, S. Kim, J. P. Park, M. Shin, K. Kim, J. H. Ryu and H. Lee, *Biomacromolecules*, 2018, **19**, 2053–2061.
181 M. Shan, C. Gong, B. Q. Li and G. L. Wu, *Polym. Chem.*, 2017, **8**, 2997–3005.
182 P. Esmaeilzadeh, A. Kowitsch, A. Liedmann, M. Menzel, B. Fuhrmann, G. Schmidt, J. Klehm and T. Groth, *ACS Appl. Mater. Interfaces*, 2018, **10**, 8507–8518.
183 Y. J. Che, D. P. Li, Y. L. Liu, Z. Yue, J. L. Zhao, Q. L. Ma, Q. Zhang, Y. B. Tan, Q. Y. Yue and F. J. Meng, *J. Polym. Res.*, 2018, **25**, 169.
184 M. Kuddushi, D. Ray, V. Aswal, C. Hoskins and N. Malek, *ACS Appl. Bio Mater.*, 2020, **3**, 4883–4894.
185 L. Zhang, Y. T. Zhou, D. D. Su, S. Y. Wu, J. Zhou and J. H. Chen, *J. Mater. Chem. B*, 2021, **9**, 5887–5897.
186 D. Wu, X. G. Shi, F. L. Zhao, S. T. F. Chilengue, L. D. Deng, A. J. Dong, D. L. Kong, W. W. Wang and J. H. Zhang, *Acta Biomater.*, 2019, **96**, 123–136.
187 Z. L. Han, P. Wang, G. Y. Mao, T. H. Yin, D. M. Zhong, B. R. B. Yiming, X. C. Hu, Z. Jia, G. D. Nian, S. X. Qu and W. Yang, *ACS Appl. Mater. Interfaces*, 2020, **12**, 12010–12017.
188 S. K. Boda, N. G. Fischer, Z. Ye and C. Aparicio, *Biomacromolecules*, 2020, **21**, 4945–4961.
189 Y. P. Liang, X. Zhao, P. X. Ma, B. L. Guo, Y. P. Du and X. Z. Han, *J. Colloid Interface Sci.*, 2019, **536**, 224–234.
190 R. Garriga, I. Jurewicz, S. Seyedin, N. Bardi, S. Totti, B. Matta-Domjan, E. G. Velliou, M. A. Alkhorayef, V. L. Cebolla, J. M. Razal, A. B. Dalton and E. Munoz, *Nanoscale*, 2017, **9**, 7791–7804.
191 M. di Luca, O. Vittorio, G. Cirillo, M. Curcio, M. Czuban, F. Voli, A. Farfalla, S. Hampel, F. P. Nicoletta and F. Iemma, *Int. J. Pharm.*, 2018, **546**, 50–60.
192 V. Yesilyurt, M. J. Webber, E. A. Appel, C. Godwin, R. Langer and D. G. Anderson, *Adv. Mater.*, 2016, **28**, 86–91.
193 R. P. Birajdar, S. B. Patil, V. V. Alange and R. V. Kulkarni, *J. Macromol. Sci., Part A: Pure Appl.Chem.*, 2019, **56**, 306–315.
194 Y. T. Zhu, Q. Zeng, Q. Zhang, K. Li, X. L. Shi, F. Liang and D. Han, *Nanoscale*, 2020, **12**, 8679–8686.
195 Y. H. Yan, L. H. Rong, J. Ge, B. D. B. Tiu, P. F. Cao and R. C. Advincula, *Macromol. Mater. Eng.*, 2019, **304**, 1800720.
196 R. Pinnaratip, M. S. A. Bhuiyan, K. Meyers, R. M. Rajachar and B. P. Lee, *Adv. Healthcare Mater.*, 2019, **8**, 1801568.
197 N. Annabi, D. Rana, E. S. Sani, R. Portillo-Lara, J. L. Gifford, M. M. Fares, S. M. Mithieux and A. S. Weiss, *Biomaterials*, 2017, **139**, 229–243.
198 X. Ke, Z. Y. Dong, S. X. Tang, W. L. Chu, X. R. Zheng, L. Zhen, X. Y. Chen, C. M. Ding, J. Luo and J. S. Li, *Biomater. Sci.*, 2020, **8**, 4346–4357.
199 Y. J. Moon, S. J. Yoon, J. H. Koo, Y. Yoon, H. J. Byun, H. S. Kim, G. Khang, H. J. Chun and D. H. Yang, *Int. J. Mol. Sci.*, 2021, **22**, 700.
200 H. F. Zhu, X. H. Mei, Y. Y. He, H. L. Mao, W. B. Tang, R. Liu, J. Yang, K. Luo, Z. Gu and L. Zhou, *ACS Appl. Mater. Interfaces*, 2020, **12**, 4241–4253.
201 X. X. Zhang, Z. F. Ma, Y. Ke, Y. Xia, X. D. Xu, J. C. Liu, Y. M. Gong, Q. Shi and J. H. Yin, *Mater. Adv.*, 2021, **2**, 5150–5159.
202 X. M. Luo, F. Ao, Q. Q. Huo, Y. Liu, X. C. Wang, H. J. Zhang, M. Yang, Y. Ma and X. H. Liu, *Biomater. Adv.*, 2022, **139**, 212983.
203 M. Rahimnejad and W. Zhong, *RSC Adv.*, 2017, **7**, 47380–47396.
204 C. Y. Sun, X. L. Zeng, S. H. Zheng, Y. L. Wang, Z. Y. Li, H. N. Zhang, L. L. Nie, Y. F. Zhang, Y. B. Zhao and X. L. Yang, *Chem. Eng. J.*, 2022, **427**, 130843.
205 D. Y. Du, X. Chen, C. Shi, Z. Y. Zhang, D. J. Shi, D. Kaneko, T. Kaneko and Z. Hua, *Acta Biomater.*, 2021, **136**, 223–232.
206 Y. Q. Zheng, K. Y. Zhang, Y. M. Yao, X. R. Li, J. Y. Yu and B. Ding, *Compos. Commun.*, 2021, **26**, 100785.
207 S. C. Lu, X. H. Zhang, Z. W. Tang, H. Xiao, M. Zhang, K. Liu, L. H. Chen, L. L. Huang, Y. H. Ni and H. Wu, *Chem. Eng. J.*, 2021, **417**, 129329.
208 Q. L. Yang, L. L. Tang, C. C. Guo, F. Deng, H. Wu, L. H. Chen, L. L. Huang, P. Lu, C. C. Ding, Y. H. Ni and M. Zhang, *Chem. Eng. J.*, 2021, **417**, 127962.
209 E. Y. Jeon, J. Lee, B. J. Kim, K. I. Joo, K. H. Kim, G. Lim and H. J. Cha, *Biomaterials*, 2019, **222**, 119439.
210 D. D. Wang, P. P. Xu, S. S. Wang, W. L. Li and W. Z. Liu, *Eur. Polym. J.*, 2020, **134**, 109763.
211 J. Qu, X. Zhao, Y. P. Liang, T. L. Zhang, P. X. Ma and B. L. Guo, *Biomaterials*, 2018, **183**, 185–199.
212 C. Dai, Z. N. Zhou, Z. P. Guan, Y. X. Wu, Y. Liu, J. P. He, P. Yu, L. J. Tu, F. M. Zhang, D. F. Chen, R. X. Wang, C. Y. Ning, L. Zhou and G. X. Tan, *Macromol. Mater. Eng.*, 2018, **303**, 1800305.
213 B. Saleh, H. K. Dhaliwal, R. Portillo-Lara, E. Shirzaei Sani, R. Abdi, M. M. Amiji and N. Annabi, *Small*, 2019, **15**, 1902232.
214 S. Baik, H. J. Lee, D. W. Kim, J. W. Kim, Y. Lee and C. Pang, *Adv. Mater.*, 2019, **31**, 1803309.
215 J.-C. Hsieh, Y. Li, H. Wang, M. Perz, Q. Tang, K. W. K. Tang, I. Pyatnitskiy, R. Reyes, H. Ding and H. Wang, *J. Mater. Chem. B*, 2022, **10**, 7260–7280.
216 X. Zhou, A. Rajeev, A. Subramanian, Y. Li, N. Rossetti, G. Natale, G. A. Lodygensky and F. Cicoira, *Acta Biomater.*, 2022, **139**, 296–306.
217 W. Dang, L. Manjakkal, W. T. Navaraj, L. Lorenzelli, V. Vinciguerra and R. Dahiya, *Biosens. Bioelectron.*, 2018, **107**, 192–202.
218 J. Zhong, Z. Li, M. Takakuwa, D. Inoue, D. Hashizume, Z. Jiang, Y. Shi, L. Ou, M. O. G. Nayeem, S. Umezu, K. Fukuda and T. Someya, *Adv. Mater.*, 2022, **34**, 2107758.

219 Q. Lin, J. Huang, J. Yang, Y. Huang, Y. Zhang, Y. Wang, J. Zhang, Y. Wang, L. Yuan, M. Cai, X. Hou, W. Zhang, Y. Zhou, S. G. Chen and C. F. Guo, *Adv. Healthcare Mater.*, 2020, **9**, 2001023.

220 S. Zhang, Y. Li, G. Tomasello, M. Anthonisen, X. Li, M. Mazzeo, A. Genco, P. Grutter and F. Cicoira, *Adv. Electron. Mater.*, 2019, **5**, 1900191.

221 H. Karimi-Maleh, F. Karimi, M. Alizadeh and A. L. Sanati, *Chem. Rec.*, 2020, **20**, 682–692.

222 P. Rebelo, E. Costa-Rama, I. Seguro, J. G. Pacheco, H. P. A. Nouws, M. N. D. S. Cordeiro and C. Delerue-Matos, *Biosens. Bioelectron.*, 2021, **172**, 112719.

223 J. Song, Y. Wei, M. Xu, J. Gao, L. Luo, H. Wu, X. Li, Y. Li and X. Wang, *ACS Appl. Polym. Mater.*, 2022, **4**, 766–772.

224 J. Gu, J. Huang, G. Chen, L. Hou, J. Zhang, X. Zhang, X. Yang, L. Guan, X. Jiang and H. Liu, *ACS Appl. Mater. Interfaces*, 2020, **12**, 40815–40827.

225 H. Liu, H. Zhang, W. Han, H. Lin, R. Li, J. Zhu and W. Huang, *Adv. Mater.*, 2021, **33**, 2004782.

226 W. Zhai, J. Zhu, Z. Wang, Y. Zhao, P. Zhan, S. Wang, G. Zheng, C. Shao, K. Dai, C. Liu and C. Shen, *ACS Appl. Mater. Interfaces*, 2022, **14**, 4562–4570.

227 Y. D. Horev, A. Maity, Y. Zheng, Y. Milyutin, M. Khatib, M. Yuan, R. Y. Suckeveriene, N. Tang, W. Wu and H. Haick, *Adv. Mater.*, 2021, **33**, 2102488.

228 X. Lin, Y. Bing, F. Li, H. Mei, S. Liu, T. Fei, H. Zhao and T. Zhang, *Adv. Mater. Technol.*, 2022, **7**, 2101312.

229 A. S. Fiorillo, C. D. Critello and S. A. Pullano, *Sens. Actuators, A*, 2018, **281**, 156–175.

230 Q. Liu, X.-X. Wang, W.-Z. Song, H.-J. Qiu, J. Zhang, Z. Fan, M. Yu and Y.-Z. Long, *ACS Appl. Mater. Interfaces*, 2020, **12**, 8288–8295.

231 J. Zhong, Y. Ma, Y. Song, Q. Zhong, Y. Chu, I. Karakurt, D. B. Bogy and L. Lin, *ACS Nano*, 2019, **13**, 7107–7116.

232 I. Șerban and A. Enesca, *Front. Chem.*, 2020, **8**, 354.

233 Y. Li, B. Cui, S. Zhang, B. Li, J. Li, S. Liu and Q. Zhao, *Small*, 2022, 2107413.

234 Y. Chen, Y. Zhang, Z. Liang, Y. Cao, Z. Han and X. Feng, *npj Flexible Electron.*, 2020, **4**, 2.

235 W. Gao, S. Emaminejad, H. Y. Y. Nyein, S. Challa, K. Chen, A. Peck, H. M. Fahad, H. Ota, H. Shiraki, D. Kiriya, D.-H. Lien, G. A. Brooks, R. W. Davis and A. Javey, *Nature*, 2016, **529**, 509–514.

236 S. Emaminejad, W. Gao, E. Wu, Z. A. Davies, H. Yin Yin Nyein, S. Challa, S. P. Ryan, H. M. Fahad, K. Chen, Z. Shahpar, S. Talebi, C. Milla, A. Javey and R. W. Davis, *Proc. Natl. Acad. Sci. U. S. A.*, 2017, **114**, 4625–4630.

237 H. Y. Y. Nyein, M. Bariya, L. Kivimäki, S. Uusitalo, T. S. Liaw, E. Jansson, C. H. Ahn, J. A. Hangasky, J. Zhao, Y. Lin, T. Happonen, M. Chao, C. Liedert, Y. Zhao, L.-C. Tai, J. Hiltunen and A. Javey, *Sci. Adv.*, 2019, **5**, eaaw9906.

238 J. Zhao, H. Y. Y. Nyein, L. Hou, Y. Lin, M. Bariya, C. H. Ahn, W. Ji, Z. Fan and A. Javey, *Adv. Mater.*, 2021, **33**, 2006444.

239 Y. Lin, M. Bariya and A. Javey, *Adv. Funct. Mater.*, 2021, **31**, 2008087.

240 H. Y. Y. Nyein, M. Bariya, B. Tran, C. H. Ahn, B. J. Brown, W. Ji, N. Davis and A. Javey, *Nat. Commun.*, 2021, **12**, 1823.

241 S. Liu, D. S. Yang, S. Wang, H. Luan, Y. Sekine, J. B. Model, A. J. Aranyosi, R. Ghaffari and J. A. Rogers, *EcoMat*, 2022, e12270.

242 Y. Sekine, S. B. Kim, Y. Zhang, A. J. Bandodkar, S. Xu, J. Choi, M. Irie, T. R. Ray, P. Kohli, N. Kozai, T. Sugita, Y. Wu, K. Lee, K.-T. Lee, R. Ghaffari and J. A. Rogers, *Lab Chip*, 2018, **18**, 2178–2186.

243 L. B. Baker, J. B. Model, K. A. Barnes, M. L. Anderson, S. P. Lee, K. A. Lee, S. D. Brown, A. J. Reimel, T. J. Roberts, R. P. Nuccio, J. L. Bonsignore, C. T. Ungaro, J. M. Carter, W. Li, M. S. Seib, J. T. Reeder, A. J. Aranyosi, J. A. Rogers and R. Ghaffari, *Sci. Adv.*, 2020, **6**, eabe3929.

244 J. T. Reeder, J. Choi, Y. Xue, P. Gutruf, J. Hanson, M. Liu, T. Ray, A. J. Bandodkar, R. Avila, W. Xia, S. Krishnan, S. Xu, K. Barnes, M. Pahnke, R. Ghaffari, Y. Huang and J. A. Rogers, *Sci. Adv.*, 2019, **5**, eaau6356.

245 L. B. Baker, M. S. Seib, K. A. Barnes, S. D. Brown, M. A. King, P. J. D. De Chavez, S. Qu, J. Archer, A. S. Wolfe, J. R. Stofan, J. M. Carter, D. E. Wright, J. Wallace, D. S. Yang, S. Liu, J. Anderson, T. Fort, W. Li, J. A. Wright, S. P. Lee, J. B. Model, J. A. Rogers, A. J. Aranyosi and R. Ghaffari, *Adv. Mater.Technol.*, 2022, 2200249.

246 L. Yin, M. Cao, K. N. Kim, M. Lin, J.-M. Moon, J. R. Sempionatto, J. Yu, R. Liu, C. Wicker, A. Trifonov, F. Zhang, H. Hu, J. R. Moreto, J. Go, S. Xu and J. Wang, *Nat. Electron.*, 2022, **5**, 694–705.

247 J. R. Sempionatto, J.-M. Moon and J. Wang, *ACS Sens.*, 2021, **6**, 1875–1883.

248 M. C. Hartel, D. Lee, P. S. Weiss, J. Wang and J. Kim, *Biosens. Bioelectron.*, 2022, **215**, 114565.

249 L. Manjakkal, L. Yin, A. Nathan, J. Wang and R. Dahiya, *Adv. Mater.*, 2021, **33**, 2100899.

250 J. R. Sempionatto, M. Lin, L. Yin, E. De la paz, K. Pei, T. Sonsa-ard, A. N. de Loyola Silva, A. A. Khorshed, F. Zhang, N. Tostado, S. Xu and J. Wang, *Nat. Biomed. Eng.*, 2021, **5**, 737–748.

251 Y. Wang, G. P. Chen, H. Zhang, C. Zhao, L. Y. Sun and Y. J. Zhao, *ACS Nano*, 2021, **15**, 5977–6007.

252 Y. Wang, H. Haick, S. Y. Guo, C. Y. Wang, S. Lee, T. Yokota and T. Someya, *Chem. Soc. Rev.*, 2022, **51**, 3759–3793.

253 G. H. Lee, H. Kang, J. W. Chung, Y. Lee, H. Yoo, S. Jeong, H. Cho, J. Y. Kim, S. G. Kang, J. Y. Jung, S. G. Hahm, J. Lee, I. J. Jeong, M. Park, G. Park, I. H. Yun, J. Y. Kim, Y. Hong, Y. Yun, S. H. Kim and B. K. Choi, *Sci. Adv.*, 2022, **8**, eabm3622.

254 Y. B. Wang, M. M. Zhu, X. D. Wei, J. Y. Yu, Z. L. Li and B. Ding, *Chem. Eng. J.*, 2021, **425**, 130599.

255 H. Jinno, T. Yokota, M. Koizumi, W. Yukita, M. Saito, I. Osaka, K. Fukuda and T. Someya, *Nat. Commun.*, 2021, **12**, 2234.

256 H. X. Wu, Z. M. Su, M. Y. Shi, L. M. Miao, Y. Song, H. T. Chen, M. D. Han and H. X. Zhang, *Adv. Funct. Mater.*, 2018, **28**, 1704641.
257 Z. L. Li, M. M. Zhu, J. L. Shen, Q. Qiu, J. Y. Yu and B. Ding, *Adv. Funct. Mater.*, 2020, **30**, 1908411.
258 C. Y. Ye, K. Dong, J. An, J. Yi, X. Peng, C. Ning and Z. L. Wang, *ACS Energy Lett.*, 2021, **6**, 1443–1452.
259 B. H. Moghadam, M. Hasanzadeh and A. Simchi, *ACS Appl. Nano Mater.*, 2020, **3**, 8742–8752.
260 F. Mokhtari, G. M. Spinks, S. Sayyar, Z. X. Cheng, A. Ruhparwar and J. Foroughi, *Adv. Mater. Technol.*, 2021, **6**, 2000841.
261 M. Piccolino, *C. R. Biol.*, 2006, **329**, 303–318.
262 G. P. Tai, M. Tai and M. Zhao, *Burns Trauma*, 2018, **6**, 20.
263 S. Xu, A. Jayaraman and J. A. Rogers, *Nature*, 2019, **571**, 319–321.
264 M. Zhao, B. Song, J. Pu, T. Wada, B. Reid, G. P. Tai, F. Wang, A. H. Guo, P. Walczysko, Y. Gu, T. Sasaki, A. Suzuki, J. V. Forrester, H. R. Bourne, P. N. Devreotes, C. D. McCaig and J. M. Penninger, *Nature*, 2006, **442**, 457–460.
265 R. Z. Luo, J. Y. Dai, J. P. Zhang and Z. Li, *Adv. Healthcare Mater.*, 2021, **10**, 2100557.
266 J. C. Liang, H. J. Zeng, L. Qiao, H. Jiang, Q. Ye, Z. L. Wang, B. Liu and Z. J. Fan, *ACS Appl. Mater. Interfaces*, 2022, **14**, 30507–30522.
267 D. Wan, J. Yang, X. J. Cui, N. C. Ma, Z. S. Wang, Y. P. Li, P. W. Li, Y. X. Zhang, Z. H. Lin, S. B. Sang and H. L. Zhang, *Nano Energy*, 2021, **89**, 106465.
268 T. Y. Y. He, H. Wang, J. H. Wang, X. Tian, F. Wen, Q. F. Shi, J. S. Ho and C. K. Lee, *Adv. Sci.*, 2019, **6**, 1901437.
269 G. Yao, L. Kang, J. Li, Y. Long, H. Wei, C. A. Ferreira, J. J. Jeffery, Y. Lin, W. B. Cai and X. D. Wang, *Nat. Commun.*, 2018, **9**, 5349.
270 M. M. Zhu, M. N. Lou, J. Y. Yu, Z. L. Li and B. Ding, *Nano Energy*, 2020, **78**, 105208.
271 Y. Wang, H. Haick, S. Guo, C. Wang, S. Lee, T. Yokota and T. Someya, *Chem. Soc. Rev.*, 2022, **51**, 3759–3793.
272 M. Zohair, K. Moyer, J. Eaves-Rathert, C. Meng, J. Waugh and C. L. Pint, *ACS Nano*, 2020, **14**, 2308–2315.
273 C. S. Kim, H. M. Yang, J. Lee, G. S. Lee, H. Choi, Y. J. Kim, S. H. Lim, S. H. Cho and B. J. Cho, *ACS Energy Lett.*, 2018, **3**, 501–507.
274 M. M. Zhu, M. N. Lou, I. Abdalla, J. Y. Yu, Z. L. Li and B. Ding, *Nano Energy*, 2020, **69**, 104429.
275 C. R. Bowen, J. Taylor, E. LeBoulbar, D. Zabek, A. Chauhan and R. Vaish, *Energy Environ. Sci.*, 2014, **7**, 3836–3856.
276 Y. B. Wang, M. M. Zhu, X. D. Wei, J. Y. Yu, Z. L. Li and B. Ding, *Chem. Eng. J.*, 2021, **425**, 130599.
277 M. Jose, A. Bronckaers, R. S. N. Kumar, D. Reenaers, T. Vandenryt, R. Thoelen and W. Deferme, *Sci. Rep.*, 2022, **12**, 10138.
278 S. Du, H. Suo, G. Xie, Q. Lyu, M. Mo, Z. Xie, N. Zhou, L. Zhang, J. Tao and J. Zhu, *Nano Energy*, 2022, **93**, 106906.
279 H. Ouyang, Z. Liu, N. Li, B. Shi, Y. Zou, F. Xie, Y. Ma, Z. Li, H. Li, Q. Zheng, X. Qu, Y. Fan, Z. L. Wang, H. Zhang and Z. Li, *Nat. Commun.*, 2019, **10**, 1821.
280 F. Zou, Y. Wang, Y. Zheng, Y. Xie, H. Zhang, J. Chen, M. I. Hussain, H. Meng and J. Peng, *Bioact. Mater.*, 2022, **17**, 471–487.
281 Z. J. Krysiak and U. Stachewicz, *Wiley Interdiscip. Rev.: Nanomed. Nanobiotechnol.*, 2023, **15**, e1829.
282 H. Wang, G. Pastorin and C. Lee, *Adv. Sci.*, 2016, **3**, 1500441.
283 T. He, H. Wang, J. Wang, X. Tian, F. Wen, Q. Shi, J. S. Ho and C. Lee, *Adv. Sci.*, 2019, **6**, 1901437.
284 Y. Lee, J. Park, A. Choe, S. Cho, J. Kim and H. Ko, *Adv. Funct. Mater.*, 2020, **30**, 1904523.
285 P. Basset, S. P. Beeby, C. Bowen, Z. J. Chew, A. Delbani, R. D. I. G. Dharmasena, B. Dudem, F. R. Fan, D. Galayko, H. Guo, J. Hao, Y. Hou, C. Hu, Q. Jing, Y. H. Jung, S. K. Karan, S. Kar-Narayan, M. Kim, S.-W. Kim, Y. Kuang, K. J. Lee, J. Li, Z. Li, Y. Long, S. Priya, X. Pu, T. Ruan, S. R. P. Silva, H. S. Wang, K. Wang, X. Wang, Z. L. Wang, W. Wu, W. Xu, H. Zhang, Y. Zhang and M. Zhu, *APL Mater.*, 2022, **10**, 109201.
286 Y. Bai, H. Jantunen and J. Juuti, *Adv. Mater.*, 2018, **30**, 1707271.
287 Z. L. Li, M. M. Zhu, J. L. Shen, Q. Qiu, J. Y. Yu and B. Ding, *Adv. Funct. Mater.*, 2019, **30**, 1908411.
288 L. Yang, H. D. Ji, C. Z. Meng, Y. H. Li, G. H. Zheng, X. Chen, G. Y. Niu, J. Y. Yan, Y. Xue, S. J. Guo and H. Y. Cheng, *ACS Appl. Mater. Interfaces*, 2022, **14**, 17818–17825.
289 D. Son, J. Kang, O. Vardoulis, Y. Kim, N. Matsuhisa, J. Y. Oh, J. W. F. To, J. W. Mun, T. Katsumata, Y. X. Liu, A. F. McGuire, M. Krason, F. Molina-Lopez, J. Ham, U. Kraft, Y. Lee, Y. Yun, J. B. H. Tok and Z. N. Bao, *Nat. Nanotechnol.*, 2018, **13**, 1057–1065.
290 Y. Q. Wang, M. Z. Guo, B. F. He and B. B. Gao, *Anal. Chem.*, 2021, **93**, 4687–4696.
291 M. Farahani and A. Shafiee, *Adv. Healthcare Mater.*, 2021, **10**, e2100477.
292 L. Y. Meng, A. P. F. Turner and W. C. Mak, *Biotechnol. Adv.*, 2020, **39**, 107398.
293 X. L. Nan, X. Wang, T. T. Kang, J. L. Zhang, L. X. Dong, J. F. Dong, P. Xia and D. L. Wei, *Micromachines*, 2022, **13**, 1395.
294 Y. Li, X. Li, S. Zhang, L. Liu, N. Hamad, S. R. Bobbara, D. Pasini and F. Cicoira, *Adv. Funct. Mater.*, 2020, **30**, 2002853.
295 Y. Li, S. Zhang, N. Hamad, K. Kim, L. Liu, M. Lerond and F. Cicoira, *Macromol. Biosci.*, 2020, **20**, 2000146.
296 Y. Li, X. Zhou, B. Sarkar, N. Gagnon-Lafrenais and F. Cicoira, *Adv. Mater.*, 2022, 2108932.
297 B. Ying and X. Liu, *iScience*, 2021, **24**, 103174.
298 Y. Peng, M. Pi, X. Zhang, B. Yan, Y. Li, L. Shi and R. Ran, *Polymer*, 2020, **196**, 122469.

299 N. Coppedè, M. Giannetto, M. Villani, V. Lucchini, E. Battista, M. Careri and A. Zappettini, *Org. Electron.*, 2020, **78**, 105579.
300 Y. Li, S. Zhang, X. Li, V. R. N. Unnava and F. Cicoira, *Flexible Printed Electron.*, 2019, **4**, 044004.
301 J.-C. Hsieh, H. Alawieh, Y. Li, F. Iwane, L. Zhao, R. Anderson, S. I. Abdullah, K. W. Kevin Tang, W. Wang, I. Pyatnitskiy, Y. Jia, J. d. R. Millán and H. Wang, *Biosens. Bioelectron.*, 2022, **218**, 114756.
302 M. Bhattacharjee, M. Soni, P. Escobedo and R. Dahiya, *Adv. Electron. Mater.*, 2020, **6**, 2000445.
303 Z. Li, W. Guo, Y. Huang, K. Zhu, H. Yi and H. Wu, *Carbon*, 2020, **164**, 164–170.
304 Q. Wang, X. Pan, C. Lin, D. Lin, Y. Ni, L. Chen, L. Huang, S. Cao and X. Ma, *Chem. Eng. J.*, 2019, **370**, 1039–1047.
305 J. Liu, X. Zhang, Y. Liu, M. Rodrigo, P. D. Loftus, J. Aparicio-Valenzuela, J. Zheng, T. Pong, K. J. Cyr, M. Babakhanian, J. Hasi, J. Li, Y. Jiang, C. J. Kenney, P. J. Wang, A. M. Lee and Z. Bao, *Proc. Natl. Acad. Sci. U. S. A.*, 2020, **117**, 14769–14778.
306 X. W. Wang, Z. Liu and T. Zhang, *Small*, 2017, **13**, 1602790.